



UNIVERSITY OF LEEDS

This is a repository copy of *Sucrose transporter ZmSut1 expression and localization uncover new insights into sucrose phloem loading*.

White Rose Research Online URL for this paper:  
<http://eprints.whiterose.ac.uk/104063/>

Version: Accepted Version

---

**Article:**

Baker, RF, Leach, KA, Boyer, NR et al. (7 more authors) (2016) Sucrose transporter ZmSut1 expression and localization uncover new insights into sucrose phloem loading. *Plant Physiology*, 172 (3). pp. 1876-1898. ISSN 0032-0889

<https://doi.org/10.1104/pp.16.00884>

---

© 2016 American Society of Plant Biologists. This is an author produced version of a paper published in *Plant Physiology*. Uploaded in accordance with the publisher's self-archiving policy.

**Reuse**

Unless indicated otherwise, fulltext items are protected by copyright with all rights reserved. The copyright exception in section 29 of the Copyright, Designs and Patents Act 1988 allows the making of a single copy solely for the purpose of non-commercial research or private study within the limits of fair dealing. The publisher or other rights-holder may allow further reproduction and re-use of this version - refer to the White Rose Research Online record for this item. Where records identify the publisher as the copyright holder, users can verify any specific terms of use on the publisher's website.

**Takedown**

If you consider content in White Rose Research Online to be in breach of UK law, please notify us by emailing [eprints@whiterose.ac.uk](mailto:eprints@whiterose.ac.uk) including the URL of the record and the reason for the withdrawal request.



[eprints@whiterose.ac.uk](mailto:eprints@whiterose.ac.uk)  
<https://eprints.whiterose.ac.uk/>

1 **Short title:** Suc phloem loading and retrieval by *ZmSut1*

2

3 **Corresponding Author:** David M. Braun, E-mail: [braundm@missouri.edu](mailto:braundm@missouri.edu)

4 116 Tucker Hall, Columbia, MO 65211

5 Phone: (573) 882-1055; Fax: (573) 882-0123

6

7 **Sucrose transporter *ZmSut1* expression and localization uncover new**  
8 **insights into sucrose phloem loading**

9 R. Frank Baker<sup>1</sup>, Kristen A. Leach<sup>1</sup>, Nathaniel R. Boyer<sup>1</sup>, Michael J. Swyers<sup>1</sup>, Yoselin  
10 Benitez-Alfonso<sup>2</sup>, Tara Skopelitis<sup>2</sup>, Anding Luo<sup>3</sup>, Anne Sylvester<sup>3</sup>, David Jackson<sup>2</sup>,  
11 David M. Braun<sup>1</sup>

12

13 <sup>1</sup>308 Tucker Hall, Division of Biological Sciences, Interdisciplinary Plant Group, and  
14 Missouri Maize Center, University of Missouri-Columbia, Columbia, MO 65211

15 <sup>2</sup>Cold Spring Harbor Laboratory, Cold Spring Harbor, NY 11724

16 <sup>3</sup>Department of Molecular Biology, University of Wyoming, Laramie, Wyoming 82071

17

18 **One sentence summary:** Maize *Sucrose transporter1* functions to load sucrose into  
19 phloem companion cells, restrict its accumulation in the apoplasm, and prevent its loss  
20 during long-distance transport.

21

22 **Author Contributions:** R.F.B. participated in the design of the study, conducted the  
23 light, epi-fluorescence, and confocal microscopy, performed the CFDA experiments, and  
24 drafted the manuscript. K.A.L. performed the qRT-PCR and helped draft the manuscript.  
25 N.B. performed genotyping to propagate transgenic events and the quantification of  
26 relative signal abundance in the RNA *in situ* hybridizations. M.S. performed genotyping  
27 and phenotyping to confirm and propagate transgenic events. Y.B.A., T.S., and D.J.  
28 constructed the pZmSut1::RFP and gSUT1-YFP transgenic lines, and A.L. and A.S.  
29 provided the PIP2-1-CFP line. D.M.B. conceived of the study, participated in its design  
30 and implementation, performed the genetic experiments, and helped draft the manuscript.  
31 All authors edited and critically revised the manuscript.

32

33 **Funding Information:** This research was supported by the US National Science  
34 Foundation Plant Genome Research Program, grants no. IOS-1025976 to DMB, and  
35 IOS-0501862 to DJ and AS.

36

37 **Present Addresses:**

38 RFB: University of Missouri Molecular Cytology Core, Bond Life Sciences Building,  
39 Columbia, MO 65211

40 MJS: Monsanto, Chesterfield, MO, 63017

41 YBA: Center for Plant Science, The Faculty of Biological Sciences, University of Leeds,  
42 Leeds, LS2 9JT, UK

43

44

45 The author responsible for distribution of materials integral to the findings presented in  
46 this article in accordance with the Journal policy described in the Instructions for Authors  
47 (<http://www.plantphysiol.org>) is: David M. Braun ([braundm@missouri.edu](mailto:braundm@missouri.edu)).

48

49 **Corresponding Author Email:** [braundm@missouri.edu](mailto:braundm@missouri.edu)

50

51

52 **Abstract**

53 Sucrose (Suc) transporters (SUTs) translocate Suc across cellular membranes, and, in  
54 eudicots, multiple SUTs are known to function in Suc phloem loading in leaves. In maize  
55 (*Zea mays* L.), the *Sucrose transporter1* (*ZmSut1*) gene has been implicated in Suc  
56 phloem loading based upon RNA expression in leaves, electrophysiological experiments,  
57 and phenotypic analysis of *zmsut1* mutant plants. However, no previous studies have  
58 examined the cellular expression of *ZmSut1* RNA or subcellular localization of the  
59 ZmSUT1 protein to assess the gene's hypothesized function in Suc phloem loading or to  
60 evaluate its potential roles, such as phloem unloading, in non-photosynthetic tissues. To  
61 this end, we performed RNA *in situ* hybridization experiments, promoter: reporter gene  
62 analyses, and ZmSUT1 localization studies to elucidate the cellular expression pattern of  
63 the *ZmSut1* transcript and protein. These data showed *ZmSut1* was expressed in multiple  
64 cell types throughout the plant, and indicated it functions in phloem companion cells to  
65 load Suc, and also in other cell types to retrieve Suc from the apoplasm to prevent its  
66 accumulation and loss to the transpiration stream. Additionally, by comparing a phloem-  
67 mobile tracer with *ZmSut1* expression, we determined that developing maize leaves  
68 dynamically switch from symplasmic to apoplasmic phloem unloading, reconciling  
69 previously conflicting reports, and suggest that *ZmSut1* does not have an apparent  
70 function in either unloading process. A model for the dual roles for *ZmSut1* function  
71 (phloem loading and apoplasmic recycling), *Sut1* evolution, and its possible use to  
72 enhance Suc export from leaves in engineering C<sub>3</sub> grasses for C<sub>4</sub> photosynthesis is  
73 discussed.

74

75 **Keywords:** apoplasm, CFDA, maize, phloem, sink, source, Suc, SUT, symplasm,  
76 ZmSUT1

77

78 **INTRODUCTION**

79 Plant growth, development, and ultimately crop yield are dependent on the transport of  
80 photosynthates from the source (net exporting) leaves to sink (net importing) tissues (e.g.,  
81 ears, tassels, stems, roots). In the coming decades, a growing world population (predicted  
82 to increase by more than two billion people by 2050) will place increasing pressure on

83 agricultural systems already challenged with the increased temperatures and more erratic  
84 precipitation patterns predicted for climate change (Godfray et al., 2010; Rosenzweig et  
85 al., 2014). Hence, understanding the transport pathways and genes functioning to control  
86 the allocation of carbohydrates in plants will be crucial to improve crop resilience to  
87 biotic and abiotic stress and to increase crop productivity (Rennie and Turgeon, 2009;  
88 Bihmidine et al., 2013; Lemoine et al., 2013; Braun et al., 2014; Jia et al., 2015; Yadav et  
89 al., 2015; Durand et al., 2016).

90

91 To sustain development and growth, photoassimilates must be transported from the  
92 leaves through the veins to various sink tissues. In the majority of crop plants, including  
93 maize (*Zea mays* L.), sucrose (Suc) is the carbohydrate translocated long-distance from  
94 source to sink tissues (Heyser et al., 1978; Ohshima et al., 1990). Suc is synthesized in  
95 the mesophyll (M) cells of mature leaves and ultimately enters the phloem tissue within  
96 the veins for long-distance transport (Lunn and Furbank, 1999; Slewinski and Braun,  
97 2010a). Suc movement from the M cells into the phloem involves a combination of  
98 symplasmic and apoplasmic transport (Braun and Slewinski, 2009). In symplasmic  
99 transport, Suc moves directly between cells through plasmodesmata (PD), cell-wall pores  
100 connecting the cytoplasms of adjacent cells. In apoplasmic transport, Suc is released into  
101 the apoplasm (the cell-wall free space) and uptaken into recipient cells (Lalonde et al.,  
102 2004; Ayre, 2011; Baker et al., 2012; Chen et al., 2012).

103

104 Suc loading and transport through the phloem primarily occur in different vein types. In  
105 maize leaves, three distinct classes of longitudinal veins (lateral, intermediate, and small)  
106 function in photoassimilate loading and transport (Russell and Evert, 1985). The majority  
107 of Suc phloem loading occurs in the small and intermediate veins, which are collectively  
108 termed the minor veins. The Suc is then funneled through small, transversely oriented  
109 veins into the lateral veins, which function primarily in long-distance transport from the  
110 leaf blade and into other plant regions (Fritz et al., 1983; Fritz et al., 1989).

111

112 Within the phloem, Suc transport occurs in the sieve tube, which is constituted of sieve  
113 elements (SE) arranged end-to-end (Evert, 1982). Upon maturation, SE lose their nucleus

114 and most other organelles to form the conducting sieve tube (Esau, 1977), and come to  
115 depend on companion cells (CC) for metabolic support and survival (van Bel and  
116 Knoblauch, 2000). The transfer of Suc, other metabolites, RNA, and proteins from the  
117 CC into the SE occurs symplasmically through the PD connecting them. Because of this  
118 dependency, the two cells are referred to as the CC/SE complex.

119

120 The phloem system can be divided into three functionally overlapping domains: the  
121 collection, transport, and release phloems (van Bel, 1996). The collection phloem is  
122 located in mature source leaf veins and is the site where Suc is loaded into the phloem  
123 (Patrick, 2012). The transport phloem connects the collection phloem to the release  
124 phloem and is the largest portion of the phloem network in a plant (van Bel, 2003). In the  
125 release phloem, Suc is unloaded from the phloem cells into surrounding cells for  
126 utilization, storage, or growth (Patrick, 2012). Once Suc enters the collection phloem, it is  
127 exported through the transport phloem in the blade and sheath (the leaf base), and then  
128 through the stem to distal sink tissues. The mechanism driving this flow of Suc and other  
129 solutes through the phloem is the hydrostatic pressure differential generated by the  
130 difference in osmotic potentials between the collection and release phloems (Patrick,  
131 2012). However, the high concentration of Suc in the sieve tubes relative to the apoplasm  
132 poses a thermodynamic challenge to its continued transport. In maize, the Suc  
133 concentration has been measured at 0.9–1.4 M in the phloem sieve tube sap (Ohshima et  
134 al., 1990; Weiner et al., 1991) and estimated to be 1–3 mM in the leaf apoplasm (Heyser  
135 et al., 1978; Lohaus et al., 2000; Lohaus et al., 2001). Thus, Suc is continually lost to the  
136 apoplasm by passive leakage across the sieve tube plasma membrane during long-  
137 distance transport through the phloem and must be continuously retrieved to maintain the  
138 hydrostatic pressure gradient between source and sink tissues (Minchin and Thorpe,  
139 1987; Patrick, 2012).

140

141 The other conducting tissue within veins, the xylem, transports water and dissolved  
142 minerals from roots to transpiring leaves within the tracheids and vessels (also called  
143 elements), which are both dead at maturity (Esau, 1977). In early organ development,  
144 vascular tissues are referred to using the prefix “proto” and are termed the protoxylem

145 and protophloem. These tissues are obliterated during organ elongation and growth and  
146 are replaced by later-forming metaxylem and metaphloem, which comprise the  
147 conducting tissues at maturity (Esau, 1977).

148

149 The different classes of maize veins are distinguished anatomically. Lateral veins contain  
150 large metaxylem elements, a protoxylem lacunae (space) produced by the rupturing of the  
151 protoxylem elements, and hypodermal sclerenchyma (HS) cells above and below the vein  
152 for structural support (Esau, 1977). Intermediate veins contain HS cells on one or both  
153 sides of the vein but lack large metaxylem vessels. Small veins lack both HS cells and  
154 large metaxylem vessels. Interestingly, ultrastructural studies of the sink-to-source  
155 transition in a maize leaf revealed that all veins classes were structurally mature prior to  
156 the cessation of phloem unloading (Evert et al., 1996a).

157

158 As a NADP-malic enzyme type of C<sub>4</sub> plant, maize exhibits Kranz anatomy in the leaf  
159 blade (Esau, 1977). In particular, two different types of photosynthetic cells  
160 concentrically enclose the vein: a single inner layer of bundle-sheath (BS) cells and a  
161 single outer layer of M cells (Fig. 2A, B). Both photosynthetic cell types share dense PD  
162 connections for facilitating the symplasmic flow of metabolites between them, including  
163 Suc (Evert et al., 1977). The BS cells similarly show abundant PD connections with the  
164 vascular parenchyma (VP) cells, which are associated with either the xylem (referred to  
165 as xylem parenchyma [XP] cells) or phloem (i.e., phloem parenchyma [PP] cells) (Evert  
166 et al., 1978). Based on the nearly complete symplasmic isolation of the CC/SE complex  
167 from other cell types in the vein, the PP cells are hypothesized to efflux Suc into the  
168 apoplasm for subsequent uptake across the plasma membrane into the CC/SE complex  
169 (Evert et al., 1978; Baker et al., 2012; Braun, 2012; Chen et al., 2012). In addition to the  
170 CC/SE, radioactive labeling studies determined that C<sup>14</sup>-Suc is retrieved from the xylem  
171 by XP cells, but the transporters responsible for Suc uptake remain unknown (Fritz et al.,  
172 1983).

173

174 Multiple classes of transporters involved in Suc flux across cell membranes have been  
175 identified, including Suc transporters (SUTs) (Aoki et al., 2003; Lalonde et al., 2004;

176 Sauer, 2007; Kühn and Grof, 2010; Ainsworth and Bush, 2011; Ayre, 2011; Baker et al.,  
177 2012; Reinders et al., 2012; Eom et al., 2015; Jung et al., 2015; Bihmidine et al., 2016).  
178 However, much remains to be clarified with respect to their particular roles in the phloem  
179 loading of Suc in photosynthetic tissues, its long-distance transport, and its unloading in  
180 sink tissues, especially in the grasses (Aoki et al., 2003; Braun and Slewinski, 2009;  
181 Bihmidine et al., 2013). Based on phylogenetic analysis, the *Sut* genes in plants have  
182 been classified into five different groups (Braun and Slewinski, 2009). The group 2  
183 (formerly type I) *Sut* genes were the first class of characterized *Sut* genes and are unique  
184 to eudicots. Some of these genes show strong expression in mature leaves, and both yeast  
185 (*Sacchomyces cerevisiae*) and *Xenopus laevis* oocyte heterologous expression studies  
186 of various SUT proteins demonstrated that they possess Suc transporter activity  
187 (Riesmeier et al., 1992; Aoki et al., 2003; Chandran et al., 2003; Carpaneto et al., 2005;  
188 Sivitz et al., 2005; Reinders et al., 2006; Sun et al., 2010). Additional mutational analyses  
189 and RNA suppression experiments supported a role for the group 2 *Sut* genes in Suc  
190 loading into the phloem (Riesmeier et al., 1994; Bürkle et al., 1998; Gottwald et al.,  
191 2000; Hackel et al., 2006; Srivastava et al., 2008). Recent experiments have also found  
192 that the *AtSUC2* gene in *Arabidopsis thaliana*, which was known to function in phloem  
193 loading, also performs Suc retrieval in the transport phloem (Srivastava et al., 2008;  
194 Gould et al., 2012).

195

196 Group 2 *Sut* genes are absent from monocot genomes; hence, the group 1 *Sut* genes,  
197 which are unique to the monocots, have been proposed to function in Suc phloem loading  
198 in leaves (Aoki et al., 2003; Sauer, 2007; Braun and Slewinski, 2009; Kühn and Grof,  
199 2010). Based on their broad expression in both source and sink tissues, some group 1 *Sut*  
200 genes have also been hypothesized to function in Suc phloem unloading in sink tissues  
201 and in the retrieval of leaked Suc along the phloem transport route, as shown by studies  
202 in rice (*Oryza sativa*), wheat (*Triticum aestivum*), maize, and sugarcane (*Saccharum*  
203 *officinarum*). In rice, OsSUT1 has been localized to the SE and CC in the veins of the  
204 mature leaf, stems, pedicel, and base of the filling grain (Scofield et al., 2007). However,  
205 despite expression in the CC/SE complex in the leaf, no effect on photosynthesis or  
206 carbohydrate contents was observed in the leaves of rice lines with strong antisense

207 repression of the *OsSUT1* RNA (Ishimaru et al., 2001; Scofield et al., 2002). Further  
208 analysis of mutant plants homozygous for a null *OsSUT1* allele produced by a *Tos17*  
209 retrotransposon insertion confirmed the absence of a phenotype in the vegetative leaves  
210 (Eom et al., 2012). These findings were interpreted as support that *OsSUT1* does not play  
211 a major role in phloem loading in the mature rice leaf (Braun et al., 2014). By contrast,  
212 grain filling and germination were impaired in the RNA-suppression lines (Ishimaru et  
213 al., 2001; Scofield et al., 2002). Moreover, in an expression analysis of an *OsSUT1*  
214 promoter:: $\beta$ -glucuronidase (GUS) transgene, the XP cells and the cells at the border of  
215 the phloem/xylem interface showed slight, sporadic expression of the transgene in the  
216 minor veins in the mature leaf under normal physiological conditions, and increased  
217 expression after aphid feeding (Scofield et al., 2007; Ibraheem et al., 2014). Based on  
218 these studies, *OsSUT1* has been proposed to function in Suc retrieval along the transport  
219 phloem and from the xylem upon insect herbivory (e.g., aphid feeding) (Scofield et al.,  
220 2007; Eom et al., 2012; Braun et al., 2014; Ibraheem et al., 2014). Similarly, the  
221 expression of wheat *TaSUT1* RNA and the localization of its encoded protein in leaves  
222 were restricted to the CC and SE, respectively (Aoki et al., 2004). Intriguingly, sugarcane  
223 *ShSUT1* was not localized to the CC/SE complex in the leaf or stem, but instead to the  
224 XP and PP cells in lateral and intermediate veins of the leaf and in non-conducting cells  
225 in the stem, indicating that like *OsSUT1*, *ShSUT1* also does not function in phloem  
226 loading, but may function to retrieve Suc lost to the apoplasm (Rae et al., 2005). These  
227 data indicate that the roles of group 1 *Sut* genes remain to be resolved and that their  
228 functions may vary between the grasses (Braun and Slewinski, 2009; Braun et al., 2014;  
229 Bihmidine et al., 2015). Moreover, these results leave in doubt whether any group 1 *Sut*  
230 gene functions in phloem loading in grasses.

231

232 Based on homology with rice *OsSut1*, the first *Sut* gene cloned from maize was *ZmSut1*  
233 (Aoki et al., 1999). *ZmSut1* was found to show high expression levels and diurnal cycling  
234 of its transcript in mature leaves and to be expressed in various sink tissues. Based on this  
235 expression profile, *ZmSut1* was proposed to function in the phloem loading of Suc in  
236 mature leaves and potentially to perform the phloem unloading of Suc into organs such as  
237 the pedicel. Subsequent oocyte expression studies supported the ability of *ZmSUT1* to

238 move Suc across a membrane in a reversible manner based on the direction of the Suc  
239 gradient across the membrane, the pH gradient, and the membrane potential (Carpaneto et  
240 al., 2005; Geiger, 2011). From these studies, the authors proposed that ZmSUT1 could  
241 function to unload Suc from the phloem in sink tissues. Consistent with a role in phloem  
242 loading, phenotypic characterization of *zmsut1* null mutants revealed stunted plant  
243 growth, frequent failure to achieve reproductive maturity, chlorotic leaves that  
244 accumulated excess levels of starch and soluble sugars (e.g., Suc, Glc, and Fru), and  
245 impaired transport of radioactively labelled Suc out of the leaves (Slewinski et al., 2009;  
246 Rotsch et al., 2015). Another intriguing phenotype of *zmsut1* mutant plants was the  
247 secretion of droplets with high Suc concentrations from the hydathodes (Supp. Fig. S1)  
248 (Slewinski et al., 2010). Because no Suc was detectable in the wild-type guttation fluid,  
249 this finding indicated a high level of Suc was present in the apoplasm (which is  
250 contiguous with the xylem transpiration stream) of *zmsut1* mutants, and supported a role  
251 for *ZmSut1* in phloem loading. In addressing this potential role, one previous study  
252 evaluated *ZmSut1* expression in vein-enriched vs. non-vein tissues dissected from the  
253 coleoptile, the protective sheath enclosing the germinating shoot, and found higher  
254 expression in the vein-enriched tissue (Bauer et al., 2000). However, to our knowledge,  
255 no previous studies have examined the cellular and subcellular expression of *ZmSut1* and  
256 the ZmSUT1 protein, respectively, to evaluate this proposed role in the phloem loading  
257 of Suc in the leaf blade. Further, only limited studies have investigated the potential role  
258 of *ZmSut1* in non-photosynthetic tissues.

259

260 Although apoplasmic phloem loading in maize is physiologically and anatomically well  
261 established (Evert et al., 1978; Heyser et al., 1978; Slewinski et al., 2009; Slewinski et  
262 al., 2012), the exact role of *ZmSut1* in this process is not well defined. Specifically, does  
263 ZmSUT1 mediate Suc phloem loading? If so, several predictions based on the model for  
264 apoplasmic phloem loading are that *ZmSut1* will be expressed in the CC/SE complex of  
265 mature leaves and that ZmSUT1 will be localized to the plasma membrane. To  
266 investigate these predictions, we used RNA *in situ* hybridization to examine *ZmSut1*  
267 expression at the cellular level in mature leaf tissues. These results were extended to  
268 additional tissues within the plant by investigating the cellular expression pattern of the

269 native *ZmSut1* promoter driving a transcriptional reporter gene encoding the monomeric  
270 red fluorescent protein (RFP). Additionally, the subcellular localization of the ZmSUT1  
271 protein translationally tagged with the yellow fluorescent protein (YFP) was determined.  
272 Coupled with the previous phenotypic characterization of *zmsut1* mutants, these findings  
273 inform our understanding of the function of *ZmSut1* in the collection and transport  
274 phloems.

275

276 In contrast to our understanding of Suc phloem loading in mature leaves, the phloem  
277 unloading pathway in maize is less resolved and has been suggested to be apoplasmic in  
278 leaves (Evert and Russin, 1993) and symplasmic in roots (Giaquinta et al., 1983;  
279 Warmbrodt, 1985; Hukin et al., 2002; Ma et al., 2009). However, Haupt et al. (2001)  
280 determined that the phloem unloading pathway in developing leaves in the related grass  
281 barley (*Hordeum vulgare*) is symplasmic rather than apoplasmic, calling into question the  
282 conclusions based upon ultrastructural studies that both barley and maize sink leaves use  
283 apoplasmic phloem unloading (Evert and Russin, 1993; Evert et al., 1996b). To better  
284 resolve the pathway utilized for phloem unloading in maize immature leaves and roots,  
285 we analyzed transport and phloem unloading of the phloem-mobile tracer  
286 carboxyfluorescein (CF) in these tissues, and investigated whether *ZmSut1* has any role in  
287 Suc efflux as proposed by Carpaneto et al. (2005). Interestingly, our data reconcile the  
288 previously contradictory results and provide a framework to understand *ZmSut1* function  
289 in the transport and release phloems. Finally, our data also suggest an enhanced role of  
290 apoplasmic Suc retrieval in nonconducting vascular cells in leaves in the context of C<sub>4</sub>  
291 photosynthesis, providing insights as to how *Sut* gene expression could be tailored for  
292 engineering C<sub>4</sub> photosynthesis and carbon transport in C<sub>3</sub> plants such as rice.

293

## 294 RESULTS

### 295 ***ZmSut1* cellular expression is consistent with phloem loading but indicates** 296 **additional functions**

297 Previous analysis of *ZmSut1* expression in the mature third leaf blades from 2-week-old  
298 greenhouse-grown plants found the transcript levels peaked at the end of the d and  
299 decreased during the night to low levels, with expression increasing again the following

300 afternoon (Aoki et al., 1999). An evaluation of the expression pattern in immature leaf  
301 tissues was limited to examining the apical-to-basal expression pattern in expanding leaf  
302 blades, which showed a gradient of very high expression at the tip to very low expression  
303 at the base (Aoki et al., 1999). To evaluate whether *ZmSut1* expression in developing leaf  
304 tissue also followed a diurnal pattern as reported for mature juvenile leaves, we  
305 performed quantitative reverse-transcription polymerase chain reaction (qRT-PCR)  
306 experiments on both mature adult (leaf 11) and immature adult (leaf 17) leaves of 6-  
307 week-old field-grown B73 plants for a period of 48 hrs during the d/night cycle (Fig. 1).  
308 In contrast to previous results, *ZmSut1* transcript abundance showed no pattern of  
309 detectable fluctuation in mature leaves over the course of the 24-h cycle, and similarly  
310 showed no diurnal pattern in immature leaf tissues. Although *ZmSut1* mRNA transcript  
311 levels tended to be slightly higher in immature than mature adult leaves, the increased  
312 expression was not significant. These differences in *ZmSut1* leaf expression prompted us  
313 to further examine its expression.

314

315 Based on previous work, it was anticipated *ZmSut1* would be expressed in the phloem of  
316 mature leaf blades because of its postulated role in Suc loading. To determine the cellular  
317 expression pattern of *ZmSut1* in mature leaf blade tissue, we performed RNA *in situ*  
318 hybridization. As evidenced by the blue precipitate indicative of gene expression, *ZmSut1*  
319 expression was indeed observed in the CC in both the minor and lateral veins (Fig. 2C-  
320 H). By contrast, *ZmSut1* expression was absent from the enucleate SE. Interestingly,  
321 *ZmSut1* expression was also strongly detected in the BS, PP, and XP cells of both lateral  
322 and minor veins (Fig. 2C, D, F). In the minor veins, *ZmSut1* expression was consistently  
323 observed in the VP cells and CC. Signal was sporadically seen in the BS cells and often  
324 observed in only a subset of them around the vein (Fig. 2C, D). In minor veins, the VP  
325 cells near the xylem (i.e., XP cells) are typically larger relative to the phloem-associated  
326 VP cells. These large XP cells usually exhibited the strongest *ZmSut1* expression  
327 compared to the other VP cells and cell types. In lateral veins, *ZmSut1* was strongly  
328 expressed in the XP cells, particularly near the metaxylem elements and protoxylem  
329 lacunae, and in the CC and sporadically in the BS cells (Fig. 2F). As a negative control,  
330 we analyzed *ZmSut1* expression in *zmsut1* mutants, which result from a *Ds* transposable

331 element insertion into the 5' untranslated region of the gene that greatly reduces *ZmSut1*  
332 RNA abundance (Slewinski et al., 2010) (Fig. 2G). These experiments showed a greatly  
333 reduced signal in the same subset of cells as in the wild-type B73 leaf. We used qRT-  
334 PCR to determine whether residual expression could account for the reduced signal  
335 observed in the mutant plants (Supp. Fig. S2). However, expression in the *zmsut1* mutant  
336 was less than 6.5% that of the wild type, suggesting the majority of the signal had a  
337 different underlying cause. Some of this signal may be due to background staining, as  
338 control sections lacking the *ZmSut1* probe displayed blue staining in the epidermis and to  
339 a limited extent in the xylem and HS cells (Fig. 2E, H). Overall, these findings  
340 demonstrate that *ZmSut1* is expressed in the CC, where it likely functions to load Suc into  
341 the phloem, as well as broadly in all other cells enclosed within the vascular bundle, with  
342 the exception of the enucleate SE and the xylem vessels, which are dead at maturity.

343

344 From the RNA *in situ* hybridization data, *ZmSut1* expression in the CC unexpectedly  
345 appeared to comprise only a small portion of the total signal. To evaluate the relative  
346 abundance of *ZmSut1* RNA expression in the CC/SE compared to the remainder of cells  
347 within the vein and the BS cells, the percentage of blue signal in each cell type in each  
348 vein class was quantified with Image J (Table 1). Based on their position within the vein  
349 and their size, the cells were classified as CC/SE, VP (XP + PP), or BS cells. For these  
350 measurements, we focused our attention on the veins; any signal detected in the xylem  
351 elements, HS cells, and epidermis was excluded as non-specific. We note that these data  
352 are only a rough approximate of the signal abundance in each cell type and do not  
353 adequately account for differences in cell size, vacuole size, signal intensity, or  
354 representation of cell types in the sections. However, they do provide an estimate of the  
355 relative amount of signal within the CC/SE compared to other cell types. In the lateral  
356 veins, the *ZmSut1* expression in the CC/SE was ~14% of the blue signal, the VP cells  
357 accounted for nearly 81% of the signal, and the BS cells ~5% (Table 1). By contrast, in  
358 the minor veins, the BS cells contained ~27% of the blue signal, while the CC  
359 represented only ~15% of the signal, with the VP cells accounting for ~55-60%. The  
360 principal differences in the relative signal abundance between the lateral and minor vein  
361 classes appeared to be due to the increased percentage of signal contained in BS cells,

362 and the corresponding decreased abundance of signal within the VP cells. Overall, there  
363 was little difference in the contribution of *ZmSut1* signal between the CC of different vein  
364 classes, and the *ZmSut1* expression pattern was highly similar between the intermediate  
365 and smallest veins. There was approximately six-to-eleven-fold more *ZmSut1* signal in  
366 the VP and BS cells compared to the CC across all vein classes (Table 1). These data  
367 suggest that the majority of *ZmSut1* RNA is expressed in vascular-associated cells other  
368 than the CC in longitudinal veins.

369

### 370 **A transcriptional reporter gene faithfully reveals *ZmSut1* cellular expression** 371 **throughout the plant**

372 Because seven *Sut* genes are present in the maize genome (Braun et al., 2014), some of  
373 the faint blue signal detected in the *zmsut1* mutant (Fig. 2G) and wild-type (Fig. 2C, D, F)  
374 leaf tissue in the RNA *in situ* hybridization might be due to expression of a closely  
375 related *Sut* gene, such as *ZmSut7*. To specifically examine the expression of *ZmSut1*, we  
376 analyzed a transgenic transcriptional reporter line. Approximately 2 kb of promoter  
377 upstream from the translation start signal was cloned in front of a version of RFP targeted  
378 to the endoplasmic reticulum (pZmSut1::RFP<sub>ER</sub>), and stably transformed into maize. The  
379 expression of the pZmSut1::RFP<sub>ER</sub> reporter gene in the mature leaf blade (Fig. 3)  
380 mirrored the expression shown by RNA *in situ* hybridization (Fig. 2). In particular, RFP  
381 expression was strong in the CC, PP, and XP cells in the lateral and minor veins in both  
382 transverse and paradermal tissue sections (Fig. 3A, C, D, F, H). Additionally, RFP  
383 expression varied in intensity between BS cells within the same vein for each vein class.  
384 Non-transgenic control sibling plants had virtually no RFP signal (Fig. 3B, E, G, I).  
385 Identical results were observed in two additional independent transformation events of  
386 the pZmSut1::RFP<sub>ER</sub> reporter gene. These results indicated that the RFP signal was the  
387 same as the expression observed by RNA *in situ* hybridization, and hence, that the  
388 pZmSut1::RFP<sub>ER</sub> transcriptional reporter gene could be used to reliably monitor *ZmSut1*  
389 expression.

390

391 To determine which cells expressed *ZmSut1* in immature leaves, we used the  
392 pZmSut1::RFP<sub>ER</sub> transgene to examine expression within the longitudinal (proximal-

393 distal) axis of the leaf (Supp. Fig. S3 and Fig. 4). We selected a leaf undergoing the sink-  
394 to-source transition, with the tip emerging out of the whorl into the light, to be able to  
395 compare pZmSut1::RFP expression with the characterized anatomical, developmental,  
396 and physiological changes that occur during this transition (Evert et al., 1996a). In  
397 developing leaf blade tissue in which metaxylem and metaphloem had fully formed in the  
398 lateral veins, pZmSut1::RFP expression was evident throughout the leaf blade,  
399 including the BS, M, and epidermal cells, but was strongest in the CC, XP, and PP cells  
400 within all vein classes (Fig. 4C, D). In leaves of non-transgenic control plants,  
401 autofluorescent red signal was visible only from the HS cell walls (Fig. 4A, B), showing  
402 that under these microscope and camera settings, none of the observed red signal in the  
403 transgenic leaves was due to chlorophyll autofluorescence. In younger, more proximal  
404 developing leaf blade and sheath tissue, in which only protoxylem and protophloem were  
405 evident within the lateral veins, strong RFP signal was observed in the XP cells bounding  
406 the protoxylem elements and in the protophloem cells (Fig. 4E-H, M, N). However,  
407 expression was largely excluded from the developing procambium of developing leaves  
408 near the meristem, with punctate signal only visible in initiating lateral veins (Fig. 4I, J).  
409 Thus, in the youngest cells at the base of the leaf, pZmSut1::RFP expression was  
410 largely confined to initiating lateral veins, and expression expanded into non-vascular  
411 cells as leaf maturation progressed.

412

413 *ZmSut1* exhibits an increasing base-to-tip gradient of expression (Supp. Fig. S3) (Aoki et  
414 al., 1999; Li et al., 2010) that mirrors and is potentially linked to the sink-to-source  
415 transition within a leaf. However, it is possible the expression pattern instead reflects the  
416 leaf developmental (age) and/or the light-regulated genetic programs. To test whether  
417 light exposure influenced pZmSut1::RFP expression, we germinated seedlings in the  
418 dark. After 8 d, leaf 1 of the etiolated seedlings had emerged from the coleoptile, and a  
419 small tissue segment located on one side of the midrib was harvested for microscopic  
420 analysis. We observed a similar pattern of pZmSut1::RFP expression as in developing  
421 leaves within the whorl (cf. Fig. 5A, C with Fig. 4C, D). The etiolated plants were  
422 subsequently exposed to white fluorescent lights in the lab for 48 hrs to induce  
423 chlorophyll synthesis and transferred into the greenhouse with high light. After 5 d in the

424 greenhouse, the other half of leaf 1, which was dark green and fully mature, was analyzed  
425 (Fig. 5B, D). We observed strong expression of pZmSut1::RFPper within the CC, XP, and  
426 PP cells within the veins in the green tissue relative to the etiolated tissue, supporting an  
427 induction of pZmSut1::RFPper expression by light, age, and/or physiological maturity as  
428 source tissue.

429

430 To further dissect which of these factors might influence the pZmSut1::RFPper expression  
431 pattern, we backcrossed the pZmSut1::RFPper reporter gene into the *striate2* (*sr2*) mutant,  
432 which displays a variegation pattern of longitudinal white and green leaf stripes (Huang  
433 and Braun, 2010). If age or light influenced pZmSut1::RFPper expression, we reasoned  
434 expression would be comparable between neighboring green and white mature leaf  
435 tissues. Alternatively, if the sink-to-source transition influenced expression, we should  
436 see differences between the white (sink) and adjacent green (source) regions, since both  
437 regions experience similar light exposure. In *sr2* mutant plants carrying pZmSut1::RFPper,  
438 we observed strong up-regulation of pZmSut1::RFPper in the XP and PP in green tissue  
439 compared to white tissue, indicating pZmSut1::RFPper is upregulated in source tissues  
440 (Fig. 6A, C, E). Non-transgenic *sr2* mutant leaves at green-white borders showed no RFP  
441 signal (Fig. 6B, D, F). Additionally, under these microscope and camera settings, no  
442 chlorophyll autofluorescence was detected using the RFP filter cube (cf. Fig. 6D, F),  
443 indicating the red signal in Fig. 6C resulted from RFP. Note the apparent difference in  
444 RFP expression in the M cells between white and green tissues in pZmSut1::RFPper; *sr2*  
445 leaves (Fig. 6C) does not result from differences in gene expression, but appears to be  
446 due to the chloroplasts masking the underlying RFP signal in green tissue. Moreover, it is  
447 worth noting the strong upregulation of pZmSut1::RFPper expression in the veins in  
448 source tissues as compared to sink tissues decreased the relative apparent signal in the M  
449 cells. Hence, by controlling for leaf age and light exposure, we determined  
450 pZmSut1::RFPper expression was enhanced in PP and XP cells in source compared with  
451 sink leaf tissue.

452

453 In addition to developing leaves, Aoki et al. (1999) reported *ZmSut1* was expressed in  
454 stems (culms), developing tassels (flowers and rachis-branches), and ears (pedicels), but

455 not in roots. We thus examined pZmSut1::RFP<sub>er</sub> expression in these and other sink  
456 tissues to determine the cell-specific expression pattern. For immature stem internode  
457 tissue, we observed strong RFP expression in veins and expanding storage parenchyma  
458 cells (Fig. 7A, B). However, the signal was strongest in the XP cells surrounding the  
459 developing protoxylem and in the protophloem cells. In mature stem internodes, the  
460 signal was strongest in the mature veins, with weaker signal in the storage parenchyma  
461 cells (Fig. 7C). No signal was visible in non-transgenic controls (Fig. 7D). Closer  
462 inspection of mature stem veins with confocal microscopy showed strong  
463 pZmSut1::RFP<sub>er</sub> expression in the CC, XP, and PP cells (Fig. 7E-G). The red signal in  
464 the xylem elements and cells surrounding the vein was due to autofluorescence, as  
465 evidenced by a non-transgenic control section (Fig. 7H-J).

466

467 In the shoot apical meristem, the rib meristem displayed limited and variable expression  
468 of the transgene, while the central and peripheral zones had absent or only very minimal  
469 RFP signal (Fig. 8A). However, the stem immediately subtending the meristem exhibited  
470 the strongest expression of pZmSut1::RFP<sub>er</sub> detected in the plant, which is indicated by  
471 the saturated orange-yellow signal in Figure 8A. Examination of the developing tassels  
472 and ears showed RFP expression was absent from the inflorescence and axillary  
473 meristems but was present in the developing tassel rachis and developing cob (Fig. 8C-  
474 F). Transverse sections through the ear demonstrated expression in the developing veins  
475 leading to the ovules (Fig. 8G-L). In the maturing tassel, expression was strong in the  
476 veins (Fig. 8M), including the vein between the anther locules in the male flower (Fig.  
477 8N).

478

479 Using northern blot assays, Aoki et al. (1999) did not detect *ZmSut1* expression in roots.  
480 By contrast, we observed strong expression in both developing and mature roots (Fig.  
481 8O-V). In immature roots, pZmSut1::RFP<sub>er</sub> expression was initially present in the  
482 developing protophloem and protoxylem (Fig. 8O). As development proceeded, its  
483 expression was maintained in the phloem, but became reduced in maturing xylem  
484 elements undergoing programmed cell death (compare Fig. 8Q and S). In mature root  
485 tissue, the phloem showed the strongest expression, with weaker signal in other cell types

486 (Fig. 8U). We observed no RFP signal in any of these tissues in non-transgenic control  
487 plants.

488

#### 489 **pZmSut1::RFP** expression is not correlated with the phloem unloading zone

490 Biochemical studies demonstrated that ZmSUT1 was capable of mediating Suc import  
491 into cells, and with the appropriate Suc concentration gradient, pH gradient, and electrical  
492 potential across the plasma membrane, it could also export Suc from cells (Carpaneto et  
493 al., 2005). Therefore, it was postulated ZmSUT1 could function to efflux Suc from the  
494 phloem into sink tissues. The strong expression of the pZmSut1::RFP transgene in the  
495 phloem of roots (Fig. 8O-V) also suggested it might be involved in phloem unloading.  
496 However, previous physiological and anatomical studies indicated that Suc was unloaded  
497 symplasmically from the root phloem, suggesting ZmSUT1 might not be involved in  
498 phloem unloading (Giaquinta et al., 1983; Warmbrodt, 1985; Hukin et al., 2002; Ma et  
499 al., 2009). To assess whether potential apoplasmic unloading via ZmSUT1 overlaps with  
500 potential symplasmic unloading via plasmodesmata in the unloading zone, we compared  
501 pZmSut1::RFP expression with the symplasmic tracer CF. Carboxyfluorescein  
502 diacetate (CFDA) is a membrane-permeable non-fluorescent dye that is converted to the  
503 membrane-impermeable, fluorescent form (CF) inside cells to trace solute movement in  
504 the phloem (Grignon et al., 1989; Ma et al., 2009; Bihmidine et al., 2015). We fed CFDA  
505 to physiologically mature source leaves of developing pZmSut1::RFP transgenic plants,  
506 and examined the overlap between RFP and CF signals in root tips. CF was translocated  
507 through the phloem and symplasmically unloaded into the pith and cortex cells basal  
508 (toward the shoot) to the root differentiation zone (Fig. 9A, B, E, F). No CF signal was  
509 detected in the root cap, root meristem, or differentiation zone. pZmSut1::RFP was  
510 expressed strongly in the phloem and xylem and to a lesser extent in the surrounding  
511 cortical cells and pith (Fig. 9C, G). pZmSut1::RFP expression was observed both  
512 basally and apically (toward the root tip) relative to the root phloem unloading zone  
513 marked by CF movement into the cortical cells (Fig. 9D, H). Importantly, the region of  
514 CF symplasmic unloading from the phloem and pZmSUT1::RFP expression were  
515 independent, indicating pZmSut1::RFP expression overlapped with, but was not  
516 restricted to, the phloem unloading zone (Fig. 9D, H).

517

518 We similarly investigated CF phloem unloading within the developing sink leaves of  
519 pZmSut1::RFP plants. Interestingly, we observed different phloem unloading pathways  
520 being utilized in different portions of the same developing leaf (Fig. 10). In enclosed  
521 developing sink leaf tissues located approximately half way between the top and base of  
522 the fed leaf sheath, we consistently observed that CF was confined to the phloem,  
523 indicating that the phloem was symplasmically isolated from surrounding cells (Fig.  
524 10C). Of note, this region represents etiolated sink tissue completely enveloped within  
525 the whorl, and is less than one-third of the length it will reach before emerging from the  
526 whorl, indicating it must import carbon for cell expansion (Evert et al., 1996a). However,  
527 at approximately 25% of the distance above the sheath base, within the same developing  
528 sink leaf, we observed CF moving symplasmically out of the phloem into adjacent cells  
529 (Fig. 10D). These data indicate that maize sink leaves undergo a transition from using  
530 symplasmic phloem unloading to apoplastic phloem unloading substantially prior to the  
531 sink-to-source transition when leaves emerge from the whorl. pZmSut1::RFP was  
532 expressed strongly in the veins and surrounding cells in both regions (Fig. 10E, F).  
533 Collectively, these results suggest that pZmSut1::RFP expression within sink tissue is  
534 not correlated with the Suc phloem unloading mechanism in root tips, and is also  
535 independent of both symplasmic and apoplastic Suc phloem unloading in developing  
536 sink leaves.

537

### 538 **ZmSUT1 localizes to the plasma membrane**

539 A prediction for ZmSUT1 functioning to transport Suc into cells from the apoplast is its  
540 localization to the plasma membrane. To test this hypothesis, we constructed a  
541 translational fusion protein of YFP attached to the C-terminus of ZmSUT1 under control  
542 of the endogenous genomic regulatory sequences, including the native promoter, all  
543 exons and introns, and both the 5' and 3' untranslated regions (referred to as gSUT1-  
544 YFP). To assess if the fusion protein was functional, we examined if the transgene  
545 complemented the *zmsut1* mutant phenotype. To this end, we twice backcrossed plants  
546 carrying gSUT1-YFP to heterozygous *Sut1/sut1* plants to generate families segregating  
547 for wild-type and *sut1* mutant plants and the presence or absence of the transgene. All

548 plants were genotyped for *ZmSut1* and the transgene. As previously reported,  
549 homozygous *zmsut1* mutant plants were stunted and did not complete their lifecycle in  
550 comparison to wild-type plants (Fig. 11) (Slewinski et al., 2009; Slewinski et al., 2010).  
551 In contrast, *zmsut1* mutant plants carrying the gSUT1-YFP transgene flowered, set seed,  
552 and completed their lifecycle, indicating the transgene was able to restore *ZmSut1*  
553 function (Fig. 11; Supp. Table S1). However, the *zmsut1* mutant plants carrying one copy  
554 of the transgene attained only ~75% of the height of their wild-type sibling plants,  
555 suggesting the transgene largely, but incompletely, complemented the *zmsut1* mutant  
556 phenotype. No difference in plant growth or flowering was observed in wild-type plants  
557 with or without the gSUT1-YFP transgene. Virtually identical results were observed in  
558 two additional independent transformation events of the gSUT1-YFP translational fusion  
559 (Supp. Table S1). We conclude that the YFP fusion to the C-terminus of ZmSUT1  
560 maintained its biochemical function, albeit partially, and that the gSUT1-YFP transgene  
561 was expressed in the correct cells and at the correct time to provide ZmSUT1 function.

562

563 To investigate whether the gSUT1-YFP translational fusion reporter gene exhibited the  
564 same expression pattern as the endogenous *ZmSut1* RNA, we crossed plants harboring  
565 this construct to plants carrying the pZmSut1::RFPper transcriptional reporter gene, which  
566 recapitulated the *ZmSut1* expression detected by RNA *in situ* hybridization studies, to  
567 generate doubly labeled plants. As seen in the minor vein of a mature leaf blade, the  
568 gSUT1-YFP construct showed the same cellular expression pattern as the  
569 pZmSut1::RFPper transgene (Supp. Fig. S4). Non-transgenic control plants displayed no  
570 YFP signal in the veins, with only weak autofluorescence detected in the M cells (Supp.  
571 Fig. S4D). Examining expression in a lateral vein of a mature leaf of a gSUT1-YFP  
572 transgenic plant, we observed YFP expression in the CC, PP, XP, and BS cells, but not in  
573 the SE (Fig. 12A-C), a pattern identical to that of the RNA *in situ* hybridization (Fig. 2)  
574 and transcriptional reporter (Fig. 3). Collectively, these data indicate that the gSUT1-YFP  
575 construct largely complemented the *zmsut1* mutation and was expressed similarly to the  
576 endogenous gene; therefore, we used it for protein localization studies.

577

578 Examination of the BS cells in a paradermal section of the mature leaf blade of a gSUT1-  
579 YFP transgenic plant revealed ZmSUT1 was present at the cell periphery, adjacent to the  
580 cell wall, and therefore likely localized to the plasma membrane (Fig. 13A-C). To  
581 evaluate this possibility, we performed co-localization studies with a known plasma  
582 membrane-localized protein, the aquaporin PIP2-1 (Zelazny et al., 2007; Mohanty et al.,  
583 2009) translationally fused to the cyan fluorescent protein (PIP2-1-CFP). Co-expression  
584 of both transgenes in doubly labelled plants confirmed gSUT1-YFP localized to the  
585 plasma membrane (Fig. 13D-F). Like PIP2-1-CFP, gSUT1-YFP localization was seen  
586 throughout the plasma membrane. However, occasional punctate localization of both  
587 gSUT1-YFP and PIP2-1-CFP in the plasma membrane was observed, which we suggest  
588 to be PD. To provide further support for this localization pattern, leaves were  
589 plasmolysed by using a concentrated NaCl solution. Prior to plasmolysis, the YFP signal  
590 was localized at the cell periphery (Fig. 13G). After plasmolysis, multiple YFP-labeled  
591 Hechtian strands were observed connecting the plasmolyzed plasma membrane to the cell  
592 wall (Fig. 13H) (Lang-Pauluzzi, 2000). Non-transgenic control plants showed only weak  
593 background autofluorescence (Fig. 13I). Because the plasma membrane is anchored at the  
594 PD, the plasmolysis results provided additional evidence for the plasma-membrane  
595 localization of the ZmSUT1-YFP protein.

596

## 597 **DISCUSSION**

598 Previous research suggested *ZmSut1* plays a role in phloem loading and potentially in  
599 phloem unloading. However, since the orthologous sugarcane and rice *Sut1* genes have  
600 no apparent function in phloem loading, the cell-type-specific expression and possible  
601 functions of the maize *Sut1* gene were uncertain. To address its role in both source and  
602 sink tissues, we used a combination of approaches to investigate the cellular expression  
603 of the *ZmSut1* transcript and protein. We determined that *ZmSut1* was expressed in all  
604 vein classes and phloem domains (e.g., collection phloem) throughout the plant.  
605 Additionally, these experiments yielded several unexpected results, including 1) a lack of  
606 diurnal cycling of the transcript in adult leaves, 2) the majority of *ZmSut1* expression in  
607 the source leaf occurring in cells other than the phloem-loading CC, and 3)  
608 pZmSut1::RFP expression in the sink tissue overlapping with but independent of the

609 sites and mechanisms of phloem unloading. These and other data provide a deeper  
610 understanding of the biological functions of *Sut1* in maize, resolve previously conflicting  
611 data on the path of Suc unloading in developing grass leaves, provide insights into the  
612 evolution of *Sut1* expression and function within grasses, and suggest *Sut1* function was  
613 enhanced in the context of the higher Suc export resulting from C<sub>4</sub> photosynthesis.

614

615 In characterizing *ZmSut1* diurnal expression, Aoki et al. (1999) found that *ZmSut1*  
616 showed rhythmic expression in juvenile leaf blades, with transcript levels peaking at the  
617 end of the d and decreasing during the night. In contrast, we observed no diurnal cycling  
618 of *ZmSut1* expression in adult source and sink leaves. There are several possible reasons  
619 for this discrepancy. First, Aoki et al. (1999) characterized *ZmSut1* expression in 2-week-  
620 old juvenile leaf 3 blade tissues, whereas we investigated expression in 6-week-old adult  
621 leaf 11 and immature leaf 17 tissues. Second, Aoki et al. (1999) characterized  
622 greenhouse-grown plants while we utilized field-grown materials. Third, we investigated  
623 the B73 genotype and Aoki et al. (1999) used a sweet corn variety. Hence, differences in  
624 the age of the plants, the growth conditions, and/or the genotypes may contribute to the  
625 different results we observed. While likely highly dependent on experimental conditions,  
626 our results demonstrate that *ZmSut1* transcript is not regulated diurnally in adult leaves.

627

628 Aoki et al. (1999) also previously determined that feeding Suc through the xylem induced  
629 *ZmSut1* expression. Additionally, previous expression analyses and the present one found  
630 that *ZmSut1* RNA accumulation mirrors the sink-to-source transition in an emerging leaf.  
631 Consistent with these data, pZmSut1::RFP expression was induced in the CC, PP and  
632 XP cells upon leaf maturation in the light and its transition to source tissue. Yet, it was  
633 possible that the increased pZmSut1::RFP expression resulted from leaf age or light-  
634 regulated gene expression. However, from experiments analyzing pZmSut1::RFP  
635 expression in variegated *sr2* leaves, we conclusively determined pZmSut1::RFP  
636 expression was not dependent on leaf age or exposure to light but correlates with source  
637 tissue. Collectively, the data suggest that pZmSut1::RFP expression is enhanced upon  
638 maturation of the collection phloem and the transition to phloem loading.

639

640 **Function of ZmSUT1 in the collection phloem**

641 Based on the expression of *ZmSut1* in the CC of source leaf veins, we propose it  
642 functions within this cell type to load Suc into the collection phloem. This conclusion is  
643 based on the results of RNA *in situ* hybridization experiments and on the expression data  
644 for both *ZmSut1* transgenes. We also determined ZmSUT1 is localized to the plasma  
645 membrane, consistent with its proposed role in apoplasmic phloem loading. We did not  
646 detect the expression of *ZmSut1* RNA or the fusion protein in the SE. Although this result  
647 is unsurprising given the lack of a nucleus in this cell type, it could have been possible to  
648 detect gSUT1-YFP protein that had been transcribed and translated in the CC and then  
649 trafficked through PD into the SE, since both wheat TaSUT1 and rice OsSUT1 proteins  
650 have been localized to the SE (Aoki et al., 2004; Scofield et al., 2007). Collectively, the  
651 localization results suggest the CC and not the SE are the site of Suc uptake into the  
652 collection phloem in maize. Once in the CC cytoplasm, Suc would enter into the sieve  
653 tube through the PD for long-distance transport. However, it is conceivable the YFP tag  
654 on the C-terminus of the ZmSUT1 protein limited protein trafficking from the CC to the  
655 SE, as previously suggested for a green fluorescent protein (GFP) fusion of LeSUT1 in  
656 tomato (*Solanum lycopersicon*) (Lalonde et al., 2003). However, subsequent  
657 immunolocalization experiments indicated LeSUT1 is present in the CC, not the SE  
658 (Schmitt et al., 2008). That the transgenic complementation we observed was incomplete  
659 may be due to the YFP fusion partially obstructing the ZmSUT1 biochemical function;  
660 nevertheless, the YFP fusion must not have compromised the biochemical activity of the  
661 protein too severely to provide the level of complementation achieved. Further, it could  
662 be argued that the constraint of the ZmSUT1-YFP fusion within the CC instead of the SE  
663 could explain that only a partial complementation of the *zmsut1* mutant was observed.  
664 Interestingly, fusion of GFP to the C-terminus of AtSUC2, which functions in the CC and  
665 therefore does not require trafficking into the SE, expressed under the control of the  
666 AtSUC2 promoter was also reduced in its effectiveness of complementing the *atsuc2*  
667 mutation (Srivastava et al., 2008). Future experiments to immunolocalize the native  
668 ZmSUT1 protein will be necessary to resolve whether it is present in the SE.

669

670 **Function of ZmSUT1 in non-conducting cells within source tissue**

671 An intriguing and surprising finding was that *ZmSut1* is strongly expressed in non-  
672 conducting leaf cells (e.g., PP, XP, and BS cells). Indeed, CC expression represented only  
673 ~15% of the RNA *in situ* hybridization signal detected within leaf veins. These data  
674 suggest this gene likely plays additional roles beyond the canonical one of Suc phloem  
675 loading in the leaf blade. A previous study on tobacco (*Nicotiana tabacum*) found the  
676 group 2 *NtSUT1* gene was expressed not only in the CC but also in the XP cells of Class I  
677 (midrib) through Class IV leaf veins (Schmitt et al., 2008). No expression outside of the  
678 CC was found in the Class V veins, the smallest vein class within the leaf. The authors  
679 speculated that one potential function for *NtSUT1* expression in the XP cells was to  
680 retrieve Suc from the xylem. A similar observation of XP cell expression has been made  
681 for group 1 *Suts* in both rice and sugarcane (Rae et al., 2005; Scofield et al., 2007;  
682 Ibraheem et al., 2014). As described in the Introduction, from functional and expression  
683 studies, rice *OsSUT1* is suggested to function in Suc retrieval into the phloem along the  
684 transport path from the leaf blade to the pedicel subtending the grain. Additionally,  
685 *OsSut1* expression in XP cells can be induced by aphid feeding, a condition that  
686 potentially increases Suc leakage from damaged cells and necessitates Suc retrieval. In  
687 sugarcane, *ShSUT1* was expressed in non-phloem cells, where it is proposed to function  
688 to prevent Suc loss to the apoplasm (Rae et al., 2005). Hence, these data suggest *OsSUT1*  
689 and *ShSUT1* function in non-conducting cells to retrieve Suc from the apoplasm, similar  
690 to the proposed role for *ZmSUT1* in cells other than CC.

691

692 Based on the previous and current results, we propose a model for *ZmSut1* function in the  
693 leaf blade. This model takes into account the molecular expression, physiological, and  
694 genetic data for *ZmSut1* as well as the previous anatomical and radiolabeling work in  
695 studies addressing routes of water and Suc movement in the maize plant. Figure 14 shows  
696 the schematic of a minor vein in the mature leaf blade. The model proposes that Suc is  
697 effluxed from the PP cells by SWEET transporters in the vicinity of the CC/SE complex.  
698 *ZmSUT1* functions on the CC plasma membrane to transport Suc into the CC cytoplasm,  
699 where it moves through PD into the SE for long-distance transport through the sieve tube  
700 to distal sink tissues. Importantly, *ZmSUT1* also functions to retrieve Suc into non-  
701 conducting cells (XP, PP, and BS cells) from the vein apoplasm (both phloem and xylem)

702 to recover any Suc not effectively loaded into the CC. ZmSUT1 expression in M cells  
703 would similarly function to recover Suc from the leaf apoplasm. Additional evidence in  
704 support of the model is enumerated below.

705

706 First, Slewinski et al. (2009, 2010) showed that *zmsut1* mutants had impaired uptake of  
707 radiolabeled Suc into the phloem of the leaf blade and that the leaf apoplasm had excess  
708 Suc (i.e., Suc droplets), supporting the previous hypothesis of Aoki et al. (1999) that  
709 ZmSUT1 functions in the phloem loading of Suc. The present RNA *in situ* hybridization,  
710 promoter: reporter gene expression analyses, and full gene translational fusion results  
711 showing the expression of *ZmSut1* in the CC provide further support for its role in this  
712 process within the collection phloem. To date, maize remains the only grass for which a  
713 group 1 *Sut* gene has been shown via expression, biochemical, physiological, and genetic  
714 analyses to directly function in Suc phloem loading.

715

716 Second, *ZmSut1* functions in the recovery of Suc from the xylem. When Fritz et al.  
717 (1983) exposed maize leaves to  $^{14}\text{CO}_2$ , the presence of radiolabel was consistently  
718 observed in the xylem elements of the small veins, suggesting leakage of photosynthate  
719 into the xylem transpiration stream. Additional studies feeding  $^{14}\text{C}$ -Suc through the  
720 xylem showed that the XP cells were the cells that took up Suc from the xylem (Fritz et  
721 al., 1983). Further, a sharp rise in the pH has been observed in the xylem exudate when  
722 Suc was fed through the xylem of a detached leaf, indicating the active uptake of Suc  
723 from it (Heyser et al., 1978). Both the Suc droplets in the *zmsut1* mutants and the strong  
724 expression of *ZmSut1* in the XP cells adjacent to the xylem elements in all of the vein  
725 classes suggest that *ZmSut1* is the gene largely responsible for this active uptake of Suc  
726 from the xylem.

727

728 Third, ZmSUT1 is proposed to also function in the PP, XP, and BS cells to retrieve Suc  
729 not loaded into CC from being eventually lost to the transpiration stream. These other cell  
730 types within the vein have abundant PD in their shared cell walls and are therefore  
731 symplasmically connected (Evert et al., 1977, 1978). Additionally, the radial and  
732 tangential cell walls of the BS cells are suberized, which has been proposed to function to

733 confine Suc within the vein apoplasm (Evert et al., 1977). Hence, ZmSUT1 expression in  
734 the PP, XP, and BS cells enables Suc recovery back to the symplasm and thereby  
735 provides another opportunity for the plant to efflux the Suc from the PP and load it into  
736 the sieve tube for long-distance transport. An intriguing possibility for future study is that  
737 the efficiency of Suc transport into the CC vs. Suc uptake from the apoplasm into non-  
738 conducting cells could serve as a Suc flux measurement that feeds back to regulate  
739 phloem loading.

740

741 One argument against *ZmSut1* functioning in Suc retrieval from the apoplasm in cells  
742 other than the CC/SE complexes is that the Suc droplets observed in *zmsut1* mutant  
743 leaves solely reflect the failure to perform phloem loading—that is, in wild-type plants,  
744 Suc leakage would not occur because ZmSUT1 would load all apoplasmically located  
745 Suc into the CC. Hence, any expression of ZmSUT1 in the non-vascular cells would  
746 represent a non-functional role. In addition to the strong expression of *ZmSut1* in non-  
747 conducting leaf cells, further evidence for ZmSUT1 functioning in Suc retrieval is that  
748 we have not observed Suc droplets in other maize mutants with an excessive  
749 accumulation of starch and sugars in the leaves, such as *Suc export defective1*,  
750 *psychedelic*, and the *tie-dyed1* and *2* mutants (Baker and Braun, 2007; Baker and Braun,  
751 2008; Ma et al., 2008; Slewinski and Braun, 2010b). In the *tie-dyed* mutants, the  
752 blockage in Suc movement appears to occur between the CC and SE, as evidenced by the  
753 CC in the mutants containing a high abundance of oil droplets relative to those in wild-  
754 type siblings (Baker et al., 2013). Hence, the process of phloem loading does not appear  
755 to be defective, but instead dramatically reduced in the *tie-dyed* mutants. If a  
756 consequence of a reduction in phloem loading is the excretion of Suc droplets, we might  
757 anticipate observing them in these other mutants.

758

759 If this model of Suc retrieval in the mature leaf blade is accurate, why might the plant  
760 maintain such tight control over apoplasmic levels of Suc? In previous studies of rice  
761 lines susceptible to pathogenic attack from *Xanthomonas oryzae* pv. *Oryzae*, it was found  
762 that bacterial transcription activator-like (TAL) effectors upregulated *OsSWEET11* or  
763 *OsSWEET14* in the leaf vascular tissues (Antony et al., 2010; Chen et al., 2010). This

764 upregulation has been proposed to lead to increased Suc release into the apoplasm and  
765 thereby facilitate bacterial growth. In resistant lines, these gene promoters are no longer  
766 recognized by the TAL effectors (Chu et al., 2006). Thus, one possibility is that the plant  
767 maintains apoplasmic Suc concentrations below a certain level as a defense mechanism  
768 against pathogenic invasion. Interestingly, the Suc droplets in *zmsut1* mutants also  
769 provide evidence that the release of Suc from the PP cells is not feedback regulated  
770 (Baker et al., 2012). Hence, if SWEETs are responsible for Suc release into the phloem  
771 apoplasm in maize, as proposed for Arabidopsis, ZmSUT1 is presumably a predominant  
772 part of the mechanism for controlling Suc apoplasmic levels. Relatedly, ZmSUT1  
773 function to load Suc into the collection phloem maintains low apoplasmic Suc levels,  
774 which provides a mechanism for homeostatic maintenance of water flow and turgor  
775 pressure within the leaf.

776

#### 777 **Functions of ZmSUT1 within sink tissues**

778 pZmSut1::RFP<sub>er</sub> was expressed in all examined sink tissues throughout the plant,  
779 including developing leaves, stems, roots, shoot apical meristems, and developing ears,  
780 tassels, and anthers. Expression was invariantly seen in the CC and surrounding non-  
781 conducting cells, with high expression levels often observed in the XP cells. With respect  
782 to *ZmSut1* function in the transport phloem, we suggest ZmSUT1 retrieves Suc passively  
783 leaked from the sieve tube during translocation to maintain the high osmotic potential and  
784 hydrostatic pressure gradient in the phloem. This function is analogous to the dual roles  
785 proposed for *ZmSut1* function in loading and retrieval in the source tissue. This proposed  
786 role has been previously suggested for OsSUT1 and ShSUT1 in the lateral veins of the  
787 mature leaf and in the veins of the transport phloem of various tissues (Rae et al., 2005;  
788 Scofield et al., 2007). This function would presumably be the primary one for ZmSUT1  
789 throughout the transport phloem of the plant. In the stem storage parenchyma cells,  
790 ZmSUT1 may function to uptake Suc from the apoplasm during expansive growth, and to  
791 retrieve Suc leaked from cells during accumulation and to maintain turgor. A similar  
792 function has been proposed during sugar accumulation in sugarcane and sweet sorghum  
793 (*Sorghum bicolor*) stems (Bihmidine et al., 2013; Patrick et al., 2013; Bihmidine et al.,  
794 2015).

795

796 pZmSut1::RFP<sub>er</sub> was also expressed in the region of the release phloem, which was  
797 marked by symplasmic CF unloading into the developing leaves and roots. In these  
798 unloading regions, a portion of the solutes are released from the phloem, but others are  
799 transported more distally through it and unloaded apoplasmically, as seen in developing  
800 leaves. Hence, the transport and release phloems overlap in these regions. Symplasmic  
801 phloem unloading has been suggested to be regulated largely by the rate at which Suc  
802 moves through the PD into post-phloem sink cells (Patrick, 2012). Suc that is not  
803 symplasmically unloaded through PD would continue along the translocation path toward  
804 the phloem terminus. We interpret these data to suggest that *ZmSut1*, although expressed  
805 in the release phloem, does not directly function to efflux Suc from the phloem as  
806 previously postulated. Our findings are consistent with the suggestion that SUT-mediated  
807 Suc efflux to the apoplasm is unlikely due to thermodynamic considerations (Zhang et  
808 al., 2007a). Additionally, these results support the previous data showing symplasmic  
809 phloem unloading in maize roots (Giaquinta et al., 1983; Warmbrodt, 1985; Hukin et al.,  
810 2002; Ma et al., 2009).

811

812 In the developing ears and tassels, pZmSut1::RFP<sub>er</sub> expression was most strongly  
813 observed in the developing veins and was largely absent in the meristematic tissue, while  
814 virtually no expression was observed in the shoot apical meristem. To our knowledge,  
815 although Suc movement at the pedicel and nucellus has been assessed at the pre- and  
816 post-pollination stages in maize (Porter et al., 1985; Makela et al., 2005; Bihmidine et al.,  
817 2013; Tang and Boyer, 2013), the process of Suc unloading in the grass inflorescence at  
818 earlier developmental stages remains to be evaluated. Based on the function of group 1  
819 *Sut* genes in the transport phloem of various grasses, we speculate that if Suc is unloaded  
820 symplasmically into the developing inflorescence tissues, the expression of  
821 pZmSut1::RFP<sub>er</sub> in the veins reflects its function in retrieving Suc leaked into the  
822 apoplasm. However, if Suc is unloaded into the apoplasm (e.g., by SWEET proteins) for  
823 subsequent uptake by these sink tissues (either as Suc directly, or as hexoses after  
824 cleavage by cell wall invertase), an intriguing idea is that the ZmSUT1 retrieval of Suc  
825 back into the phloem competes with the sink cell for Suc (Hafke et al., 2005). Thus, Suc

826 recovery in the phloem might act as a feedback mechanism to signal insufficient sink  
827 capacity and excess Suc production to the photosynthetic cells through virtue of a  
828 decrease in bulk flow. This mechanism is consistent with the expression reported for  
829 grass *Sut1* genes in sink tissues and could be a conserved aspect of its function in these  
830 tissues. Future studies will need to be performed to address these various possibilities.

831

### 832 **Developing maize leaves dynamically switch from symplasmic to apoplasmic phloem** 833 **unloading**

834 Based on anatomical, dye-tracer, and viral movement studies, Haupt et al. (2001)  
835 concluded that Suc unloading in the developing barley leaf occurs symplasmically.  
836 However, both barley and maize leaves were proposed to use apoplasmic phloem  
837 unloading based on ultrastructural studies, which found that the CC/SE complexes in  
838 these developing leaves were symplasmically isolated from surrounding cells (Evert and  
839 Russin, 1993; Evert et al., 1996b). Our data examining CF unloading into developing  
840 maize leaves likely explain the previous discrepancy and reconcile these contradictory  
841 reports. We discovered that maize leaves dynamically switch from using symplasmic  
842 phloem unloading near the base of the leaf (younger tissue) to apoplasmic phloem  
843 unloading in the older regions. Such a dynamic switch in phloem unloading mechanism  
844 has been reported previously in many plants and tissues (see Braun et al. (2014) for a  
845 review). Hence, we suggest that the barley and maize developing leaves examined by  
846 Evert's group for ultrastructural studies were more mature regions employing apoplasmic  
847 unloading, while the data of Haupt et al. (2001) reflect symplasmic phloem unloading  
848 occurring in younger tissues. This dynamic switch in the phloem unloading mechanism in  
849 developing leaves is likely a common feature of grass leaves. More research is necessary  
850 to understand the changes during leaf development in PD frequency or conductivity, such  
851 as occlusion by callose, that may regulate the symplasmic vs. apoplasmic phloem  
852 unloading process.

853

### 854 **Evolution of group 1 *Suts* in the grasses**

855 Based on the foundational work in rice, expression studies in other grasses, and the  
856 present findings, we propose a model for the evolution of group 1 *Sut* genes in the

857 vegetative portions of the plant and suggest the increased importance of *Sut1* function in  
858 the evolution of C<sub>4</sub> photosynthesis.

859

860 It is currently hypothesized that the monocot leaf blade evolved from the petiole or the  
861 lower leaf zone (leaf base and stipule) of eudicots, with the original leaf lamina present  
862 only residually in the tips of the first few seedling leaves (see Slewinski (2013) and  
863 references therein). As the petiole flattened, corresponding veins rearranged from a netted  
864 to a linear pattern. Within this evolutionary context, the veins formerly contributing to  
865 long-distance transport (i.e., transport phloem), now located in the leaf blade, would now  
866 function to acquire photosynthate from the photosynthetic cells (i.e., become collection  
867 phloem) (Slewinski et al., 2013). A shared trait of group 1 *Sut* genes is their expression in  
868 the transport phloem, suggesting that the default role of these genes was to retrieve Suc  
869 leaked from the sieve tube along the transport path and potentially in developing tissues.  
870 The group 1 *Sut* genes might have replaced the function of other *Sut* genes that may have  
871 originally contributed to phloem loading in the former leaf blade (Slewinski et al., 2013).  
872 Similarly, the observed expression in the XP cells of transport phloem and sink tissues in  
873 the grasses suggests group 1 *Sut* genes could have been co-opted to function for Suc  
874 retrieval, particularly in response to breaches in the xylem/phloem barrier. One prediction  
875 is that the expression of the group 1 *Sut* genes might have been upregulated to  
876 accommodate this increased demand. In this context, it is interesting that we see  
877 induction of pZmSut1::RFP expression in the leaf veins upon maturation as source  
878 tissue.

879

880 A key consideration in the present study is that Suc leakage from sieve tubes during long-  
881 distance transport is a constant challenge to the plant. In previous studies, C<sub>4</sub> grasses  
882 (e.g., maize and sorghum) have been shown to have a substantially higher rate of export  
883 of photosynthates than C<sub>3</sub> grasses (e.g., wheat and barley) (Grodzinski et al., 1998).  
884 Consistent with this idea, Suc content in maize phloem sap is substantially higher than  
885 that measured for wheat or rice (Fukumorita and Chino, 1982; Hayashi and Chino, 1986;  
886 Ohshima et al., 1990; Weiner et al., 1991). This substantial increase in the translocation  
887 of photosynthate would presumably lead to the increased loss of Suc from the phloem in

888 photosynthetic tissues, and would also have demanded a greater reliance on Suc retrieval  
889 systems within transport phloem and developing tissues, as the Suc flux increased.  
890 Hence, during the shift to C<sub>4</sub> photosynthesis, the group 1 *Sut* genes might have acquired a  
891 more imperative role in C<sub>4</sub> plants as compared to C<sub>3</sub> plants. The strong expression of  
892 *ZmSut1* and *ShSut1* in non-conducting vascular cells, coupled with the expression of  
893 *TaSut1* only in CC/SE, supports this possibility.

894

895 Within the framework of this model, it will be of interest to determine whether variants of  
896 sugarcane will express a ShSUT1 homolog in the CC, and whether *shsut1* mutants will  
897 also condition a Suc-droplet phenotype. In rice, the absence of an effect on Suc flux in  
898 the mature leaf blade of *ossut1* mutants might partly reflect lower photosynthate  
899 production in C<sub>3</sub> compared to C<sub>4</sub> grasses. A limitation of this model is that the *Sut1* genes  
900 have been studied in only a few grasses. Moreover, only two C<sub>4</sub> grasses are represented  
901 in studies of *Sut1* expression and function, and both are of the NADP-malic enzyme type.  
902 More studies will need to be performed to address the validity of this hypothesis.

903

#### 904 **Modulating Suc retrieval activity in engineering C<sub>3</sub> grasses for C<sub>4</sub> photosynthesis**

905 The rapidity and frequency of C<sub>4</sub> evolution within the grasses suggest that this group of  
906 plants might be pre-adapted for evolving C<sub>4</sub> metabolism (Slewinski, 2013). The  
907 expression of group 1 *Sut1* genes within the non-conducting cell types of the leaf blade  
908 might represent one such preadaptation for accommodating increased flux from the  
909 photosynthetic cells accompanying the higher rates of assimilate export in C<sub>4</sub> plants. Our  
910 present results suggest the role of Suc retrieval in the leaf blade is enhanced in maize,  
911 potentially as a product of C<sub>4</sub> photosynthesis, resulting in higher levels of Suc production.  
912 If so, increased capacity of Suc retrieval may be required for successfully engineering C<sub>3</sub>  
913 grasses to perform C<sub>4</sub> photosynthesis. If the existing regulatory program for addressing  
914 cell damage and Suc leakage in C<sub>3</sub> plants is sufficient for an appropriate response to the  
915 increased assimilate flux, the modulation of *Sut1* activity might not be necessary for  
916 tailoring C<sub>4</sub> photosynthesis. However, the issue of increased Suc flux will need to be  
917 considered if insufficient carbon export occurs or photosynthesis is impaired. If so,

918 further adjustment of *Sut1* regulation might facilitate an improved export rate in C<sub>4</sub>-  
919 engineered plants.

920

## 921 **MATERIALS AND METHODS**

### 922 *Tissue collection, RNA extraction, and cDNA synthesis*

923 Maize (*Zea mays* L.) plants were grown in the field at the University of Missouri South  
924 Farm Agricultural Experiment Station. The inbred line B73 was used for the time course  
925 experiment. At the v11 stage, approximately 6 weeks after planting, the fully mature leaf  
926 11 and the immature leaf 17, which was etiolated and ensconced within the whorl, of 10  
927 individual plants were harvested at 4 h intervals over the course of 48 hrs beginning at  
928 04:30 am on d 1. Collected tissue was immediately placed in liquid nitrogen and stored at  
929 -80°C until processing. 100 mg of frozen leaf tissue was finely ground in a mortar and  
930 pestle, total RNA was extracted with Trizol, 50 pg luciferase RNA (Promega, Madison,  
931 WI) was added as the reference gene to 1 µg of total RNA, and cDNA was synthesized as  
932 described (Bihmidine et al., 2015).

### 933 *qRT-PCR*

934 *ZmSut1* gene-specific primers were designed and validated according to Bihmidine et al.  
935 (2015). Primer sequences and annealing temperatures are listed in Supp. Table S2. For  
936 the time course expression analysis, reactions were run in 384-well plates on a CFX384  
937 Real Time System (Bio-Rad, Hercules, CA). The d prior to running the qRT-PCR  
938 experiment, 4 µL containing 10 ng of cDNA was added to each well of the 384-well plate  
939 and then centrifuged. Nuclease-free water was added to a well in place of cDNA as a no  
940 template control. The plates were placed in a 30°C incubator overnight to evaporate the  
941 water. The following d 5 µL of a reaction mix containing 2.5 µL SsoFast EvaGreen  
942 Supermix with low ROX (Bio-Rad, Hercules, CA) and 0.5 µM of both the forward and  
943 reverse primers was added. The qRT-PCR experiment was run with the following  
944 conditions: 95°C for 30s, with 40 cycles of 95°C for 5s and the appropriate annealing  
945 temperature for each primer set for 30s. After 40 cycles, a melt curve analysis was  
946 performed to check that a single PCR product was amplified.

947 To quantify *ZmSut1* expression in *zmsut1-m4* mutants compared to wild type, a  
948 segregating family was planted in the greenhouse illuminated with supplemental lighting

949 provided by 600-watt high-pressure sodium fixtures under a 16/8 h light: dark regime  
950 ( $1000 \mu\text{mols m}^{-2} \text{sec}^{-1}$ ), with the temperatures maintained between 26-31°C during the d  
951 and 20-24°C during the night. Individuals were genotyped according to Slewinski et al.  
952 (2010). Five individuals homozygous for either the mutant or for the wild-type allele  
953 were grown to the v5 stage, upon which the fully expanded fifth leaf was collected and  
954 placed into liquid nitrogen. The RNA extraction and cDNA synthesis were performed as  
955 outlined above. For the *zmsut1-m4* and wild-type expression analysis, the 10  $\mu\text{L}$  reaction  
956 mix consisted of 10 ng cDNA, 5  $\mu\text{L}$  SsoFast EvaGreen Supermix with low ROX (Bio-  
957 Rad, Hercules, CA), and 0.5  $\mu\text{M}$  of both *ZmSut1* or luciferase forward and reverse  
958 primers (Supp. Table S2).

959 Quantitative cycle values were determined using a regression method and were analyzed  
960 using the standard curve method (Larionov et al., 2005). The time course experiment  
961 consisted of 10 individual (biological) samples for each time point with 5 technical  
962 replicates each, whereas the *zmsut1-m4* expression experiment was composed of 5  
963 biological replicates for each genotype with 4 technical replicates each. The standard  
964 curve used for the time course analysis was composed of a pool of cDNA from each  
965 individual at each time point, while the standard curve for *zmsut1-m4* expression was  
966 composed of a cDNA pool from the wild-type individuals in the experiment. Statistically  
967 significant differences at  $p < 0.05$  were determined using Proc GLM (SAS v9.3).

#### 968 *RNA In Situ Hybridization*

969 Small tissue segments ( $3 \times 1 \text{ mm}$ ) dissected from fully emerged leaves 12 and 13 of  
970 greenhouse-grown 13-week-old B73 and *zmsut1-m4* mutant plants were fixed overnight  
971 in ice-cold acetone, dehydrated through an acetone/xylene series, and embedded in  
972 paraffin, as described (Zhang et al., 2007b). The embedded tissue was sectioned at a  
973 thickness of 12  $\mu\text{m}$  and adhered to glass slides on heating plates. The subsequent probe  
974 selection, hybridization, and fast-blue color development were conducted by Affymetrix  
975 (San Diego, CA, USA) as described (Bowling et al., 2014). ImageJ was used to compare  
976 the relative percentage of signal within the CC/SE to the signal in the PP, XP, and BS  
977 cells in lateral ( $n = 5$ ), intermediate ( $n = 5$ ), and small ( $n = 10$ ) veins using the “Color  
978 Pixel Counter” plug-in (<http://rsb.info.nih.gov/ij/>). The xylem vessel elements in all vein

979 classes, the epidermis, and the HS cells in the lateral and intermediate veins were  
980 excluded from the analysis.

### 981 *Transgenic plants*

982 Maize lines carrying transgenic constructs expressing 1) RFP targeted to the endoplasmic  
983 reticulum under the control of the *ZmSut1* promoter region (pZmSut1::RFP<sub>er</sub>), 2) YFP  
984 translationally fused to the C-terminus of the ZmSUT1 protein using the full-length  
985 *ZmSut1* genomic sequence (gSUT1-YFP), and 3) CFP translationally fused to the N-  
986 terminus of PIP2-1 (AQUAPORIN) using the *PIP2-1* genomic sequence (PIP2-1-CFP)  
987 were obtained from the Maize Cell Genomics Project, and were constructed as described  
988 at <http://maize.jcvi.org/cellgenomics/index.php>. These constructs were backcrossed into  
989 the B73 inbred line at least 3 times prior to analyses. Plants carrying YFP and RFP  
990 transgenes were PCR-genotyped using primers listed in Supp. Table S2, or plants  
991 carrying the transgenes (YFP, RFP, or CFP) were visually identified by fluorescent  
992 microscopy.

993 For the etiolated seedling light-shift experiment, a family segregating for  
994 pZmSut1::RFP<sub>er</sub> was germinated in the dark for 8 d, at which time leaf 1 and the tip of  
995 leaf 2 had emerged from the coleoptile. The etiolated seedlings were brought into the lab,  
996 and a small portion of leaf 1 was harvested from one side of the midrib for microscopy.  
997 The plants were left under dim fluorescent white lighting ( $5 \mu\text{mols m}^{-2} \text{sec}^{-1}$ ) for 48 hrs to  
998 induce chlorophyll synthesis, then moved into the greenhouse to transition to source  
999 tissues. After 5 d, tissue was harvested from leaf 1 opposite to the location of the initial  
1000 sampling.

1001 For the *sr2* leaf variegation experiment, plants carrying the pZmSut1::RFP<sub>er</sub> construct  
1002 were used as males and backcrossed twice to *sr2* mutants.

1003 For the transgenic complementation test of gSUT1-YFP, plants carrying the transgene  
1004 were crossed to plants heterozygous for the *zmsut1-m1* mutant allele (Slewinski et al.,  
1005 2009). Plants carrying the transgene and *zmsut1-m1* allele were identified by genotyping  
1006 (Rotsch et al., 2015; Leach et al., 2016) and backcrossed to *ZmSut1/zmsut1-m1*  
1007 heterozygous plants to generate families for analyses. Morphometric and statistical  
1008 analyses were conducted as described (Braun et al., 2006; Baker and Braun, 2008; Ma et  
1009 al., 2008).

1010 *Light, Fluorescent, and Confocal Microscopy of Reporter Lines*

1011 For each type of illumination within a figure, all images were captured using identical  
1012 microscope and camera settings, unless otherwise noted. Bright-field and epi-  
1013 fluorescence microscopy of organs and tissues from plants expressing the  
1014 pZmSut1::RFP<sub>er</sub>, gSUT1-YFP, and PIP2-1-CFP constructs were performed on a Nikon  
1015 Eclipse 80i microscope equipped with a 100-W mercury bulb and a DXM1200F camera  
1016 (Huang et al., 2009). Filter cubes used were: UV (360- to 370-nm excitation filter and a  
1017 420-nm long-pass emission filter), CFP (412- to 462-nm excitation filter and a 460- to  
1018 500-nm band-pass emission filter), YFP (465- to 495-nm excitation filter and a 515- to  
1019 555-nm band-pass emission filter), and RFP (530- to 560-nm excitation filter and a 590-  
1020 to 650-nm band-pass emission filter). The excitation peaks for chlorophyll *a* (430, 662  
1021 nm in methanol) and *b* (453, 642 nm in methanol) occurred well outside the range of the  
1022 RFP filter (530-560 nm), resulting in the virtual absence of chlorophyll autofluorescence  
1023 and allowing a simple assessment of RFP signal within leaves. For examination, shoot  
1024 apical meristems were dissected from 2-week-old greenhouse-grown seedlings; roots,  
1025 developing leaves, and stems from 6-week-old greenhouse-grown plants; developing  
1026 tassels from 8-week-old greenhouse-grown plants; and maturing tassels and developing  
1027 ears from 10-week-old greenhouse-grown plants. For examining mature leaf tissue,  
1028 transverse hand-cut or paradermal sections were generated using a razor blade and  
1029 mounted in dH<sub>2</sub>O, while reproductive structures and meristems were whole-mounted in  
1030 dH<sub>2</sub>O after dissection from the plant. Images were captured using Nikon NIS Elements F  
1031 software (version 3.0).

1032 For visualizing RFP expression in an emerging leaf 5 of 2-week-old seedlings carrying  
1033 the pZmSut1::RFP<sub>er</sub> construct, we used a Leica MZFLIII dissecting stereomicroscope  
1034 equipped with a dsRed-bandpass filter (Leica Microsystems, Bannockburn, IL) and a 12-  
1035 bit color CCD camera (Optronics Laboratories, Inc., Goleta, CA). The plants were  
1036 examined when the tip of leaf 5 was just emerging from the whorl. The leaf was dissected  
1037 from the plant and divided into ten 10-mm segments, and representative regions from  
1038 each leaf segment were photographed. All photographs were taken using the same  
1039 exposure time, microscope, and camera settings.

1040 A Zeiss 510 META laser scanning confocal microscope (Carl Zeiss Microscopy, LLC)  
1041 was used to evaluate the cellular expression of the pZmSut1::RFPper construct in mature  
1042 leaves and internodes. RFP was excited with a 543-nm HeNe laser, and fluorescence was  
1043 recorded using a 565- to 615-nm band-pass filter. Chloroplast autofluorescence was  
1044 induced by a 488-nm argon laser line and recorded using a 650- to 710-nm band-pass  
1045 filter. For visualization of the cell walls, the samples were stained with 0.005% aniline  
1046 blue (w/v) in 0.15 M potassium phosphate buffer (pH 8.2) (Ruzin, 1999) and excited with  
1047 a 458-nm argon laser line, with fluorescence recorded using a 535- to 590-nm band-pass  
1048 filter.

1049 For evaluating gSUT1-YFP subcellular localization alone or in double-labelled lines  
1050 relative to PIP2-1-CFP or pZmSut1::RFPper, a Zeiss TCP SP8 MP inverted spectral  
1051 confocal microscope with a tunable white laser and fixed visible laser lines was used with  
1052 the following settings: YFP (tunable white laser light): excitation, 514 nm; emission band  
1053 path, 525 to 575 nm; RFP (tunable white laser light): excitation, 584 nm; emission band  
1054 path, 590 to 660 nm; UV (405-nm laser line): excitation, 405 nm; emission band path,  
1055 420 to 500 nm; CFP (458-nm argon-laser line): excitation, 458 nm; emission band path,  
1056 465 to 520 nm; chlorophyll autofluorescence (tunable white laser light): excitation, 488  
1057 nm; emission band path, 650 to 800 nm. UV excitation was used to visualize the cell  
1058 walls.

1059 To further investigate the subcellular localization of the gSUT1-YFP translational fusion  
1060 protein, we performed live-cell imaging of paradermal leaf sections with an Olympus IX-  
1061 71 inverted microscope (Center Valley, PA) equipped with a Yokogawa CSU-X1 5000-  
1062 rpm spinning disc unit (Tokyo, Japan), Andor iXon Ultra 897 High Speed EMCCD  
1063 camera (Belfast, United Kingdom), PZ-2000 XYZ series automated stage with Piezo Z-  
1064 axis top plate (Applied Scientific Instrumentation, Eugene, OR), and a 60 $\times$ -silicon oil  
1065 objective (Olympus UPlanSApo 60 $\times$ /1.30 Sil), as described in Smith et al. (2014). YFP  
1066 was excited with a Spectra Physics 515-nm diode laser (Santa Clara, CA), with  
1067 fluorescence collected through a 488-, 515-, and 561-nm dichroic beamsplitter  
1068 (ZT405/514/561TPC-XR; Chroma Technology Corp., Rockingham, VA) and 515–569-  
1069 nm band-pass filter (FF01-542/27-25; Semrock Brightline, Rochester, NY). For verifying  
1070 that gSUT1-YFP localized to the plasma membrane, paradermal leaf sections were

1071 plasmalysed by exposure to a solution of 0.75 M NaCl for 10 minutes and then mounted  
1072 for examination. Images were captured using Andor iQ2 software (Belfast, United  
1073 Kingdom).

#### 1074 *CFDA Dye Movement Assays*

1075 A solution of CFDA in water (50 µg/ml) was prepared from a stock solution as  
1076 previously described (Bihmidine et al., 2015). For the root studies, the cut end of the fully  
1077 mature leaf 4 of 10-week-old greenhouse-grown plants expressing the pZmSut1::RFPer  
1078 construct was submerged in a 30-mL solution of CFDA in a 50-mL conical tube for 1 h.  
1079 Afterwards, the dye was allowed to move through the plant for an additional 3 hrs. The  
1080 tips of aerial prop roots that penetrated the soil were harvested, cut longitudinally through  
1081 the center under a dissecting scope with a razor blade, and assessed for CF signal with  
1082 fluorescence microscopy, as previously described (Bihmidine et al., 2015). For  
1083 examining phloem unloading in developing sink leaves, a mature source leaf 9 of a 38-d-  
1084 old pZmSut1::RFPer transgenic plant was fed CF for 20 min, followed by translocation  
1085 within the plant for 5 hrs prior to tissue harvest and analysis. Cross-sections from the  
1086 enclosed developing sink leaves were taken at 50% and 25% of the distance between the  
1087 base and top of the sheath of the fed leaf.

1088

#### 1089 **Supplemental Material**

1090 Figure S1. *zmsut1* mutant leaves excrete droplets of Suc.

1091 Figure S2. qRT-PCR analysis of *zmsut1-m4* homozygous mutant and wild-type leaves.

1092 Figure S3. Expression of pZmSut1::RFPer in a leaf undergoing the sink-to-source  
1093 transition.

1094 Figure S4. gSUT1-YFP exhibits the same cellular expression pattern as pZmSut1::RFPer.

1095 Table S1. Morphometric analyses of gSUT1-YFP transgenic complementation test.

1096 Table S2. List of PCR primers used.

1097

#### 1098 **Acknowledgments**

1099 We thank two anonymous reviewers, Ben Julius, Priya Voothuluru, and Rachel Mertz for  
1100 constructive comments on the manuscript. We thank Aleksandr Jurkevic, Arpine  
1101 Mikayelyan, and Joseph Mercurio in the MU Molecular Cytology Center for their helpful

1102 advice and technical expertise. We thank Jerry Kermicle for the gift of *sr2* seeds. We also  
1103 thank Michelle Brooks at the Sears Plant Growth Facility, and Chris Browne and Matt  
1104 Boyer of the Missouri Maize Center for the maintenance and care of our plants. We also  
1105 thank Peter Cornish, Antje Hesse, and Michelle Leslie for the generous training and use  
1106 of the spinning disc confocal equipment. We thank Wilson Lew, Erik Hasal, and  
1107 Maureen Hughes from Affymetrix for technical assistance with the *in situ*.  
1108

1109 **Tables**

1110 Table 1. Quantification of *ZmSut1* RNA *in situ* hybridization signal in different cell types  
1111 within vein classes

1112

<b>Vein Class</b>	<b>Blue pixels in CC/ total blue pixels</b>	<b>Blue pixels in VP/ total blue pixels</b>	<b>Blue pixels in BS/ total blue pixels</b>	<b>Ratio VP+BS /CC</b>
Lateral	13.6±3.0	81.1±3.6	5.4±2.7	8.3±2.2
Intermediate	16.3±6.4	55.2±9.8	27.1±5.5	6.2±3.8
Small	12.6±9.3	60.0±18.3	27.4±15.9	11.0±8.1

1113

1114 Blue pixels within each vein were identified in companion cells (CC), vascular  
1115 parenchyma (VP) cells, or bundle sheath (BS) cells. Numbers of blue pixels are the  
1116 average percent values for the specified cell type within each vein class ± the standard  
1117 deviation. The last column is the ratio of blue pixels in the VP and BS cells compared to  
1118 the CC.

1119

1120 **Figure legends**

1121 **Figure 1.** *ZmSut1* expression is stable and does not cycle diurnally in adult maize leaves.  
1122 qRT-PCR expression of *ZmSut1* in B73 mature and immature leaves over 48 hrs.  
1123 Samples were harvested every 4 hrs. Measurements are average expression values for 10  
1124 biological samples of *ZmSut1* relative to exogenously supplied luciferase mRNA used as  
1125 a normalization control. Values are relative units. Red squares indicate mature leaf 11  
1126 source tissue and blue diamonds indicate immature leaf 17 sink tissue. Error bars show  
1127 standard error.

1128

1129 **Figure 2.** RNA *in situ* hybridization demonstrates that *ZmSut1* is expressed in the CC,  
1130 XP, PP, and BS cells of mature leaf blades. Expression is revealed by the blue precipitate.  
1131 A, B. Transverse section through a B73 leaf showing the anatomy of a lateral vein (left)  
1132 and a small vein (right) under bright-field (A) and UV autofluorescence (B). The  
1133 different cell types are labelled: BS, bundle sheath, CC, companion cell, E, epidermis,  
1134 HS, hypodermal sclerenchyma, M, mesophyll, MX, metaxylem element, PP, phloem  
1135 parenchyma, PX, protoxylem lacunae, SE, sieve element, XP, xylem parenchyma. C, D,  
1136 F. Wild-type (WT) B73 mature leaf sections hybridized with *ZmSut1* probe. G. *zmsut1*  
1137 mutant leaf section hybridized with *ZmSut1* probe. E, H. Wild-type B73 mature leaf  
1138 sections developed without probe. C, E show small veins, D shows an intermediate vein,  
1139 and F-H show lateral veins. Black arrows point to CC; red arrows to SE; blue arrows to  
1140 BS cells; arrowheads to large XP cells. Scale bar = 50  $\mu$ m.

1141

1142 **Figure 3.** The pZmSut1::RFPper transcriptional reporter gene recapitulates *ZmSut1*  
1143 expression observed by RNA *in situ* hybridization. A-I. Confocal images showing  
1144 expression of pZmSut1::RFPper transgene in transverse and paradermal leaf sections. A.  
1145 Transverse section of a minor vein showing RFP is expressed in the CC (white arrow),  
1146 XP (arrowhead), PP, and to a more limited extent in the BS cells (yellow arrow). The cell  
1147 outlines were visualized with aniline-blue staining; the green signal represents  
1148 chlorophyll autofluorescence. B. Transverse section of a minor vein from a plant lacking  
1149 the transgene. C. Transverse section of a lateral vein showing RFP expression in CC, XP,  
1150 PP, and to a lesser extent in BS cells. Blue signal shows cell walls and green signal is

1151 chlorophyll autofluorescence. D. Same image as in C, but only showing RFP expression.  
1152 E. Transverse section of a lateral vein of a non-transgenic control showing no RFP  
1153 expression. Blue signal shows cellular anatomy. F. Paradermal section of a minor vein  
1154 showing RFP expression in the CC, PP, and to a lesser extent in the BS cells. G.  
1155 Paradermal section of non-transgenic control showing no RFP expression. Blue signal  
1156 shows cell walls and green signal is chlorophyll autofluorescence. H. Same section as in  
1157 F showing only RFP signal. I. Same section as in G showing only red channel. BS,  
1158 bundle sheath cell, CC, companion cell, PP, phloem parenchyma cell. Scale bar = 25  $\mu\text{m}$ .  
1159

1160 **Figure 4.** pZmSut1::RFP<sub>er</sub> is expressed early in vein development in sink leaves. Epi-  
1161 fluorescence microscope images of pZmSut1::RFP<sub>er</sub> expression in developing leaves. A-  
1162 J. Transverse cross-sections through inner developing leaves of 2-week-old seedlings. A,  
1163 B. Non-transgenic control sections. Panel A shows autofluorescence of HS cell walls. C-  
1164 J. Transverse sections of pZmSut1::RFP<sub>er</sub> transgenic leaves located approximately half-  
1165 way between the blade-sheath boundary and the base of the enclosing mature leaf (C, D),  
1166 at the base of immature blade tissue (E, F), in immature sheath tissue (G, H), and located  
1167 just above the meristem (I, J). Panels C, E, G, I, K, M show RFP images. Panels B, D, F,  
1168 H, J, L, N show UV autofluorescence images. K, L. Close up of the lateral vein in middle  
1169 of panels C, D. M, N. Close up of a developing lateral vein in panels E, F. Expression is  
1170 observed in the protophloem (white arrow). Note that with the RFP filter cube, at these  
1171 exposure settings, virtually no red signal from chlorophyll is detected (cf. Fig. 4A, B).  
1172 Scale bar in A-J = 100  $\mu\text{m}$ . Scale bar in K-N = 25  $\mu\text{m}$ .

1173  
1174 **Figure 5.** pZmSut1::RFP<sub>er</sub> expression in leaves is induced in veins upon shifting plants  
1175 from growth in the dark to the light. A, B. RFP images. C, D. UV autofluorescence  
1176 images. A, C show an etiolated sink-leaf cross-section. B, D show a leaf cross-section  
1177 after shifting plants into the light and the leaf matured as source tissue. Note that with the  
1178 RFP filter cube, at these exposure settings, virtually none of the red signal is from  
1179 chlorophyll. Scale bar = 100  $\mu\text{m}$ .

1180

1181 **Figure 6.** pZmSut1::RFPper expression is induced in veins of mature source tissue  
1182 compared with albino sink tissue in variegated *sr2* mutant leaves. A, C, E show a cross-  
1183 section through a green-white border of a *sr2* leaf expressing pZmSut1::RFPper. B, D, F  
1184 show a non-transgenic control variegated *sr2* mutant leaf. A, B. Bright-field. C, D. RFP  
1185 signal. E, F. UV autofluorescence. Note that with the RFP filter cube, at these exposure  
1186 settings, virtually no red signal from chlorophyll is detected (cf. Fig. 6D, F). Scale bar =  
1187 100  $\mu$ m.

1188

1189 **Figure 7.** pZmSut1::RFPper expression is broad initially in developing stem, but becomes  
1190 restricted in mature stem veins. Transverse sections showing expression of the  
1191 pZmSut1::RFPper transgene in immature (A) and mature stem (C). B. UV  
1192 autofluorescence of tissue shown in panel A. D. Transverse section of mature stem of  
1193 non-transgenic control. A, C, D. RFP channel. A. Expression of the transgene is initially  
1194 strongest in the protoxylem and protophloem, with lower signal in the developing  
1195 parenchyma cells. C. At maturity pZmSut1::RFPper expression is highest in veins, with  
1196 low level in the storage parenchyma. E-G. Confocal images of mature stem vein showing  
1197 pZmSut1::RFPper expression in the XP cells (arrowhead) and CC (arrow). H-J. Confocal  
1198 images of mature stem vein of non-transgenic control exhibiting autofluorescence. E, H.  
1199 RFP channel. F, I. UV autofluorescence showing cell walls. G. Merged image of E and F.  
1200 J. Merged image of H and I. Note that with the RFP filter cube, at these exposure  
1201 settings, virtually no red signal is detected from chlorophyll (cf. Fig. 7C, D). Scale bar in  
1202 A, B = 250  $\mu$ m; in C, D = 500  $\mu$ m; in E-J = 25  $\mu$ m.

1203

1204 **Figure 8.** pZmSut1::RFPper displays broad expression in multiple vegetative and  
1205 reproductive sink tissues. Epi-fluorescent microscope images of pZmSut1::RFPper  
1206 expression in the shoot apical meristem, in developing tassels and ears, and in developing  
1207 roots. A, C, E, G, I, K, M, N, O, Q, S, U. RFP signal. B, D, F, H, J, L, P, R, T, V. UV  
1208 autofluorescence of corresponding tissue. A, B. Shoot apical meristem. C, D. Developing  
1209 tassel. E-L. Developing ear. G-L represent cross-sections through the developing ear. M,  
1210 N. Maturing tassel. O-V. Developing root. O. Transverse section near the root tip  
1211 showing RFP expression is largely restricted to the phloem (arrow) and xylem

1212 (arrowhead). Q. Section slightly higher than that of O showing RFP expression in the  
1213 phloem and developing xylem elements. S. Section at cusp between developing and  
1214 mature xylem cells. Arrowhead indicates xylem element presumably undergoing  
1215 autolysis. Arrow indicates phloem. U. Mature root. RFP expression can be seen in the  
1216 phloem and diffusely throughout the root. Scale bar = 100  $\mu\text{m}$  for A, B, K, L, O-V; 250  
1217  $\mu\text{m}$  for C-J, N; 500  $\mu\text{m}$  for M. Exposure times for panels A, E, G, I, N = 750 ms; for C =  
1218 4 s; for K, M = 2 s. for O, Q, S, U = 1 s.

1219

1220 **Figure 9.** pZmSut1::RFP expression pattern differs from that of the phloem unloading  
1221 zone identified by CF efflux into cortical cells of a pZmSut1::RFP transgenic root. A,  
1222 E. UV autofluorescence. B, F. CF signal. White arrow indicates region of CF efflux from  
1223 phloem into cortical cells. C, G. RFP signal. D, H. Overlay of the CF and RFP signals. E,  
1224 F, G, and H are closer views of A, B, C, and D, respectively. Scale bar in A-D = 500  $\mu\text{m}$ ;  
1225 in E-H = 250  $\mu\text{m}$ .

1226

1227 **Figure 10.** Developing leaves exhibit either symplasmic or apoplasmic phloem unloading  
1228 in distinct regions that overlap pZmSut1::RFP expression. A, C, E. Cross-section taken  
1229 approximately half-way up the blade of a developing pZmSut1::RFP expressing sink  
1230 leaf. B, D, F. Cross-section taken approximately a quarter-way up the blade from the base  
1231 of the same developing sink leaf. A, B. UV autofluorescence. C, D. CF signal. C. Arrow  
1232 shows CF confinement within the symplasmically isolated phloem. D. Arrowhead shows  
1233 vein symplasmically unloading CF into adjacent cells. CF movement marked by white  
1234 bracket. E, F. RFP signal. Scale bar = 100  $\mu\text{m}$ .

1235

1236 **Figure 11.** The gSut1-YFP transgene largely complements the *zmsut1* mutant phenotype.  
1237 *zmsut1* homozygous mutant plants carrying the transgene (middle) grew to near wild-type  
1238 height (left), and produced tassels that shed pollen and ears that produced silks. By  
1239 contrast, the *zmsut1* homozygous mutants (right) that lacked the transgene and survived  
1240 were stunted and typically failed to undergo anthesis or produce ears.

1241

1242 **Figure 12.** A ZmSUT1 protein translational fusion shows the same cellular expression  
1243 pattern as observed with RNA *in situ* hybridization. Confocal images of the ZmSUT1  
1244 protein translationally fused at the C-terminus with YFP in transverse and paradermal  
1245 leaf sections. A, B. Transverse section of a leaf lateral vein showing gSUT1-YFP is  
1246 expressed in CC (arrows), XP (arrowheads), PP, and BS cells (blue arrow). Asterisks  
1247 indicate SE. C. Paradermal section of a leaf minor vein showing gSUT1-YFP expression.  
1248 A, C. YFP signal. B. Combined YFP, cell wall autofluorescence in blue, and chlorophyll  
1249 autofluorescence in red. BS, bundle sheath cells, CC, companion cells, PP, phloem  
1250 parenchyma cells, SE, sieve element. Scale bar = 25  $\mu$ m.

1251

1252 **Figure 13.** ZmSUT1 localizes to the plasma membrane. Confocal images of the  
1253 expression of the SUT1 protein fused at the C-terminus with YFP. A-C. Paradermal  
1254 section of a leaf minor vein focused on the BS cells. A. YFP signal. Arrowheads indicate  
1255 YFP localization in two adjacent cells, separated by their shared cell wall. B. Combined  
1256 YFP and chloroplasts (green). C. Combined YFP, chloroplasts, and cell wall (blue). D-F,  
1257 Paradermal section of a leaf minor vein focused on the BS cells of a gSUT1-YFP and  
1258 PIP2-1-CFP transgenic plant. D. YFP signal. E. CFP signal. F. Combined YFP and CFP  
1259 signal. G-I. Spinning disc confocal image supporting ZmSUT1-YFP plasma membrane  
1260 localization. G. Pre-plasmolysis YFP signal located at cell periphery. H. After plasmolysis  
1261 with 0.75 M NaCl the plasma membrane has retracted; however, the plasma membrane is  
1262 attached to the cell wall at the PD, resulting in the Hechtian strands (arrows). I. Non-  
1263 transgenic control section. Scale bar = 10  $\mu$ m for A-C; = 25  $\mu$ m for D-I.

1264

1265 **Figure 14.** Model for dual functions of *ZmSut1* in phloem loading and retrieval. Red  
1266 arrow indicates ZmSUT1 loading Suc into CC. Purple arrows indicate ZmSUT1  
1267 retrieving Suc into non-conducting vascular cells. Yellow arrows show symplasmic Suc  
1268 movement. Grey rectangles represent symplasmic connectivity through PD. Light blue  
1269 rectangles with black arrows represent SWEET proteins effluxing Suc to the apoplast of  
1270 PP cells. Beige color represents vein apoplast. BS, bundle sheath cell, CC, companion  
1271 cell, M, mesophyll cell, PP, phloem parenchyma cell, SE, sieve element, TST, thick-  
1272 walled sieve element, XE, xylem element, XP, xylem parenchyma cell.

1273 **Supplementary Material**

1274 **Supplemental Figure S1.** The hydathodes of *zmsut1* mutant leaves excrete droplets with  
1275 high concentrations of Suc (left).

1276 **Supplementary Figure S2.** qRT-PCR analysis shows that the *zmsut1-m4* homozygous  
1277 mutant leaves (mut) express a very low level of *ZmSut1* transcript compared to wild-type  
1278 (WT) siblings.

1279 **Supplemental Figure S3.** Expression of the pZmSut1::RFPper transgene in an emerging  
1280 leaf (leaf 5) undergoing the sink-to-source transition.

1281 **Supplemental Figure S4.** gSUT1-YFP exhibits the same cellular expression pattern as  
1282 pZmSut1::RFPper.

1283

1284 **Supplemental Figure S1.** The hydathodes of *zmsut1* mutant leaves excrete droplets with  
1285 high concentrations of Suc (left). The droplets dry to form Suc beads (arrowhead).  
1286 Equivalent excretions are not observed in the wild-type leaf (right).

1287

1288 **Supplementary Figure S2.** qRT-PCR analysis shows that the *zmsut1-m4* homozygous  
1289 mutant leaves (mut) express a very low level of *ZmSut1* transcript compared to wild-type  
1290 (WT) siblings. Values are relative units. Error bars are standard error. Asterisk indicates  
1291 statistically significant difference at  $p < 0.05$ .

1292

1293 **Supplemental Figure S3.** Expression of the pZmSut1::RFPper transgene in an emerging  
1294 leaf (leaf 5) undergoing the sink-to-source transition. The tip of the leaf (A) has emerged  
1295 out of the whorl into the light. Each panel A-J is an image taken from a consecutive 1 cm  
1296 segment of the leaf. The bottom segment at the leaf base (J) represents the region 10 cm  
1297 proximal from the leaf tip. The grey triangle represents the gradient of exported carbon  
1298 from the source tissue. The physiological, anatomical, and developmental events  
1299 indicated are approximately positioned, correspond coarsely to cross-sections shown in  
1300 Fig. 4, and are extrapolated from Evert et al. (1996a). Scale bar = 1 mm for all panels.

1301

1302 **Supplemental Figure S4.** gSUT1-YFP exhibits the same cellular expression pattern as  
1303 pZmSut1::RFPper. A-D. Paradermal section of a leaf minor vein of a gSUT1-YFP;

1304 pSut1::RFP<sub>er</sub> transgenic plant. E-H. Paradermal section of a leaf minor vein of a non-  
1305 transgenic control sibling plant. A, E. YFP signal. B, F. RFP signal. C, G. Combined YFP  
1306 and RFP signals. D, H. Combined YFP, RFP, chlorophyll, and UV autofluorescence  
1307 signals. Scale bar = 25  $\mu$ m.  
1308

1309 **Literature Cited**

1310

- 1311 **Ainsworth EA, Bush DR** (2011) Carbohydrate export from the leaf: a highly  
1312 regulated process and target to enhance photosynthesis and productivity.  
1313 *Plant Physiol* **155**: 64-69
- 1314 **Antony G, Zhou J, Huang S, Li T, Liu B, White F, Yang B** (2010) Rice *xa13* recessive  
1315 resistance to bacterial blight is defeated by induction of the disease  
1316 susceptibility gene *Os-11N3*. *Plant Cell* **22**: 3864-3876
- 1317 **Aoki N, Hirose T, Scofield GN, Whitfield PR, Furbank RT** (2003) The sucrose  
1318 transporter gene family in rice. *Plant Cell Physiol* **44**: 223-232
- 1319 **Aoki N, Hirose T, Takahashi S, Ono K, Ishimaru K, Ohsugi R** (1999) Molecular  
1320 cloning and expression analysis of a gene for a sucrose transporter in maize  
1321 (*Zea mays* L.). *Plant Cell Physiol* **40**: 1072-1078
- 1322 **Aoki N, Scofield GN, Wang X-D, Patrick JW, Offler CE, Furbank RT** (2004)  
1323 Expression and localisation analysis of the wheat sucrose transporter  
1324 TaSUT1 in vegetative tissues. *Planta* **219**: 176-184
- 1325 **Ayre BG** (2011) Membrane-transport systems for sucrose in relation to whole-plant  
1326 carbon partitioning. *Mol Plant* **4**: 377-394
- 1327 **Baker RF, Braun DM** (2007) *tie-dyed1* functions non-cell autonomously to control  
1328 carbohydrate accumulation in maize leaves. *Plant Physiol* **144**: 867-878
- 1329 **Baker RF, Braun DM** (2008) *tie-dyed2* functions with *tie-dyed1* to promote  
1330 carbohydrate export from maize leaves. *Plant Physiol* **146**: 1085-1097
- 1331 **Baker RF, Leach KA, Braun DM** (2012) SWEET as sugar: new sucrose effluxers in  
1332 plants. *Mol Plant* **5**: 766-768
- 1333 **Baker RF, Slewinski TL, Braun DM** (2013) The *Tie-dyed* pathway promotes  
1334 symplastic trafficking in the phloem. *Plant Sig Behav* **8**: e24540
- 1335 **Bauer CS, Hoth S, Haga K, Philippar K, Aoki N, Hedrich R** (2000) Differential  
1336 expression and regulation of K<sup>+</sup> channels in the maize coleoptile: molecular  
1337 and biophysical analysis of cells isolated from cortex and vasculature. *Plant J*  
1338 **24**: 139-145
- 1339 **Bihmidine S, Baker RF, Hoffner C, Braun DM** (2015) Sucrose accumulation in  
1340 sweet sorghum stems occurs by apoplasmic phloem unloading and does not  
1341 involve differential *Sucrose transporter* expression. *BMC Plant Biol* **15**: 186
- 1342 **Bihmidine S, Hunter III CT, Johns CE, Koch KE, Braun DM** (2013) Regulation of  
1343 assimilate import into sink organs: Update on molecular drivers of sink  
1344 strength. *Front Plant Sci* **4**: 177. doi: 110.3389/fpls.2013.00177
- 1345 **Bihmidine S, Julius BT, Dweikat I, Braun DM** (2016) *Tonoplast Sugar*  
1346 *Transporters (SbTSTs)* putatively control sucrose accumulation in sweet  
1347 sorghum stems. *Plant Sig Behav* **11**: e1117721
- 1348 **Bowling AJ, Pence HE, Church JB** (2014) Application of a novel and automated  
1349 branched DNA *in situ* hybridization method for the rapid and sensitive  
1350 localization of mRNA molecules in plant tissues. *App Plant Sci* **2**: 1400011
- 1351 **Braun DM** (2012) SWEET! The pathway is complete. *Science* **335**: 173-174
- 1352 **Braun DM, Ma Y, Inada N, Muszynski MG, Baker RF** (2006) *tie-dyed1* regulates  
1353 carbohydrate accumulation in maize leaves. *Plant Physiol* **142**: 1511-1522

- 1354 **Braun DM, Slewinski TL** (2009) Genetic control of carbon partitioning in grasses:  
1355 Roles of *Sucrose Transporters* and *Tie-dyed* loci in phloem loading. *Plant*  
1356 *Physiol* **149**: 71-81
- 1357 **Braun DM, Wang L, Ruan Y-L** (2014) Understanding and manipulating sucrose  
1358 phloem loading, unloading, metabolism, and signalling to enhance crop yield  
1359 and food security. *J Exp Bot* **65**: 1713-1735
- 1360 **Bürkle L, Hibberd JM, Quick WP, Kühn C, Hirner B, Frommer WB** (1998) The H<sup>+</sup>-  
1361 sucrose cotransporter NtSUT1 is essential for sugar export from tobacco  
1362 leaves. *Plant Physiol* **118**: 59-68
- 1363 **Carpaneto A, Geiger D, Bamberg E, Sauer N, Fromm J, Hedrich R** (2005) Phloem-  
1364 localized, proton-coupled sucrose carrier ZmSUT1 mediates sucrose efflux  
1365 under the control of the sucrose gradient and the proton motive force. *J Biol*  
1366 *Chem* **280**: 21437-21443
- 1367 **Chandran D, Reinders A, Ward JM** (2003) Substrate specificity of the *Arabidopsis*  
1368 *thaliana* sucrose transporter AtSUC2. *J Biol Chem* **278**: 44320-44325
- 1369 **Chen L-Q, Hou B-H, Lalonde S, Takanaga H, Hartung ML, Qu X-Q, Guo W-J, Kim J-**  
1370 **G, Underwood W, Chaudhuri B, Chermak D, Antony G, White FF,**  
1371 **Somerville SC, Mudgett MB, Frommer WB** (2010) Sugar transporters for  
1372 intercellular exchange and nutrition of pathogens. *Nature* **468**: 527-532
- 1373 **Chen L-Q, Qu X-Q, Hou B-H, Sosso D, Osorio S, Fernie AR, Frommer WB** (2012)  
1374 Sucrose efflux mediated by SWEET proteins as a key step for phloem  
1375 transport. *Science* **335**: 207-211
- 1376 **Chu Z, Yuan M, Yao J, Ge X, Yuan B, Xu C, Li X, Fu B, Li Z, Bennetzen JL, Zhang Q,**  
1377 **Wang S** (2006) Promoter mutations of an essential gene for pollen  
1378 development result in disease resistance in rice. *Genes Dev* **20**: 1250-1255
- 1379 **Durand M, Porcheron B, Hennion N, Maurousset L, Lemoine R, Pourtau N**  
1380 (2016) Water deficit enhances C export to the roots in *Arabidopsis thaliana*  
1381 plants with contribution of sucrose transporters in both shoot and roots.  
1382 *Plant Physiol* **170**: 1460-1479
- 1383 **Eom J-S, Chen L-Q, Sosso D, Julius BT, Lin IW, Qu X-Q, Braun DM, Frommer WB**  
1384 (2015) SWEETs, transporters for intracellular and intercellular sugar  
1385 translocation. *Curr Opin Plant Biol* **25**: 53-62
- 1386 **Eom J-S, Choi S-B, Ward JM, Jeon J-S** (2012) The mechanism of phloem loading in  
1387 rice (*Oryza sativa*). *Molec Cells* **33**: 431-438
- 1388 **Esau K** (1977) *Anatomy of Seed Plants*, Ed 2nd. John Wiley and Sons, New York
- 1389 **Evert RF** (1982) Sieve-tube structure in relation to function. *Bioscience* **32**: 789-  
1390 795
- 1391 **Evert RF, Eschrich W, Heyser W** (1977) Distribution and structure of the  
1392 plasmodesmata in mesophyll and bundle sheath cells of *Zea mays* L. *Planta*  
1393 **136**: 77-89
- 1394 **Evert RF, Eschrich W, Heyser W** (1978) Leaf structure in relation to solute  
1395 transport and phloem loading in *Zea mays* L. *Planta* **138**: 279-294
- 1396 **Evert RF, Russin WA** (1993) Structurally, phloem unloading in the maize leaf  
1397 cannot be symplastic. *Am J Bot* **80**: 1310-1317

- 1398 **Evert RF, Russin WA, Bosabalidis AM** (1996a) Anatomical and ultrastructural  
 1399 changes associated with sink-to-source transition in developing maize leaves.  
 1400 Int J Plant Sci **157**: 247-261
- 1401 **Evert RF, Russin WA, Botha CEJ** (1996b) Distribution and frequency of  
 1402 plasmodesmata in relation to photoassimilate pathways and phloem loading  
 1403 in the barley leaf. Planta **198**: 572-579
- 1404 **Fritz E, Evert RF, Heyser W** (1983) Microautoradiographic studies of phloem  
 1405 loading and transport in the leaf of *Zea mays* L. Planta **159**: 193-206
- 1406 **Fritz E, Evert RF, Nasse H** (1989) Loading and transport of assimilates in different  
 1407 maize leaf bundles - Digital image analysis of <sup>14</sup>C microautoradiographs.  
 1408 Planta **178**: 1-9
- 1409 **Fukumorita T, Chino M** (1982) Sugar, amino acid and inorganic contents in rice  
 1410 phloem sap. Plant Cell Physiol **23**: 273-283
- 1411 **Geiger D** (2011) Plant sucrose transporters from a biophysical point of view. Mol  
 1412 Plant **4**: 395-406
- 1413 **Giaquinta RT, Lin W, Sadler NL, Franceschi VR** (1983) Pathway of phloem  
 1414 unloading of sucrose in corn roots. Plant Physiol **72**: 362-367
- 1415 **Godfray HCJ, Beddington JR, Crute IR, Haddad L, Lawrence D, Muir JF, Pretty J,**  
 1416 **Robinson S, Thomas SM, Toulmin C** (2010) Food security: The challenge of  
 1417 feeding 9 billion people. Science **327**: 812-818
- 1418 **Gottwald JR, Krysan PJ, Young JC, Evert RF, Sussman MR** (2000) Genetic  
 1419 evidence for the *in planta* role of phloem-specific plasma membrane sucrose  
 1420 transporters. Proc Natl Acad Sci USA **97**: 13979-13984
- 1421 **Gould N, Thorpe MR, Pritchard J, Christeller JT, Williams LE, Roeb G, Schurr U,**  
 1422 **Minchin PEH** (2012) *AtSUC2* has a role for sucrose retrieval along the  
 1423 phloem pathway: Evidence from carbon-11 tracer studies. Plant Sci **188-**  
 1424 **189**: 97-101
- 1425 **Grignon N, Touraine B, Durand M** (1989) 6(5)Carboxyfluorescein as a tracer of  
 1426 phloem sap translocation. Am J Bot **76**: 871-877
- 1427 **Grodzinski B, Jiao J, Leonardos ED** (1998) Estimating photosynthesis and  
 1428 concurrent export rates in C<sub>3</sub> and C<sub>4</sub> species at ambient and elevated CO<sub>2</sub>.  
 1429 Plant Physiol **117**: 207-215
- 1430 **Hackel A, Schauer N, Carrari F, Fernie AR, Grimm B, Kühn C** (2006) Sucrose  
 1431 transporter LeSUT1 and LeSUT2 inhibition affects tomato fruit development  
 1432 in different ways. Plant J. **45**: 180-192
- 1433 **Hafke JB, van Amerongen J-K, Kelling F, Furch ACU, Gaupels F, van Bel AJE**  
 1434 (2005) Thermodynamic battle for photosynthate acquisition between sieve  
 1435 tubes and adjoining parenchyma in transport phloem. Plant Physiol **138**:  
 1436 1527-1537
- 1437 **Haupt S, Duncan GH, Holzberg S, Oparka KJ** (2001) Evidence for symplastic  
 1438 phloem unloading in sink leaves of barley. Plant Physiol **125**: 209-218
- 1439 **Hayashi H, Chino M** (1986) Collection of pure phloem sap from wheat and its  
 1440 chemical composition. Plant Cell Physiol **27**: 1387-1393
- 1441 **Heyser W, Evert RF, Fritz E, Eschrich W** (1978) Sucrose in the free space of  
 1442 translocating maize leaf bundles. Plant Physiol **62**: 491-494

- 1443 **Huang M, Braun DM** (2010) Genetic analyses of cell death in maize (*Zea mays*,  
1444 Poaceae) leaves reveal a distinct pathway operating in the *camouflage1*  
1445 mutant. *Am J Bot* **97**: 357-364
- 1446 **Huang M, Slewinski TL, Baker RF, Janick-Buckner D, Buckner B, Johal GS,**  
1447 **Braun DM** (2009) Camouflage patterning in maize leaves results from a  
1448 defect in porphobilinogen deaminase. *Mol Plant* **2**: 773-789
- 1449 **Hukin D, Doering-Saad C, Thomas C, Pritchard J** (2002) Sensitivity of cell  
1450 hydraulic conductivity to mercury is coincident with symplasmic isolation  
1451 and expression of plasmalemma aquaporin genes in growing maize roots.  
1452 *Planta* **215**: 1047-1056
- 1453 **Ibraheem O, Botha CEJ, Bradley G, Dealtry G, Roux S** (2014) Rice sucrose  
1454 transporter1 (OsSUT1) up-regulation in xylem parenchyma is caused by  
1455 aphid feeding on rice leaf blade vascular bundles. *Plant Biol* **16**: 783-791
- 1456 **Ishimaru K, Hirose T, Aoki N, Takahashi S, Ono K, Yamamoto S, Wu J, Saji S,**  
1457 **Baba T, Ugaki M, Matsumoto T, Ohsugi R** (2001) Antisense expression of a  
1458 rice sucrose transporter OsSUT1 in rice (*Oryza sativa* L.). *Plant Cell Physiol*  
1459 **42**: 1181-1185
- 1460 **Jia W, Zhang L, Wu D, Liu S, Gong X, Cui Z, Cui N, Cao H, Rao L, Wang C** (2015)  
1461 Sucrose transporter AtSUC9 mediated by a low sucrose level is involved in  
1462 Arabidopsis abiotic stress resistance by regulating sucrose distribution and  
1463 ABA accumulation. *Plant Cell Physiol* **56**: 1574-1587
- 1464 **Jung B, Ludewig F, Schulz A, Meißner G, Wöstefeld N, Flügge U-I, Pommerrenig**  
1465 **B, Wirsching P, Sauer N, Koch W, Sommer F, Mühlhaus T, Schroda M,**  
1466 **Cuin TA, Graus D, Marten I, Hedrich R** (2015) Identification of the  
1467 transporter responsible for sucrose accumulation in sugar beet taproots. *Nat*  
1468 *Plants* **1**: 14001
- 1469 **Kühn C, Grof CPL** (2010) Sucrose transporters of higher plants. *Curr Opin Plant Biol*  
1470 **13**: 287-297
- 1471 **Lalonde S, Weise A, Walsh R, Ward JM, Frommer WB** (2003) Fusion to GFP  
1472 blocks intercellular trafficking of the sucrose transporter SUT1 leading to  
1473 accumulation in companion cells. *BMC Plant Biol* **3**: 8
- 1474 **Lalonde S, Wipf D, Frommer WB** (2004) Transport mechanisms for organic forms  
1475 of carbon and nitrogen between source and sink. *Annu Rev Plant Biol* **55**:  
1476 341-372
- 1477 **Lang-Pauluzzi I** (2000) The behaviour of the plasma membrane during  
1478 plasmolysis: a study by UV microscopy. *J Micro* **198**: 188-198
- 1479 **Larionov A, Krause A, Miller W** (2005) A standard curve based method for relative  
1480 real time PCR data processing. *BMC Bioinform* **6**: 1-16
- 1481 **Leach KA, McSteen PC, Braun DM** (2016) Genomic DNA isolation from maize (*Zea*  
1482 *mays*) leaves using a simple, high-throughput protocol. *Curr Prot Plant Biol* **1**:  
1483 15-27
- 1484 **Lemoine R, La Camera S, Atanassova R, Dédaldéchamp F, Allario T, Pourtau N,**  
1485 **Bonnemain J-L, Laloi M, Coutos-Thévenot P, Maurousset L, Faucher M,**  
1486 **Girousse C, Lemonnier P, Parrilla J, Durand M** (2013) Source to sink  
1487 transport and regulation by environmental factors. *Front Plant Sci* **4**: 272.  
1488 doi:210.3389/fpls.2013.00272

1489 **Li P, Ponnala L, Gandotra N, Wang L, Si Y, Tausta SL, Kebrom TH, Provart N,**  
1490 **Patel R, Myers CR, Reidel EJ, Turgeon R, Liu P, Sun Q, Nelson T, Brutnell**  
1491 **TP** (2010) The developmental dynamics of the maize leaf transcriptome. *Nat*  
1492 *Genet* **42**: 1060-1067

1493 **Lohaus G, Hussmann M, Pennewiss K, Schneider H, Zhu J-J, Sattelmacher B**  
1494 (2000) Solute balance of a maize (*Zea mays* L.) source leaf as affected by salt  
1495 treatment with special emphasis on phloem retranslocation and ion leaching.  
1496 *J Exp Bot* **51**: 1721-1732

1497 **Lohaus G, Pennewiss K, Sattelmacher B, Hussmann M, Muehling KH** (2001) Is  
1498 the infiltration-centrifugation technique appropriate for the isolation of  
1499 apoplastic fluid? A critical evaluation with different plant species. *Phys Plant*  
1500 **111**: 457-465

1501 **Lunn JE, Furbank RT** (1999) Tansley Review No. 105. Sucrose biosynthesis in C<sub>4</sub>  
1502 plants. *New Phytol* **143**: 221-237

1503 **Ma Y, Baker RF, Magallanes-Lundback M, DellaPenna D, Braun DM** (2008) *Tie-*  
1504 *dyed1* and *Sucrose export defective1* act independently to promote  
1505 carbohydrate export from maize leaves. *Planta* **227**: 527-538

1506 **Ma Y, Slewinski TL, Baker RF, Braun DM** (2009) *Tie-dyed1* encodes a novel,  
1507 phloem-expressed transmembrane protein that functions in carbohydrate  
1508 partitioning. *Plant Physiol* **149**: 181-194

1509 **Makela P, McLaughlin JE, Boyer JS** (2005) Imaging and quantifying carbohydrate  
1510 transport to the developing ovaries of maize. *Ann Bot* **96**: 939-949

1511 **Minchin PEH, Thorpe MR** (1987) Measurement of unloading and reloading of  
1512 photo-assimilate within the stem of bean. *J Exp Bot* **38**: 211-220

1513 **Mohanty A, Luo A, DeBlasio S, Ling X, Yang Y, Tuthill DE, Williams KE, Hill D,**  
1514 **Zadrozny T, Chan A, Sylvester AW, Jackson D** (2009) Advancing cell  
1515 biology and functional genomics in maize using fluorescent protein-tagged  
1516 lines. *Plant Physiol* **149**: 601-605

1517 **Ohshima T, Hayashi H, Chino M** (1990) Collection and chemical composition of  
1518 pure phloem sap from *Zea mays* L. *Plant Cell Physiol* **31**: 735-737

1519 **Patrick JW** (2012) Fundamentals of phloem transport physiology. *In* *Phloem*.  
1520 Wiley-Blackwell, pp 30-59

1521 **Patrick JW, Botha FC, Birch RG** (2013) Metabolic engineering of sugars and simple  
1522 sugar derivatives in plants. *Plant Biotech J* **11**: 142-156

1523 **Porter GA, Knievel DP, Shannon JC** (1985) Sugar efflux from maize (*Zea mays* L.)  
1524 pedicel tissue. *Plant Physiol* **77**: 524-531

1525 **Rae AL, Perroux JM, Grof CPL** (2005) Sucrose partitioning between vascular  
1526 bundles and storage parenchyma in the sugarcane stem: a potential role for  
1527 the ShSUT1 sucrose transporter. *Planta* **220**: 817-825

1528 **Reinders A, Sivitz A, Hsi A, Grof C, Perroux J, Ward JM** (2006) Sugarcane ShSUT1:  
1529 analysis of sucrose transport activity and inhibition by sucralose. *Plant Cell*  
1530 *Environ* **29**: 1871-1880

1531 **Reinders A, Sivitz AB, Ward JM** (2012) Evolution of plant sucrose uptake  
1532 transporters. *Front Plant Sci* **3**: 22. doi: 10.3389/fpls.2012.00022

1533 **Rennie EA, Turgeon R** (2009) A comprehensive picture of phloem loading  
1534 strategies. *Proc Natl Acad Sci USA* **106**: 14162-14167

1535 **Riesmeier JW, Willmitzer L, Frommer WB** (1992) Isolation and characterization  
1536 of a sucrose carrier cDNA from spinach by functional expression in yeast.  
1537 EMBO J **11**: 4705-4713

1538 **Riesmeier JW, Willmitzer L, Frommer WB** (1994) Evidence for an essential role  
1539 of the sucrose transporter in phloem loading and assimilate partitioning.  
1540 EMBO J **13**: 1-7

1541 **Rosenzweig C, Elliott J, Deryng D, Ruane AC, Müller C, Arneth A, Boote KJ,**  
1542 **Folberth C, Glotter M, Khabarov N, Neumann K, Piontek F, Pugh TAM,**  
1543 **Schmid E, Stehfest E, Yang H, Jones JW** (2014) Assessing agricultural risks  
1544 of climate change in the 21st century in a global gridded crop model  
1545 intercomparison. Proc Natl Acad Sci USA **111**: 3268-3273

1546 **Rotsch D, Brossard T, Bihmidine S, Ying W, Gaddam V, Harmata M, Robertson**  
1547 **JD, Swyers M, Jurisson SS, Braun DM** (2015) Radiosynthesis of 6'-deoxy-  
1548 6'<sup>[18F]</sup>fluorosucrose via automated synthesis and its utility to study *in vivo*  
1549 sucrose transport in maize (*Zea mays*) leaves. PLOS ONE **10**: e0128989

1550 **Russell SH, Evert RF** (1985) Leaf vasculature in *Zea mays* L. Planta **164**: 448-458

1551 **Ruzin S** (1999) Plant Microtechnique and Microscopy. Oxford University Press, New  
1552 York

1553 **Sauer N** (2007) Molecular physiology of higher plant sucrose transporters. FEBS  
1554 Lett **581**: 2309-2317

1555 **Schmitt B, Stadler R, Sauer N** (2008) Immunolocalization of Solanaceous SUT1  
1556 proteins in companion cells and xylem parenchyma: New perspectives for  
1557 phloem loading and transport. Plant Physiol **148**: 187-199

1558 **Scofield G, Hirose T, Gaudron J, Upadhyaya N, Ohsugi R, Furbank RT** (2002)  
1559 Antisense suppression of the rice sucrose transporter gene, *OsSUT1*, leads to  
1560 impaired grain filling and germination but does not affect photosynthesis.  
1561 Funct Plant Biol **29**: 815-826

1562 **Scofield GN, Hirose T, Aoki N, Furbank RT** (2007) Involvement of the sucrose  
1563 transporter, OsSUT1, in the long-distance pathway for assimilate transport in  
1564 rice. J Exp Bot **58**: 3155-3169

1565 **Sivitz AB, Reinders A, Ward JM** (2005) Analysis of the transport activity of barley  
1566 sucrose transporter HvSUT1. Plant Cell Physiol **46**: 1666-1673

1567 **Slewinski TL** (2013) Using evolution as a guide to engineer Kranz-type C<sub>4</sub>  
1568 photosynthesis. Front Plant Sci **4**: 212. doi:210.3389/fpls.2013.00212

1569 **Slewinski TL, Baker RF, Stubert A, Braun DM** (2012) *Tie-dyed2* encodes a callose  
1570 synthase that functions in vein development and affects symplastic  
1571 trafficking within the phloem of maize leaves. Plant Physiol **160**: 1540-1550

1572 **Slewinski TL, Braun DM** (2010a) Current perspectives on the regulation of whole-  
1573 plant carbohydrate partitioning. Plant Sci **178**: 341-349

1574 **Slewinski TL, Braun DM** (2010b) The *psychedelic* genes of maize redundantly  
1575 promote carbohydrate export from leaves. Genetics **185**: 221-232

1576 **Slewinski TL, Garg A, Johal GS, Braun DM** (2010) Maize SUT1 functions in phloem  
1577 loading. Plant Sig Behav **5**: 687-690

1578 **Slewinski TL, Meeley R, Braun DM** (2009) *Sucrose transporter1* functions in  
1579 phloem loading in maize leaves. J Exp Bot **60**: 881-892

1580 **Slewinski TL, Zhang C, Turgeon R** (2013) Structural and functional heterogeneity  
1581 in phloem loading and transport. *Front Plant Sci* **4**: 244. doi:  
1582 210.3389/fpls.2013.00244

1583 **Smith JM, Leslie ME, Robinson SJ, Korasick DA, Zhang T, Backues SK, Cornish**  
1584 **PV, Koo AJ, Bednarek SY, Heese A** (2014) Loss of *Arabidopsis thaliana*  
1585 Dynamin-Related Protein 2B reveals separation of innate immune signaling  
1586 pathways. *PLoS Pathog* **10**: e1004578

1587 **Srivastava AC, Ganesan S, Ismail IO, Ayre BG** (2008) Functional characterization  
1588 of the *Arabidopsis thaliana* AtSUC2 Suc/H<sup>+</sup> symporter by tissue-specific  
1589 complementation reveals an essential role in phloem loading but not in long-  
1590 distance transport. *Plant Physiol* **147**: 200-211

1591 **Sun Y, Reinders A, LaFleur KR, Mori T, Ward JM** (2010) Transport activity of rice  
1592 sucrose transporters OsSUT1 and OsSUT5. *Plant Cell Physiol* **51**: 114-122

1593 **Tang A-C, Boyer JS** (2013) Differences in membrane selectivity drive phloem  
1594 transport to the apoplast from which maize florets develop. *Ann Bot* **111**:  
1595 551-562

1596 **van Bel AJE** (1996) Interaction between sieve element and companion cell and the  
1597 consequences for photoassimilate distribution. Two structural hardware  
1598 frames with associated physiological software packages in dicotyledons? *J*  
1599 *Exp Bot* **47**: 1129-1140

1600 **van Bel AJE** (2003) Transport phloem: low profile, high impact. *Plant Physiol* **131**:  
1601 1509-1510

1602 **van Bel AJE, Knoblauch M** (2000) Sieve element and companion cell: the story of  
1603 the comatose patient and the hyperactive nurse. *Funct Plant Biol* **27**: 477-  
1604 487

1605 **Warmbrodt RD** (1985) Studies on the root of *Zea mays* L.-structure of the  
1606 adventitious roots with respect to phloem unloading. *Bot Gazet*: 169-180

1607 **Weiner H, Blechschmidt-Schneider S, Mohme H, Eschrich W, Heldt HW** (1991)  
1608 Phloem transport of amino acids, comparison of amino acid contents of  
1609 maize leaves and of the sieve tube exudate. *Plant Physiol Biochem* **29**: 19-23

1610 **Yadav UP, Ayre BG, Bush DR** (2015) Transgenic approaches to altering carbon and  
1611 nitrogen partitioning in whole plants: assessing the potential to improve crop  
1612 yields and nutritional quality. *Front Plant Sci* **6**: 275. doi:  
1613 210.3389/fpls.2015.00275

1614 **Zelazny E, Borst JW, Muylaert M, Batoko H, Hemminga MA, Chaumont F** (2007)  
1615 FRET imaging in living maize cells reveals that plasma membrane aquaporins  
1616 interact to regulate their subcellular localization. *Proc Natl Acad Sci USA* **104**:  
1617 12359-12364

1618 **Zhang WH, Zhou YC, Dibley KE, Tyerman SD, Furbank RT, Patrick JW** (2007a)  
1619 Nutrient loading of developing seeds. *Funct Plant Biol* **34**: 314-331

1620 **Zhang X, Madi S, Borsuk L, Nettleton D, Elshire RJ, Buckner B, Janick-Buckner**  
1621 **D, Beck J, Timmermans M, Schnable PS, Scanlon MJ** (2007b) Laser  
1622 microdissection of *narrow sheath* mutant maize uncovers novel gene  
1623 expression in the shoot apical meristem. *PLoS Genet* **3**: e101  
1624  
1625

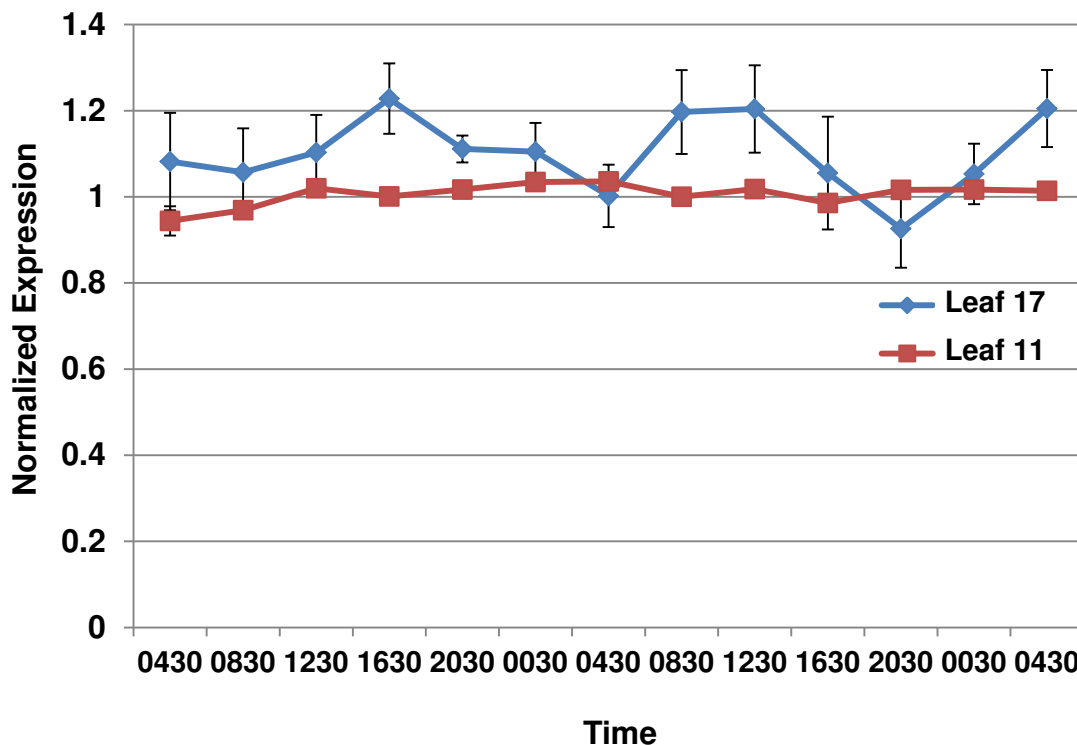


**Figure 1.** ZmSut1 expression is stable and does not cycle diurnally in adult maize leaves. qRT-PCR expression of ZmSut1 in B73 mature and immature leaves over 48 hrs. Samples were harvested every 4 hrs. Measurements are average expression values for 10 biological samples of ZmSut1 relative to exogenously supplied luciferase mRNA used as a normalization control. Values are relative units. Red squares indicate mature leaf 11 source tissue and blue diamonds indicate immature leaf 17 sink tissue. Error bars show standard error.

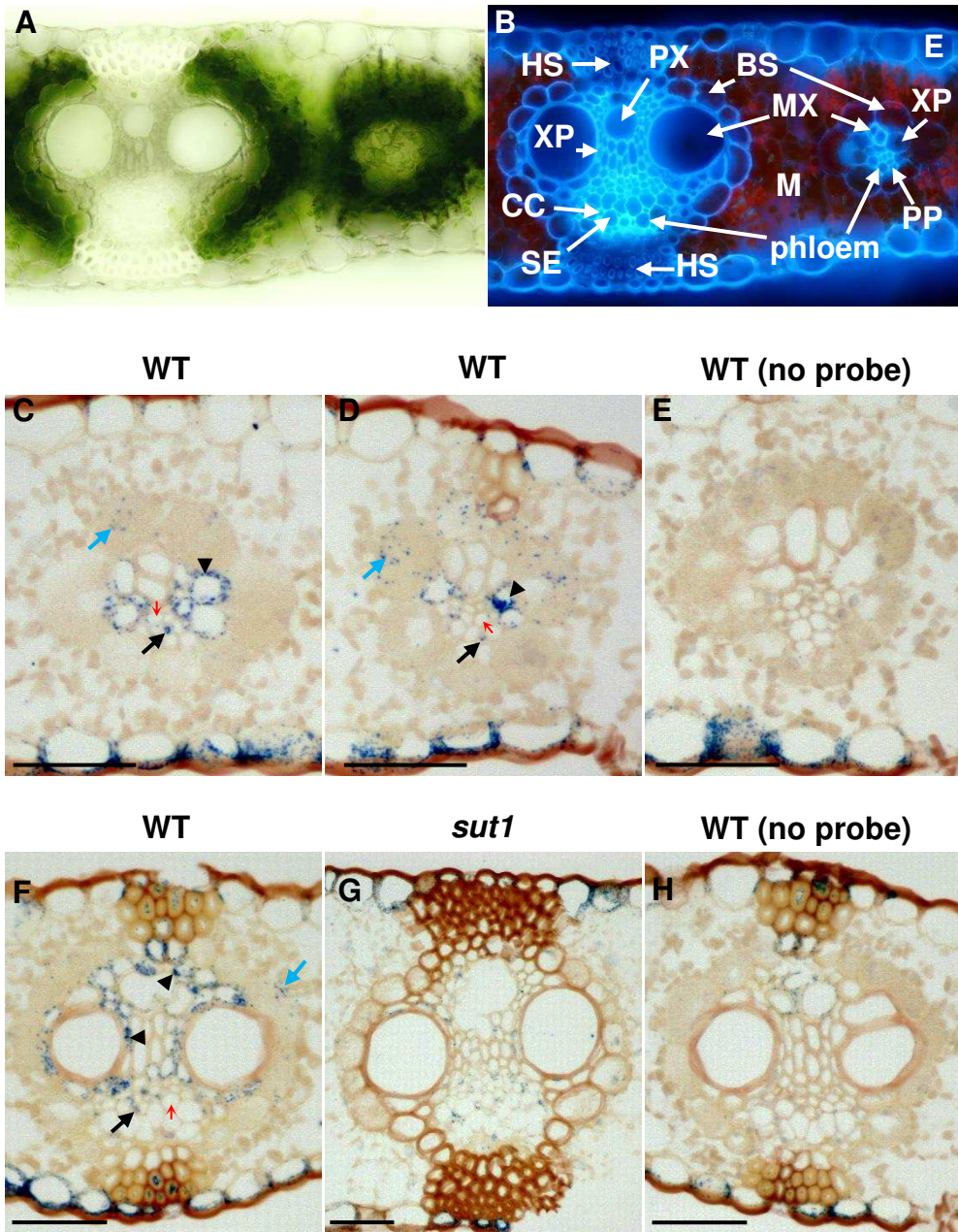


**Figure 2.** RNA in situ hybridization demonstrates that *ZmSut1* is expressed in the CC, XP, PP, and BS cells of mature leaf blades. Expression is revealed by the blue precipitate. A, B. Transverse section through a B73 leaf showing the anatomy of a lateral vein (left) and a small vein (right) under bright-field (A) and UV autofluorescence (B). The different cell types are labelled: BS, bundle sheath, CC, companion cell, E, epidermis, HS, hypodermal sclerenchyma, M, mesophyll, MX, metaxylem element, PP, phloem parenchyma, PX, protoxylem lacunae, SE, sieve element, XP, xylem parenchyma. C, D, F. Wild-type (WT) B73 mature leaf sections hybridized with *ZmSut1* probe. G. *zmsut1* mutant leaf section hybridized with *ZmSut1* probe. E, H. Wild-type B73 mature leaf sections developed without probe. C, E show small veins, D shows an intermediate vein, and F-H show lateral veins. Black arrows point to CC; red arrows to SE; blue arrows to BS cells; arrowheads to large XP cells. Scale bar = 50  $\mu\text{m}$ .

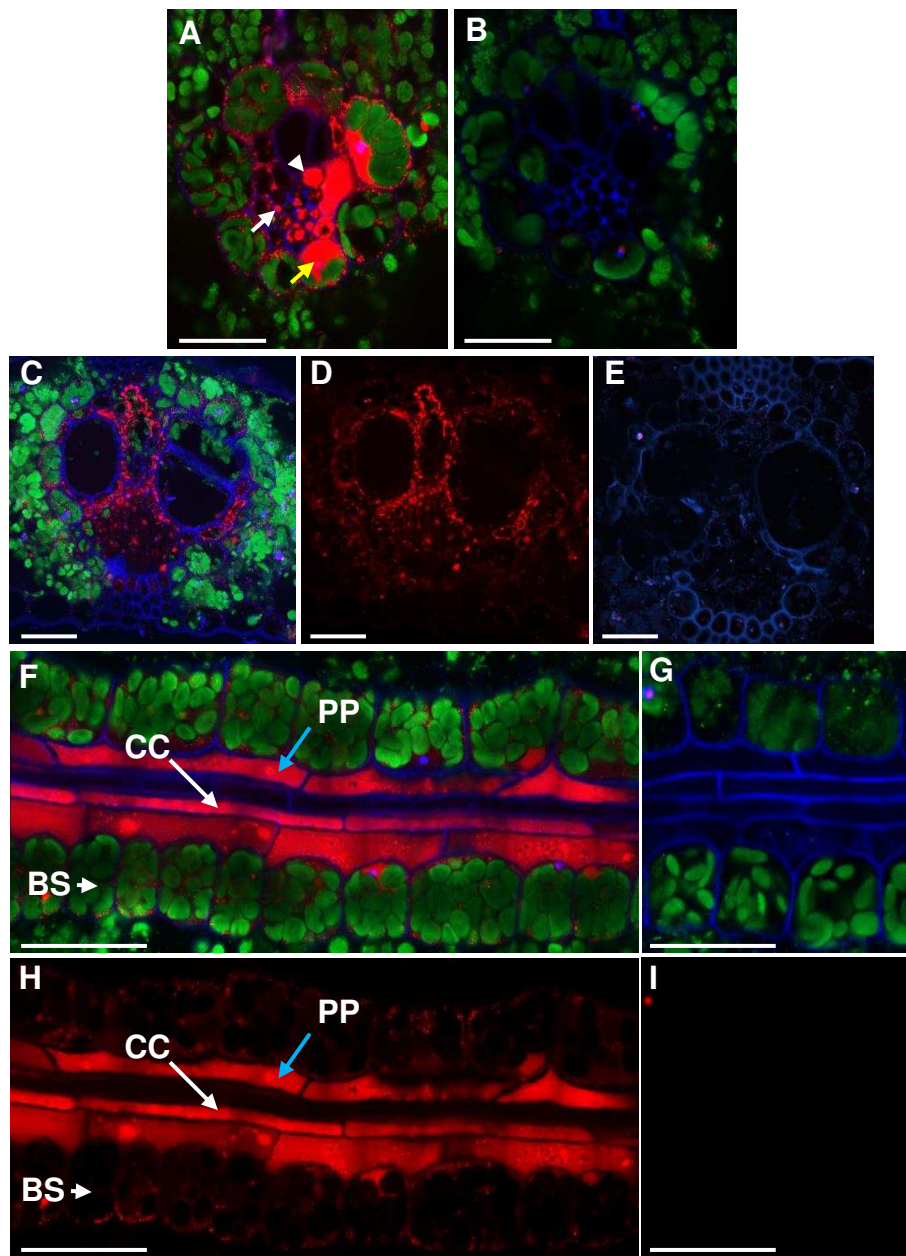


**Figure 3.** The pZmSut1::RFP transcriptional reporter gene recapitulates ZmSut1 expression observed by RNA in situ hybridization. A-I. Confocal images showing expression of pZmSut1::RFP transgene in transverse and paradermal leaf sections. A. Transverse section of a minor vein showing RFP is expressed in the CC (white arrow), XP (arrowhead), PP, and to a more limited extent in the BS cells (yellow arrow). The cell outlines were visualized with aniline-blue staining; the green signal represents chlorophyll autofluorescence. B. Transverse section of a minor vein from a plant lacking the transgene. C. Transverse section of a lateral vein showing RFP expression in CC, XP, PP, and to a lesser extent in BS cells. Blue signal shows cell walls and green signal is chlorophyll autofluorescence. D. Same image as in C, but only showing RFP expression. E. Transverse section of a lateral vein of a non-transgenic control showing no RFP expression. Blue signal shows cellular anatomy. F. Paradermal section of a minor vein showing RFP expression in the CC, PP, and to a lesser extent in the BS cells. G. Paradermal section of non-transgenic control showing no RFP expression. Blue signal shows cell walls and green signal is chlorophyll autofluorescence. H. Same section as in F showing only RFP signal. I. Same section as in G showing only red channel. BS, bundle sheath cell, CC, companion cell, PP, phloem parenchyma cell. Scale bar = 25  $\mu\text{m}$ .

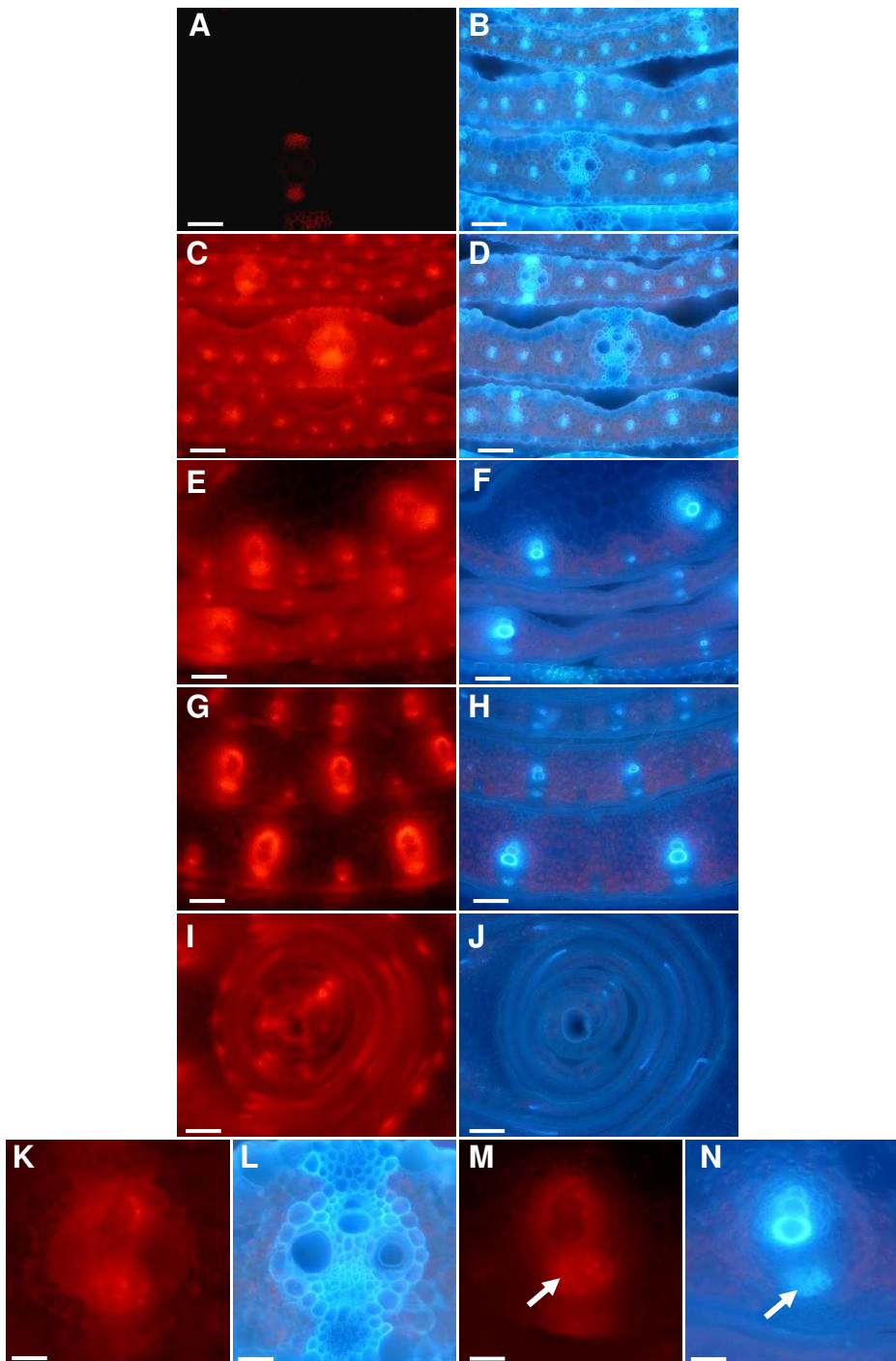


**Figure 4.** pZmSut1::RFP is expressed early in vein development in sink leaves. Epi-fluorescence microscope images of pZmSut1::RFP expression in developing leaves. A-J. Transverse cross-sections through inner developing leaves of 2-week-old seedlings. A, B. Non-transgenic control sections. Panel A shows autofluorescence of HS cell walls. C-J. Transverse sections of pZmSut1::RFP transgenic leaves located approximately half-way between the blade-sheath boundary and the base of the enclosing mature leaf (C, D), at the base of immature blade tissue (E, F), in immature sheath tissue (G, H), and located just above the meristem (I, J). Panels C, E, G, I, K, M show RFP images. Panels B, D, F, H, J, L, N show UV autofluorescence images. K, L. Close up of the lateral vein in middle of panels C, D. M, N. Close up of a developing lateral vein in panels E, F. Expression is observed in the protophloem (white arrow). Note with the RFP filter cube, at these exposure settings, virtually no red signal from chlorophyll is detected (cf. Fig. 4A, B). Scale bar in A-J = 100  $\mu$ m. Scale bars in K-N = 25  $\mu$ m.

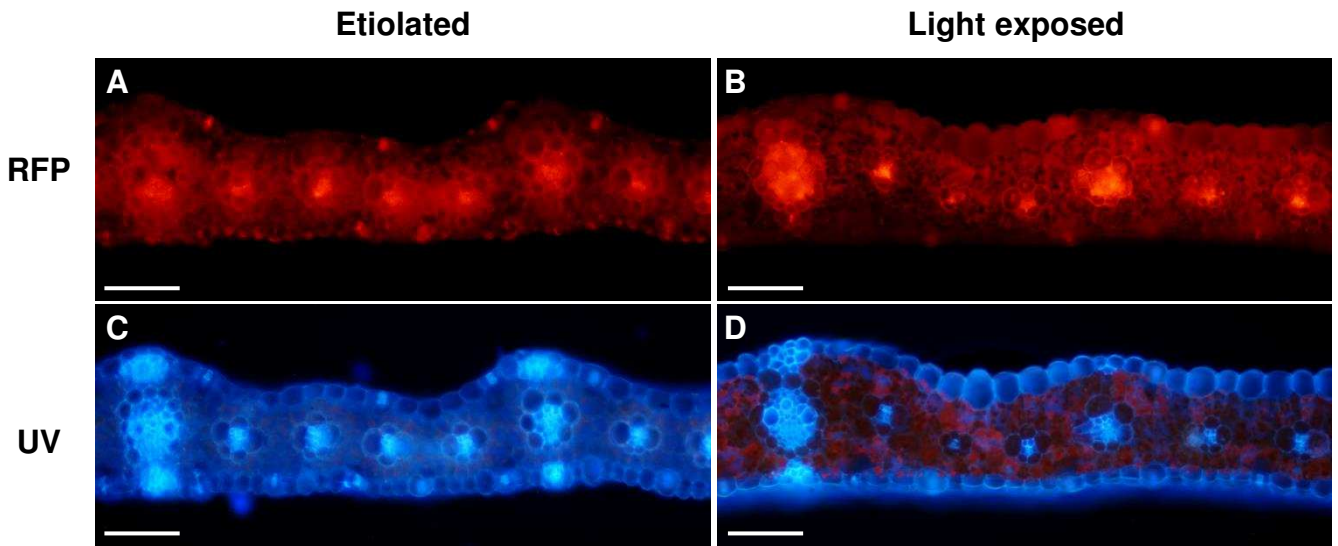


**Figure 5.** pZmSut1::RFP expression in leaves is induced in veins upon shifting plants from growth in the dark to the light. A, B. RFP images. C, D. UV autofluorescence images. A, C show an etiolated sink-leaf cross-section. B, D show a leaf cross-section after shifting plants into the light and the leaf matured as source tissue. Note with the RFP filter cube, at these exposure settings, virtually none of the red signal is from chlorophyll. Scale bar = 100  $\mu$ m.

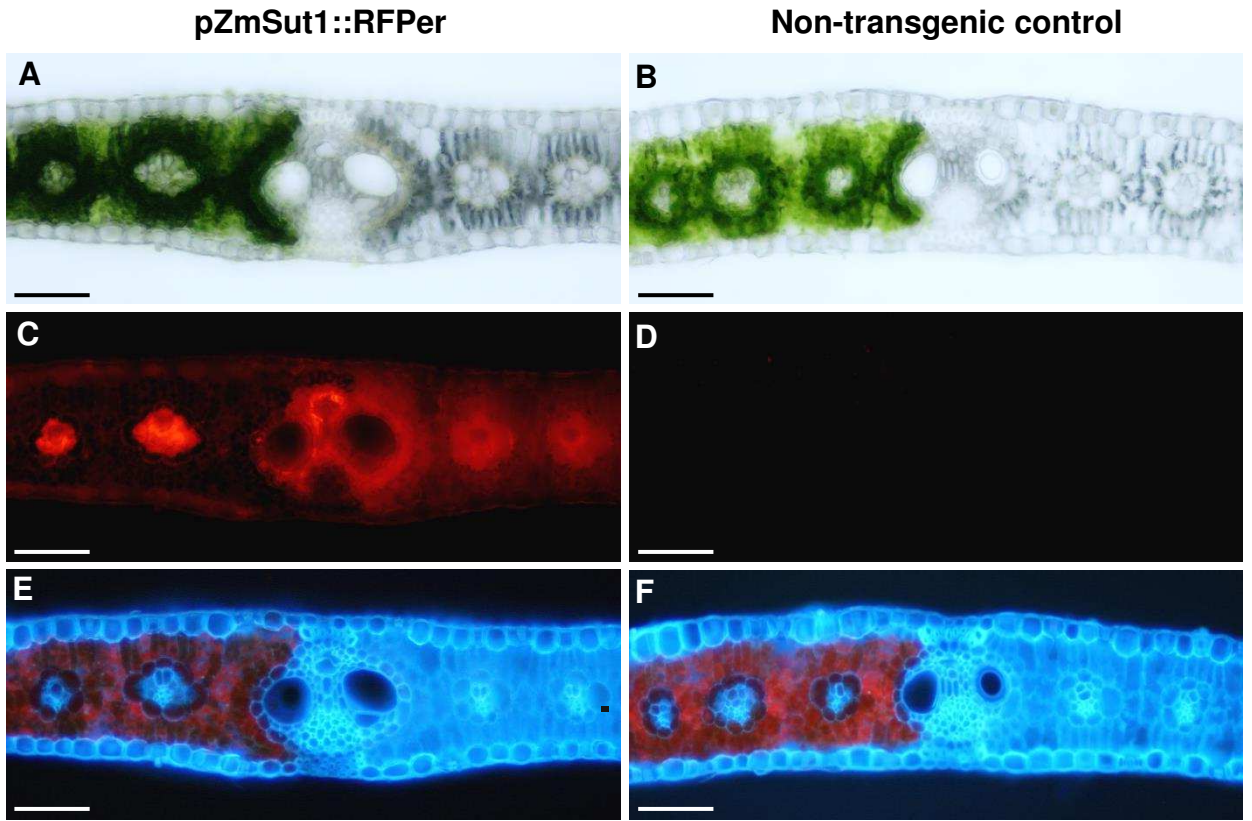


**Figure 6.** pZmSut1::RFP expression is induced in veins of mature source tissue compared with albino sink tissue in variegated *sr2* mutant leaves. A, C, E show a cross-section through a green-white border of a *sr2* leaf expressing pZmSut1::RFP. B, D, F show a non-transgenic control variegated *sr2* mutant leaf. A, B. Bright-field. C, D. RFP signal. E, F. UV autofluorescence. Note with the RFP filter cube, at these exposure settings, virtually no red signal from chlorophyll is detected (cf. Fig. 6D, F). Scale bar = 100  $\mu$ m.

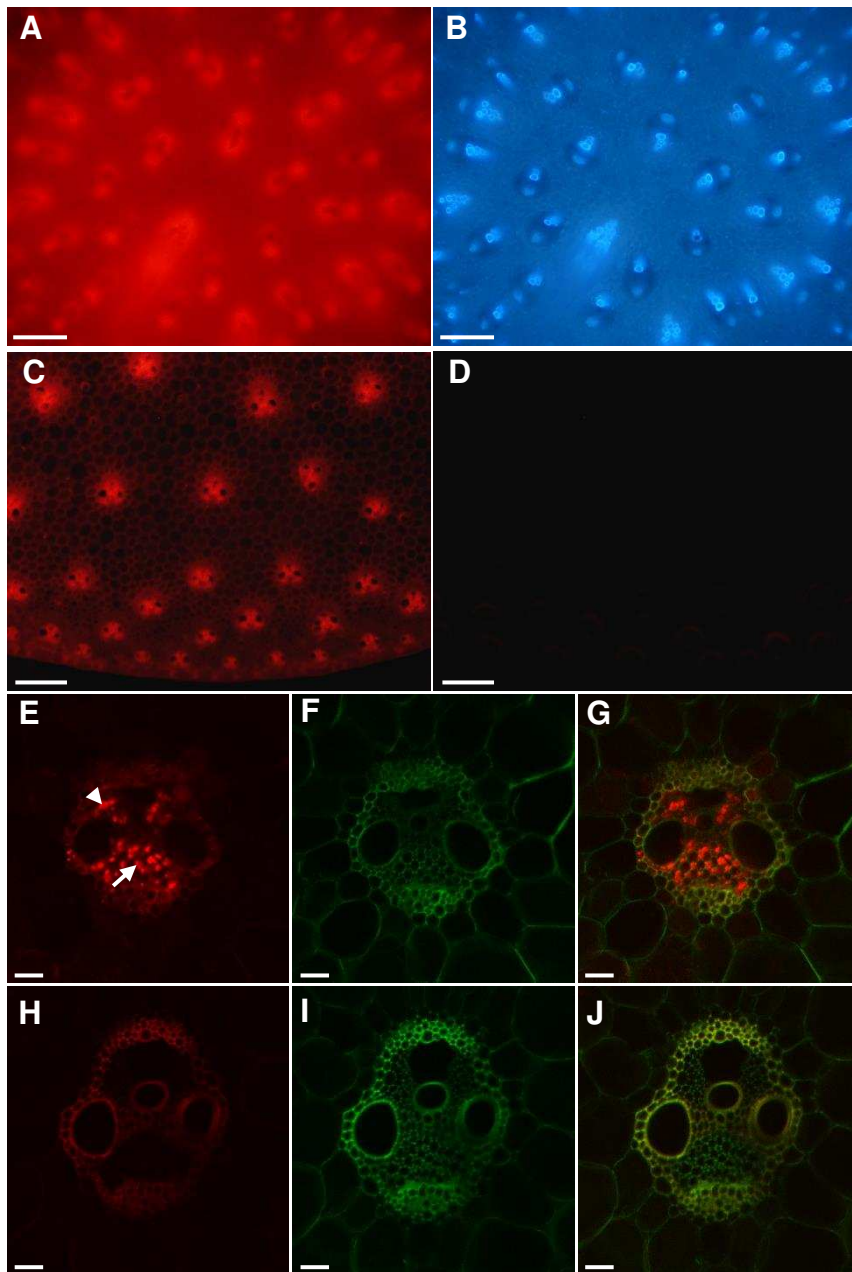


**Figure 7.** pZmSut1::RFP expression is broad initially in developing stem, but becomes restricted in mature stem veins. Transverse sections showing expression of the pZmSut1::RFP transgene in immature (A) and mature stem (C). B. UV autofluorescence of tissue shown in panel A. D. Transverse section of mature stem of non-transgenic control. A, C, D. RFP channel. A. Expression of the transgene is initially strongest in the protoxylem and protophloem, with lower signal in the developing parenchyma cells. C. At maturity pZmSut1::RFP expression is highest in veins, with low level in the storage parenchyma. E-G. Confocal images of mature stem vein showing pZmSut1::RFP expression in the XP cells (arrowhead) and CC (arrow). H-J. Confocal images of mature stem vein of non-transgenic control exhibiting autofluorescence. E, H. RFP channel. F, I. UV autofluorescence showing cell walls. G. Merged image of E and F. J. Merged image of H and I. Note with the RFP filter cube, at these exposure settings, virtually no red signal from chlorophyll is detected (cf. Fig. 7C, D). Scale bar in A, B = 250  $\mu$ m; in C, D = 500  $\mu$ m; in E-J = 25  $\mu$ m.

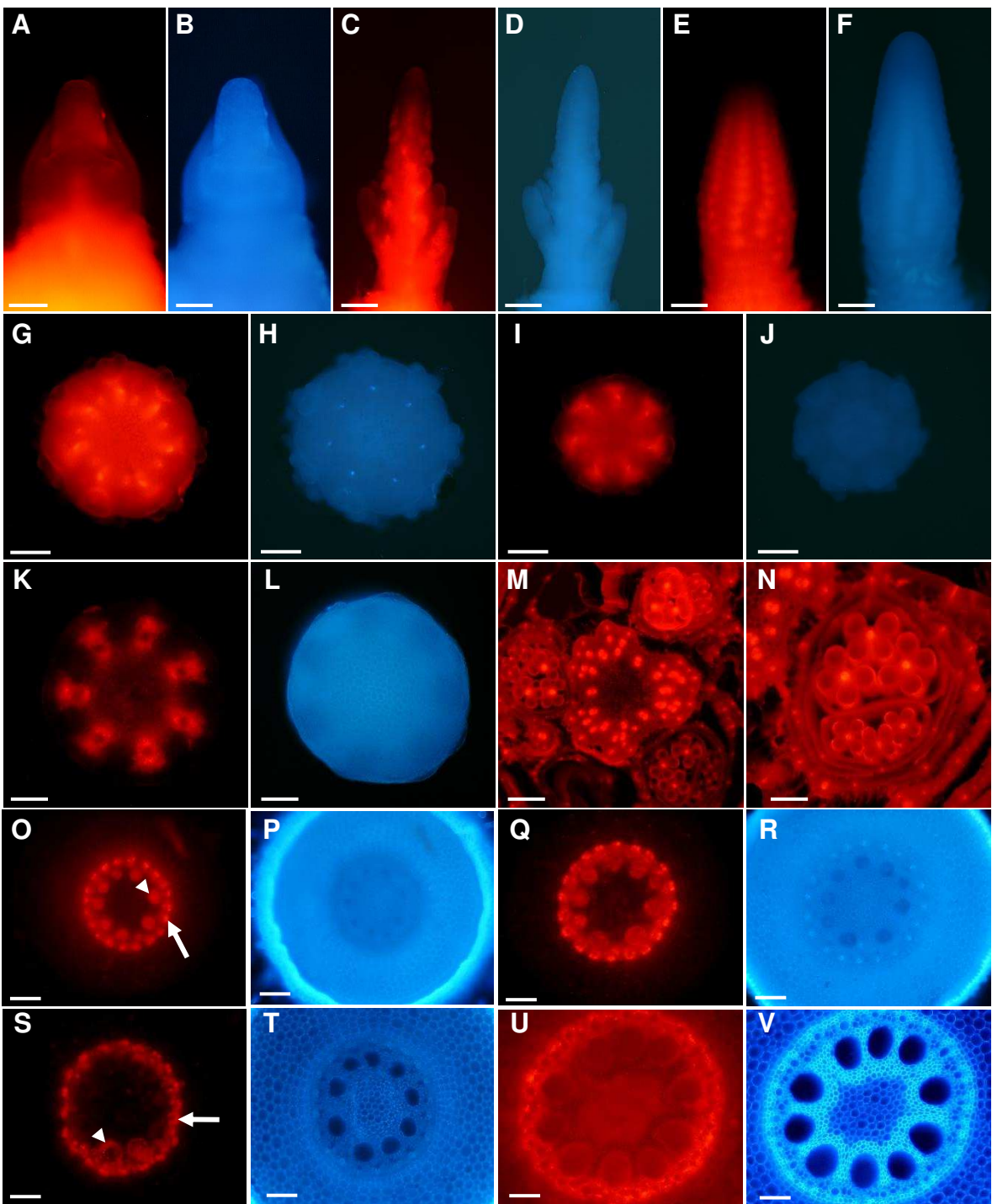


**Figure 8.** pZmSut1::RFP displays broad expression in multiple vegetative and reproductive sink tissues. Epi-fluorescent microscope images of pZmSut1::RFP expression in the shoot apical meristem, in developing tassels and ears, and in developing roots. A, C, E, G, I, K, M, N, O, Q, S, U. RFP signal. B, D, F, H, J, L, P, R, T, V. UV autofluorescence of corresponding tissue. A, B. Shoot apical meristem. C, D. Developing tassel. E-L. Developing ear. G-L represent cross-sections through the developing ear. M, N. Maturing tassel. O-V. Developing root. O. Transverse section near the root tip showing RFP expression is largely restricted to the phloem (arrow) and xylem (arrowhead). Q. Section slightly higher than that of O showing RFP expression in the phloem and developing xylem elements. S. Section at cusp between developing and mature xylem cells. Arrowhead indicates xylem element presumably undergoing autolysis. Arrow indicates phloem. U. Mature root. RFP expression can be seen in the phloem and diffusely throughout the root. Scale bar = 100  $\mu$ m for A, B, K, L, O-V; 250  $\mu$ m for C-J, N; 500  $\mu$ m for M. Exposure times for panels A, E, G, I, N = 750 ms; for C = 4 s; for K, M = 2 s. for O, Q, S, U = 1 s.

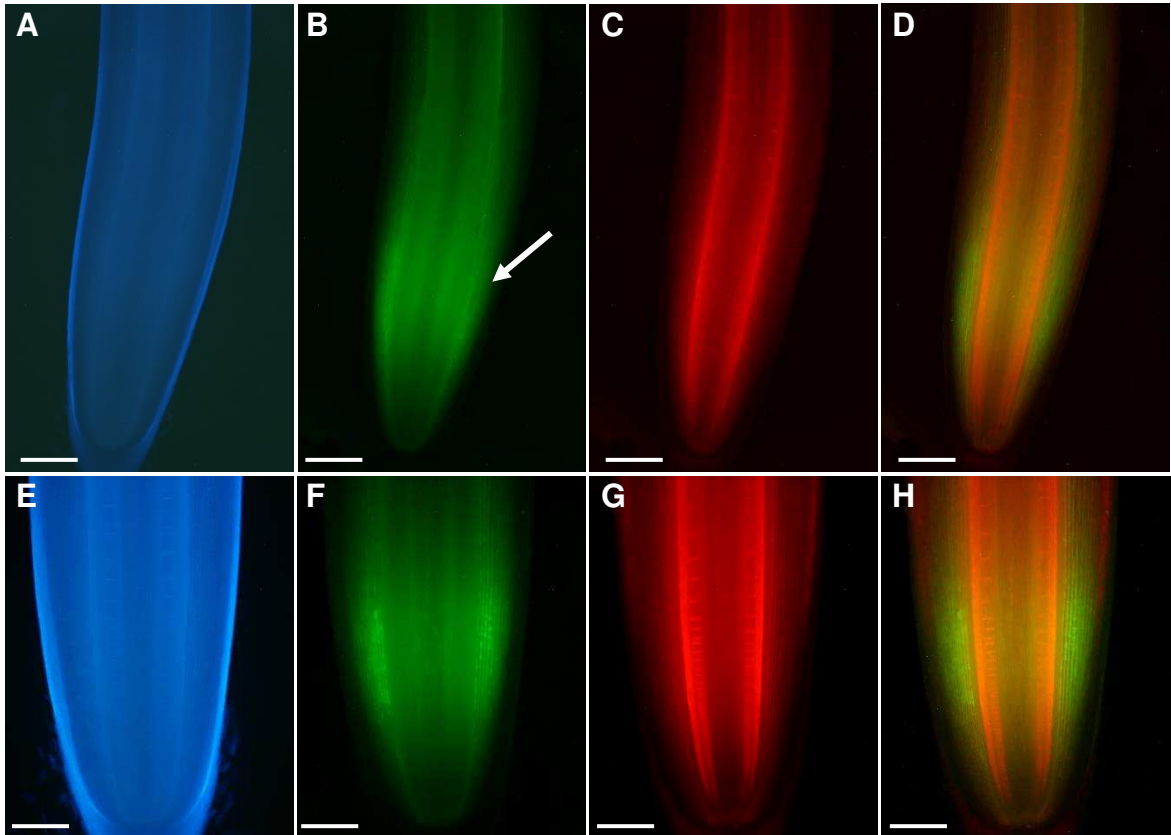


**Figure 9.** pZmSut1::RFP expression overlaps the phloem unloading zone identified by CF efflux into cortical cells of a pZmSut1::RFP transgenic root. A, E. UV autofluorescence. B, F. CF signal. White arrow indicates region of CF efflux from phloem into cortical cells. C, G. RFP signal. D, H. Overlay of the CF and RFP signals. E, F, G, and H are closer views of A, B, C, and D, respectively. Scale bar in A-D = 500  $\mu$ m; E-H = 250  $\mu$ m.

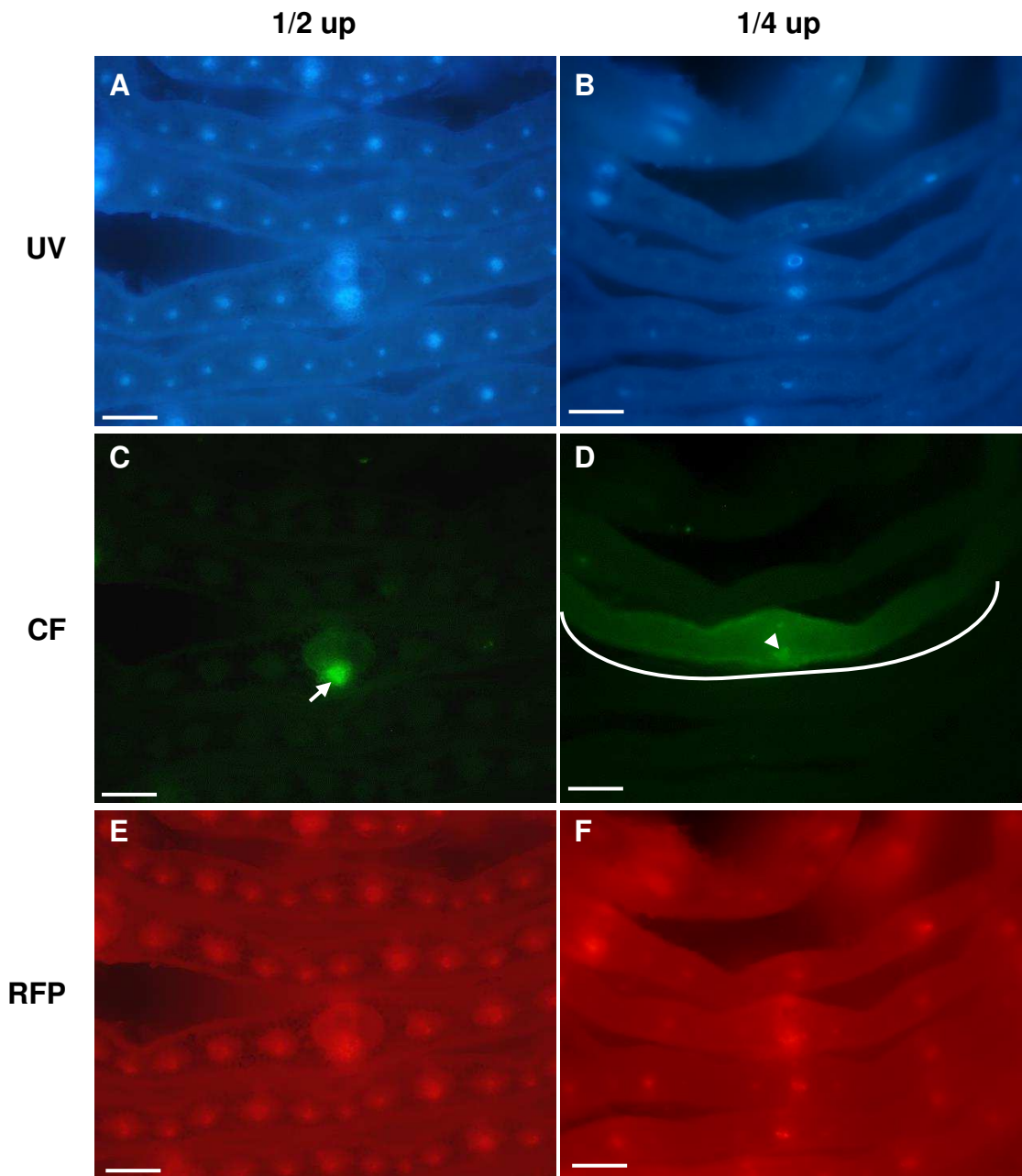


**Figure 10.** Developing leaves exhibit either symplasmic or apoplasmic phloem unloading in distinct regions that overlap pZmSut1::RFP expression. A, C, E show a cross-section taken approximately half-way up the blade of a developing pZmSut1::RFP expressing sink leaf. B, D, F show a cross-section taken approximately a quarter-way up the blade from the base of the same developing sink leaf. A, B. UV autofluorescence. C, D. CF signal. C. Arrow shows CF confinement within the symplasmically isolated phloem. D. Arrowhead shows vein symplasmically unloading CF into adjacent cells. CF movement marked by white bracket. E, F. RFP signal. Scale bar = 100  $\mu$ m.

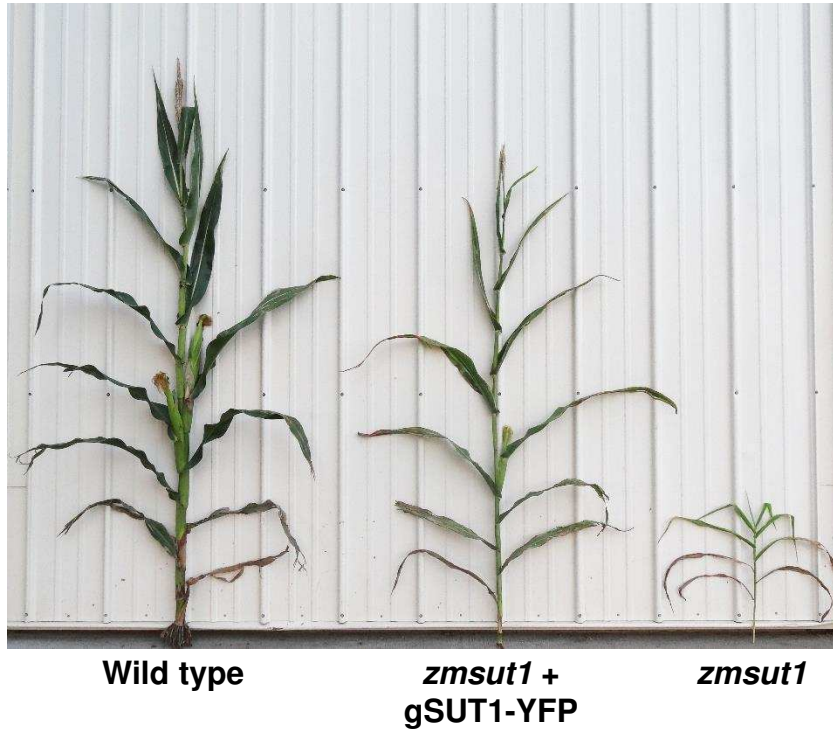


**Figure 11.** The gSut1-YFP transgene largely complements the *zmsut1* mutant phenotype. *zmsut1* homozygous mutant plants carrying the transgene (middle) grew to near wild-type height (left), and produced tassels that shed pollen and ears that produced silks. By contrast, the *zmsut1* homozygous mutants (right) that lacked the transgene and survived were stunted and typically failed to undergo anthesis or produce ears.

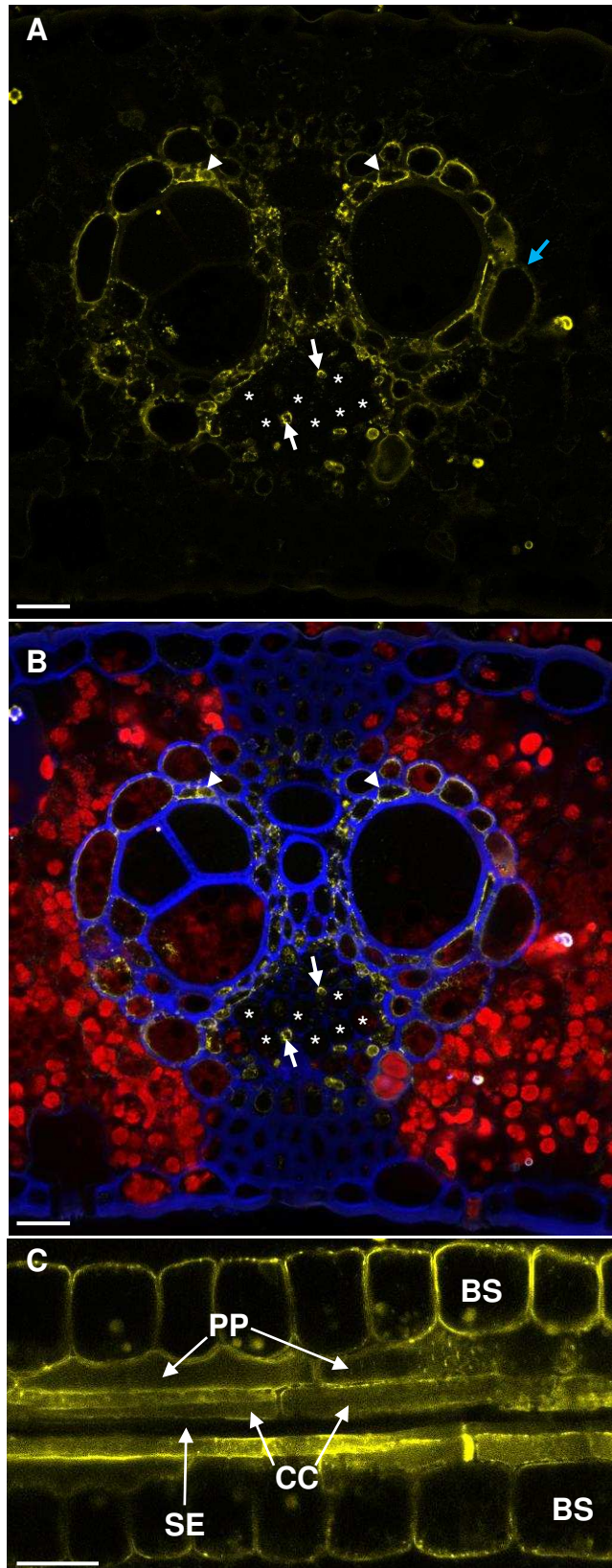


**Figure 12.** A ZmSUT1 protein translational fusion shows the same cellular expression pattern as observed with RNA in situ hybridization. Confocal images of the ZmSUT1 protein translationally fused at the C-terminus with YFP in transverse and paradermal leaf sections. A, B. Transverse section of a leaf lateral vein showing gSUT1-YFP is expressed in CC (arrows), XP (arrowheads), PP, and BS cells (blue arrow). Asterisks indicate SE. C. Paradermal section of a leaf minor vein showing gSUT1-YFP expression. A,C. YFP signal. B. Combined YFP, cell wall autofluorescence in blue, and chlorophyll autofluorescence in red. BS, bundle sheath cells, CC, companion cells, PP, phloem parenchyma cells, SE, sieve element. Scale bar = 25 μm.

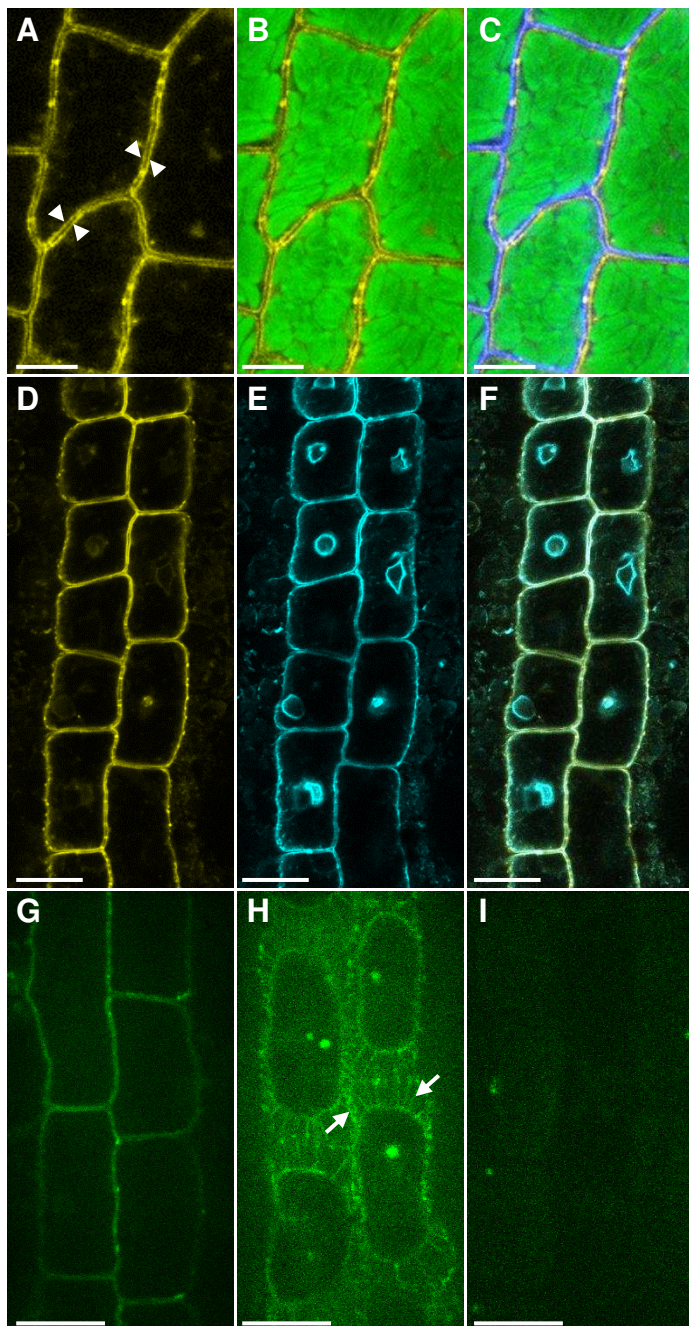


**Figure 13.** ZmSUT1 localizes to the plasma membrane. Confocal images of the expression of the SUT1 protein fused at the C-terminus with YFP. A-C. Paradermal section of a leaf minor vein focused on the BS cells. A. YFP signal. Arrowheads indicate YFP localization in two adjacent cells, separated by their shared cell wall. B. Combined YFP and chloroplasts (green). C. Combined YFP, chloroplasts, and cell wall (blue). D-F. Paradermal section of a leaf minor vein focused on the BS cells of a gSUT1-YFP and PIP2-1-CFP transgenic plant. D. YFP signal. E. CFP signal. F. Combined YFP and CFP signal. G-I. Spinning disc confocal image supporting ZmSUT1-YFP plasma membrane localization. G. Pre-plasmolysis YFP signal located at cell periphery. H. After plasmolysis with 0.75 M NaCl the plasma membrane has retracted; however, the plasma membrane is attached to the cell wall at the PD, resulting in the Hechtian strands (arrows). I. Non-transgenic control section. Scale bar = 10  $\mu\text{m}$  for A-C, = 25  $\mu\text{m}$  for D-I.

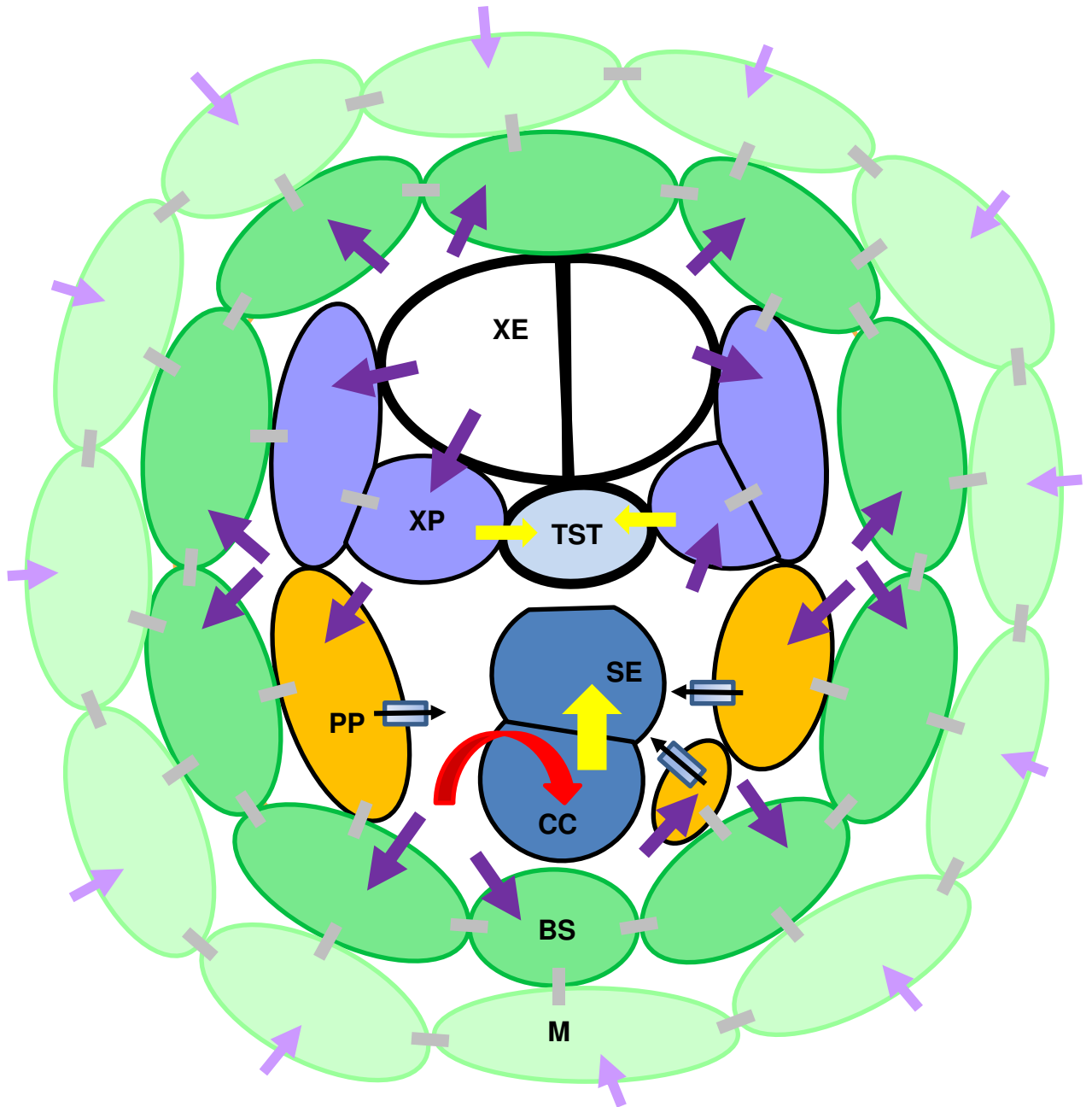


**Figure 14.** Model for dual functions of ZmSut1 in phloem loading and retrieval. Red arrow indicates ZmSUT1 loading sucrose into CC. Dark purple arrows indicate ZmSUT1 retrieving sucrose into non-conducting vascular cells; light purple arrows show ZmSUT1 recovering sucrose from leaf apoplast into M cells. Yellow arrows show symplasmic sucrose movement. Grey rectangles represent symplasmic connectivity through PD. Light blue rectangles with black arrows represent SWEET proteins effluxing sucrose to the apoplast of PP cells. Beige color represents vein apoplast. BS, bundle sheath cell, CC, companion cell, M, mesophyll cell, PP, phloem parenchyma cell, SE, sieve element, TST, thick-walled sieve element, XE, xylem element, XP, xylem parenchyma cell.

## Parsed Citations

**Ainsworth EA, Bush DR (2011) Carbohydrate export from the leaf: a highly regulated process and target to enhance photosynthesis and productivity. Plant Physiol 155: 64-69**

Pubmed: [Author and Title](#)

CrossRef: [Author and Title](#)

Google Scholar: [Author Only](#) [Title Only](#) [Author and Title](#)

**Antony G, Zhou J, Huang S, Li T, Liu B, White F, Yang B (2010) Rice xa13 recessive resistance to bacterial blight is defeated by induction of the disease susceptibility gene Os-11N3. Plant Cell 22: 3864-3876**

Pubmed: [Author and Title](#)

CrossRef: [Author and Title](#)

Google Scholar: [Author Only](#) [Title Only](#) [Author and Title](#)

**Aoki N, Hirose T, Scofield GN, Whitfield PR, Furbank RT (2003) The sucrose transporter gene family in rice. Plant Cell Physiol 44: 223-232**

Pubmed: [Author and Title](#)

CrossRef: [Author and Title](#)

Google Scholar: [Author Only](#) [Title Only](#) [Author and Title](#)

**Aoki N, Hirose T, Takahashi S, Ono K, Ishimaru K, Ohsugi R (1999) Molecular cloning and expression analysis of a gene for a sucrose transporter in maize (*Zea mays* L.). Plant Cell Physiol 40: 1072-1078**

Pubmed: [Author and Title](#)

CrossRef: [Author and Title](#)

Google Scholar: [Author Only](#) [Title Only](#) [Author and Title](#)

**Aoki N, Scofield GN, Wang X-D, Patrick JW, Offler CE, Furbank RT (2004) Expression and localisation analysis of the wheat sucrose transporter TaSUT1 in vegetative tissues. Planta 219: 176-184**

Pubmed: [Author and Title](#)

CrossRef: [Author and Title](#)

Google Scholar: [Author Only](#) [Title Only](#) [Author and Title](#)

**Ayre BG (2011) Membrane-transport systems for sucrose in relation to whole-plant carbon partitioning. Mol Plant 4: 377-394**

Pubmed: [Author and Title](#)

CrossRef: [Author and Title](#)

Google Scholar: [Author Only](#) [Title Only](#) [Author and Title](#)

**Baker RF, Braun DM (2007) tie-dyed1 functions non-cell autonomously to control carbohydrate accumulation in maize leaves. Plant Physiol 144: 867-878**

Pubmed: [Author and Title](#)

CrossRef: [Author and Title](#)

Google Scholar: [Author Only](#) [Title Only](#) [Author and Title](#)

**Baker RF, Braun DM (2008) tie-dyed2 functions with tie-dyed1 to promote carbohydrate export from maize leaves. Plant Physiol 146: 1085-1097**

Pubmed: [Author and Title](#)

CrossRef: [Author and Title](#)

Google Scholar: [Author Only](#) [Title Only](#) [Author and Title](#)

**Baker RF, Leach KA, Braun DM (2012) SWEET as sugar: new sucrose effluxers in plants. Mol Plant 5: 766-768**

Pubmed: [Author and Title](#)

CrossRef: [Author and Title](#)

Google Scholar: [Author Only](#) [Title Only](#) [Author and Title](#)

**Baker RF, Slewinski TL, Braun DM (2013) The Tie-dyed pathway promotes symplastic trafficking in the phloem. Plant Sig Behav 8: e24540**

Pubmed: [Author and Title](#)

CrossRef: [Author and Title](#)

Google Scholar: [Author Only](#) [Title Only](#) [Author and Title](#)

**Bauer CS, Hoth S, Haga K, Philippar K, Aoki N, Hedrich R (2000) Differential expression and regulation of K<sup>+</sup> channels in the maize coleoptile: molecular and biophysical analysis of cells isolated from cortex and vasculature. Plant J 24: 139-145**

Pubmed: [Author and Title](#)

CrossRef: [Author and Title](#)

Google Scholar: [Author Only](#) [Title Only](#) [Author and Title](#)

**Bihmidine S, Baker RF, Hoffner C, Braun DM (2015) Sucrose accumulation in sweet sorghum stems occurs by apoplasmic phloem unloading and does not involve differential Sucrose transporter expression. BMC Plant Biol 15: 186**

Pubmed: [Author and Title](#)

CrossRef: [Author and Title](#)

Google Scholar: [Author Only](#) [Title Only](#) [Author and Title](#)

**Bihmidine S, Hunter III CT, Johns CE, Koch KE, Braun DM (2013) Regulation of assimilate import into sink organs: Update on molecular drivers of sink strength. Front Plant Sci 4: 177. doi: 110.3389/fpls.2013.00177**

Pubmed: [Author and Title](#)

CrossRef: [Author and Title](#)

Google Scholar: [Author Only](#) [Title Only](#) [Author and Title](#)

**Bihmidine S, Julius BT, Dweikat I, Braun DM (2016) Tonoplast Sugar Transporters (SbTSTs) putatively control sucrose accumulation in sweet sorghum stems. Plant Sig Behav 11: e1117721**

Pubmed: [Author and Title](#)  
CrossRef: [Author and Title](#)  
Google Scholar: [Author Only](#) [Title Only](#) [Author and Title](#)

**Bowling AJ, Pence HE, Church JB (2014) Application of a novel and automated branched DNA in situ hybridization method for the rapid and sensitive localization of mRNA molecules in plant tissues. *App Plant Sci* 2: 1400011**

Pubmed: [Author and Title](#)  
CrossRef: [Author and Title](#)  
Google Scholar: [Author Only](#) [Title Only](#) [Author and Title](#)

**Braun DM (2012) SWEET! The pathway is complete. *Science* 335: 173-174**

Pubmed: [Author and Title](#)  
CrossRef: [Author and Title](#)  
Google Scholar: [Author Only](#) [Title Only](#) [Author and Title](#)

**Braun DM, Ma Y, Inada N, Muszynski MG, Baker RF (2006) tie-dyed1 regulates carbohydrate accumulation in maize leaves. *Plant Physiol* 142: 1511-1522**

Pubmed: [Author and Title](#)  
CrossRef: [Author and Title](#)  
Google Scholar: [Author Only](#) [Title Only](#) [Author and Title](#)

**Braun DM, Slewinski TL (2009) Genetic control of carbon partitioning in grasses: Roles of Sucrose Transporters and Tie-dyed loci in phloem loading. *Plant Physiol* 149: 71-81**

Pubmed: [Author and Title](#)  
CrossRef: [Author and Title](#)  
Google Scholar: [Author Only](#) [Title Only](#) [Author and Title](#)

**Braun DM, Wang L, Ruan Y-L (2014) Understanding and manipulating sucrose phloem loading, unloading, metabolism, and signalling to enhance crop yield and food security. *J Exp Bot* 65: 1713-1735**

Pubmed: [Author and Title](#)  
CrossRef: [Author and Title](#)  
Google Scholar: [Author Only](#) [Title Only](#) [Author and Title](#)

**Bürkle L, Hibberd JM, Quick WP, Kühn C, Hirner B, Frommer WB (1998) The H<sup>+</sup>-sucrose cotransporter NtSUT1 is essential for sugar export from tobacco leaves. *Plant Physiol* 118: 59-68**

Pubmed: [Author and Title](#)  
CrossRef: [Author and Title](#)  
Google Scholar: [Author Only](#) [Title Only](#) [Author and Title](#)

**Carpaneto A, Geiger D, Bamberg E, Sauer N, Fromm J, Hedrich R (2005) Phloem-localized, proton-coupled sucrose carrier ZmSUT1 mediates sucrose efflux under the control of the sucrose gradient and the proton motive force. *J Biol Chem* 280: 21437-21443**

Pubmed: [Author and Title](#)  
CrossRef: [Author and Title](#)  
Google Scholar: [Author Only](#) [Title Only](#) [Author and Title](#)

**Chandran D, Reinders A, Ward JM (2003) Substrate specificity of the Arabidopsis thaliana sucrose transporter AtSUC2. *J Biol Chem* 278: 44320-44325**

Pubmed: [Author and Title](#)  
CrossRef: [Author and Title](#)  
Google Scholar: [Author Only](#) [Title Only](#) [Author and Title](#)

**Chen L-Q, Hou B-H, Lalonde S, Takanaga H, Hartung ML, Qu X-Q, Guo W-J, Kim J-G, Underwood W, Chaudhuri B, Chermak D, Antony G, White FF, Somerville SC, Mudgett MB, Frommer WB (2010) Sugar transporters for intercellular exchange and nutrition of pathogens. *Nature* 468: 527-532**

Pubmed: [Author and Title](#)  
CrossRef: [Author and Title](#)  
Google Scholar: [Author Only](#) [Title Only](#) [Author and Title](#)

**Chen L-Q, Qu X-Q, Hou B-H, Sosso D, Osorio S, Fernie AR, Frommer WB (2012) Sucrose efflux mediated by SWEET proteins as a key step for phloem transport. *Science* 335: 207-211**

Pubmed: [Author and Title](#)  
CrossRef: [Author and Title](#)  
Google Scholar: [Author Only](#) [Title Only](#) [Author and Title](#)

**Chu Z, Yuan M, Yao J, Ge X, Yuan B, Xu C, Li X, Fu B, Li Z, Bennetzen JL, Zhang Q, Wang S (2006) Promoter mutations of an essential gene for pollen development result in disease resistance in rice. *Genes Dev* 20: 1250-1255**

Pubmed: [Author and Title](#)  
CrossRef: [Author and Title](#)  
Google Scholar: [Author Only](#) [Title Only](#) [Author and Title](#)

**Durand M, Porcheron B, Hennion N, Maurousset L, Lemoine R, Pourtau N (2016) Water deficit enhances C export to the roots in Arabidopsis thaliana plants with contribution of sucrose transporters in both shoot and roots. *Plant Physiol* 170: 1460-1479**

Pubmed: [Author and Title](#)  
CrossRef: [Author and Title](#)  
Google Scholar: [Author Only](#) [Title Only](#) [Author and Title](#)

**Eom J-S, Chen L-Q, Sosso D, Julius BT, Lin IW, Qu X-Q, Braun DM, Frommer WB (2015) SWEETs, transporters for intracellular and intercellular sugar translocation. *Curr Opin Plant Biol* 25: 53-62**

Pubmed: [Author and Title](#)

CrossRef: [Author and Title](#)  
Google Scholar: [Author Only Title Only Author and Title](#)

**Eom J-S, Choi S-B, Ward JM, Jeon J-S (2012) The mechanism of phloem loading in rice (*Oryza sativa*). *Molec Cells* 33: 431-438**

Pubmed: [Author and Title](#)  
CrossRef: [Author and Title](#)  
Google Scholar: [Author Only Title Only Author and Title](#)

**Esau K (1977) Anatomy of Seed Plants, Ed 2nd. John Wiley and Sons, New York**

Pubmed: [Author and Title](#)  
CrossRef: [Author and Title](#)  
Google Scholar: [Author Only Title Only Author and Title](#)

**Evert RF (1982) Sieve-tube structure in relation to function. *Bioscience* 32: 789-795**

Pubmed: [Author and Title](#)  
CrossRef: [Author and Title](#)  
Google Scholar: [Author Only Title Only Author and Title](#)

**Evert RF, Eschrich W, Heyser W (1977) Distribution and structure of the plasmodesmata in mesophyll and bundle sheath cells of *Zea mays* L. *Planta* 136: 77-89**

Pubmed: [Author and Title](#)  
CrossRef: [Author and Title](#)  
Google Scholar: [Author Only Title Only Author and Title](#)

**Evert RF, Eschrich W, Heyser W (1978) Leaf structure in relation to solute transport and phloem loading in *Zea mays* L. *Planta* 138: 279-294**

Pubmed: [Author and Title](#)  
CrossRef: [Author and Title](#)  
Google Scholar: [Author Only Title Only Author and Title](#)

**Evert RF, Russin WA (1993) Structurally, phloem unloading in the maize leaf cannot be symplastic. *Am J Bot* 80: 1310-1317**

Pubmed: [Author and Title](#)  
CrossRef: [Author and Title](#)  
Google Scholar: [Author Only Title Only Author and Title](#)

**Evert RF, Russin WA, Bosabalidis AM (1996a) Anatomical and ultrastructural changes associated with sink-to-source transition in developing maize leaves. *Int J Plant Sci* 157: 247-261**

Pubmed: [Author and Title](#)  
CrossRef: [Author and Title](#)  
Google Scholar: [Author Only Title Only Author and Title](#)

**Evert RF, Russin WA, Botha CEJ (1996b) Distribution and frequency of plasmodesmata in relation to photoassimilate pathways and phloem loading in the barley leaf. *Planta* 198: 572-579**

Pubmed: [Author and Title](#)  
CrossRef: [Author and Title](#)  
Google Scholar: [Author Only Title Only Author and Title](#)

**Fritz E, Evert RF, Heyser W (1983) Microautoradiographic studies of phloem loading and transport in the leaf of *Zea mays* L. *Planta* 159: 193-206**

Pubmed: [Author and Title](#)  
CrossRef: [Author and Title](#)  
Google Scholar: [Author Only Title Only Author and Title](#)

**Fritz E, Evert RF, Nasse H (1989) Loading and transport of assimilates in different maize leaf bundles - Digital image analysis of <sup>14</sup>C microautoradiographs. *Planta* 178: 1-9**

Pubmed: [Author and Title](#)  
CrossRef: [Author and Title](#)  
Google Scholar: [Author Only Title Only Author and Title](#)

**Fukumorita T, Chino M (1982) Sugar, amino acid and inorganic contents in rice phloem sap. *Plant Cell Physiol* 23: 273-283**

Pubmed: [Author and Title](#)  
CrossRef: [Author and Title](#)  
Google Scholar: [Author Only Title Only Author and Title](#)

**Geiger D (2011) Plant sucrose transporters from a biophysical point of view. *Mol Plant* 4: 395-406**

Pubmed: [Author and Title](#)  
CrossRef: [Author and Title](#)  
Google Scholar: [Author Only Title Only Author and Title](#)

**Giaquinta RT, Lin W, Sadler NL, Franceschi VR (1983) Pathway of phloem unloading of sucrose in corn roots. *Plant Physiol* 72: 362-367**

Pubmed: [Author and Title](#)  
CrossRef: [Author and Title](#)  
Google Scholar: [Author Only Title Only Author and Title](#)

**Godfray HCJ, Beddington JR, Crute IR, Haddad L, Lawrence D, Muir JF, Pretty J, Robinson S, Thomas SM, Toulmin C (2010) Food security: The challenge of feeding 9 billion people. *Science* 327: 812-818**

Pubmed: [Author and Title](#)  
CrossRef: [Author and Title](#)  
Google Scholar: [Author Only Title Only Author and Title](#)

- Gottwald JR, Krysan PJ, Young JC, Evert RF, Sussman MR (2000) Genetic evidence for the in planta role of phloem-specific plasma membrane sucrose transporters. Proc Natl Acad Sci USA 97: 13979-13984**  
Pubmed: [Author and Title](#)  
CrossRef: [Author and Title](#)  
Google Scholar: [Author Only](#) [Title Only](#) [Author and Title](#)
- Gould N, Thorpe MR, Pritchard J, Christeller JT, Williams LE, Roeb G, Schurr U, Minchin PEH (2012) AtSUC2 has a role for sucrose retrieval along the phloem pathway: Evidence from carbon-11 tracer studies. Plant Sci 188-189: 97-101**  
Pubmed: [Author and Title](#)  
CrossRef: [Author and Title](#)  
Google Scholar: [Author Only](#) [Title Only](#) [Author and Title](#)
- Grignon N, Touraine B, Durand M (1989) 6(5)Carboxyfluorescein as a tracer of phloem sap translocation. Am J Bot 76: 871-877**  
Pubmed: [Author and Title](#)  
CrossRef: [Author and Title](#)  
Google Scholar: [Author Only](#) [Title Only](#) [Author and Title](#)
- Grodzinski B, Jiao J, Leonardos ED (1998) Estimating photosynthesis and concurrent export rates in C3 and C4 species at ambient and elevated CO2. Plant Physiol 117: 207-215**  
Pubmed: [Author and Title](#)  
CrossRef: [Author and Title](#)  
Google Scholar: [Author Only](#) [Title Only](#) [Author and Title](#)
- Hackel A, Schauer N, Carrari F, Fernie AR, Grimm B, Kühn C (2006) Sucrose transporter LeSUT1 and LeSUT2 inhibition affects tomato fruit development in different ways. Plant J. 45: 180-192**  
Pubmed: [Author and Title](#)  
CrossRef: [Author and Title](#)  
Google Scholar: [Author Only](#) [Title Only](#) [Author and Title](#)
- Hafke JB, van Amerongen J-K, Kelling F, Furch ACU, Gaupels F, van Bel AJE (2005) Thermodynamic battle for photosynthate acquisition between sieve tubes and adjoining parenchyma in transport phloem. Plant Physiol 138: 1527-1537**  
Pubmed: [Author and Title](#)  
CrossRef: [Author and Title](#)  
Google Scholar: [Author Only](#) [Title Only](#) [Author and Title](#)
- Haupt S, Duncan GH, Holzberg S, Oparka KJ (2001) Evidence for symplastic phloem unloading in sink leaves of barley. Plant Physiol 125: 209-218**  
Pubmed: [Author and Title](#)  
CrossRef: [Author and Title](#)  
Google Scholar: [Author Only](#) [Title Only](#) [Author and Title](#)
- Hayashi H, Chino M (1986) Collection of pure phloem sap from wheat and its chemical composition. Plant Cell Physiol 27: 1387-1393**  
Pubmed: [Author and Title](#)  
CrossRef: [Author and Title](#)  
Google Scholar: [Author Only](#) [Title Only](#) [Author and Title](#)
- Heyser W, Evert RF, Fritz E, Eschrich W (1978) Sucrose in the free space of translocating maize leaf bundles. Plant Physiol 62: 491-494**  
Pubmed: [Author and Title](#)  
CrossRef: [Author and Title](#)  
Google Scholar: [Author Only](#) [Title Only](#) [Author and Title](#)
- Huang M, Braun DM (2010) Genetic analyses of cell death in maize (Zea mays, Poaceae) leaves reveal a distinct pathway operating in the camouflage1 mutant. Am J Bot 97: 357-364**  
Pubmed: [Author and Title](#)  
CrossRef: [Author and Title](#)  
Google Scholar: [Author Only](#) [Title Only](#) [Author and Title](#)
- Huang M, Slewinski TL, Baker RF, Janick-Buckner D, Buckner B, Johal GS, Braun DM (2009) Camouflage patterning in maize leaves results from a defect in porphobilinogen deaminase. Mol Plant 2: 773-789**  
Pubmed: [Author and Title](#)  
CrossRef: [Author and Title](#)  
Google Scholar: [Author Only](#) [Title Only](#) [Author and Title](#)
- Hukin D, Doering-Saad C, Thomas C, Pritchard J (2002) Sensitivity of cell hydraulic conductivity to mercury is coincident with symplasmic isolation and expression of plasmalemma aquaporin genes in growing maize roots. Planta 215: 1047-1056**  
Pubmed: [Author and Title](#)  
CrossRef: [Author and Title](#)  
Google Scholar: [Author Only](#) [Title Only](#) [Author and Title](#)
- Ibraheem O, Botha CEJ, Bradley G, Dealtry G, Roux S (2014) Rice sucrose transporter1 (OsSUT1) up-regulation in xylem parenchyma is caused by aphid feeding on rice leaf blade vascular bundles. Plant Biol 16: 783-791**  
Pubmed: [Author and Title](#)  
CrossRef: [Author and Title](#)  
Google Scholar: [Author Only](#) [Title Only](#) [Author and Title](#)
- Ishimaru K, Hirose T, Aoki N, Takahashi S, Ono K, Yamamoto S, Wu J, Saji S, Baba T, Ugaki M, Matsumoto T, Ohsugi R (2001) Antisense expression of a rice sucrose transporter OsSUT1 in rice (Oryza sativa L.). Plant Cell Physiol 42: 1181-1185**  
Pubmed: [Author and Title](#)  
CrossRef: [Author and Title](#)  
Google Scholar: [Author Only](#) [Title Only](#) [Author and Title](#)

**Jia W, Zhang L, Wu D, Liu S, Gong X, Cui Z, Cui N, Cao H, Rao L, Wang C (2015) Sucrose transporter AtSUC9 mediated by a low sucrose level is involved in Arabidopsis abiotic stress resistance by regulating sucrose distribution and ABA accumulation. Plant Cell Physiol 56: 1574-1587**

Pubmed: [Author and Title](#)

CrossRef: [Author and Title](#)

Google Scholar: [Author Only](#) [Title Only](#) [Author and Title](#)

**Jung B, Ludewig F, Schulz A, Meißner G, Wöstefeld N, Flügge U-I, Pommerrenig B, Wirsching P, Sauer N, Koch W, Sommer F, Mühlhaus T, Schroda M, Cuin TA, Graus D, Marten I, Hedrich R (2015) Identification of the transporter responsible for sucrose accumulation in sugar beet taproots. Nat Plants 1: 14001**

Pubmed: [Author and Title](#)

CrossRef: [Author and Title](#)

Google Scholar: [Author Only](#) [Title Only](#) [Author and Title](#)

**Kühn C, Grof CPL (2010) Sucrose transporters of higher plants. Curr Opin Plant Biol 13: 287-297**

Pubmed: [Author and Title](#)

CrossRef: [Author and Title](#)

Google Scholar: [Author Only](#) [Title Only](#) [Author and Title](#)

**Lalonde S, Weise A, Walsh R, Ward JM, Frommer WB (2003) Fusion to GFP blocks intercellular trafficking of the sucrose transporter SUT1 leading to accumulation in companion cells. BMC Plant Biol 3: 8**

Pubmed: [Author and Title](#)

CrossRef: [Author and Title](#)

Google Scholar: [Author Only](#) [Title Only](#) [Author and Title](#)

**Lalonde S, Wipf D, Frommer WB (2004) Transport mechanisms for organic forms of carbon and nitrogen between source and sink. Annu Rev Plant Biol 55: 341-372**

Pubmed: [Author and Title](#)

CrossRef: [Author and Title](#)

Google Scholar: [Author Only](#) [Title Only](#) [Author and Title](#)

**Lang-Pauluzzi I (2000) The behaviour of the plasma membrane during plasmolysis: a study by UV microscopy. J Micro 198: 188-198**

Pubmed: [Author and Title](#)

CrossRef: [Author and Title](#)

Google Scholar: [Author Only](#) [Title Only](#) [Author and Title](#)

**Larionov A, Krause A, Miller W (2005) A standard curve based method for relative real time PCR data processing. BMC Bioinform 6: 1-16**

Pubmed: [Author and Title](#)

CrossRef: [Author and Title](#)

Google Scholar: [Author Only](#) [Title Only](#) [Author and Title](#)

**Leach KA, McSteen PC, Braun DM (2016) Genomic DNA isolation from maize (Zea mays) leaves using a simple, high-throughput protocol. Curr Prot Plant Biol 1: 15-27**

Pubmed: [Author and Title](#)

CrossRef: [Author and Title](#)

Google Scholar: [Author Only](#) [Title Only](#) [Author and Title](#)

**Lemoine R, La Camera S, Atanassova R, Dédaldéchamp F, Alario T, Pourtau N, Bonnemain J-L, Laloi M, Coutos-Thévenot P, Maurousset L, Faucher M, Girousse C, Lemonnier P, Parrilla J, Durand M (2013) Source to sink transport and regulation by environmental factors. Front Plant Sci 4: 272. doi:210.3389/fpls.2013.00272**

Pubmed: [Author and Title](#)

CrossRef: [Author and Title](#)

Google Scholar: [Author Only](#) [Title Only](#) [Author and Title](#)

**Li P, Ponnala L, Gandotra N, Wang L, Si Y, Tausta SL, Kebrom TH, Provar N, Patel R, Myers CR, Reidel EJ, Turgeon R, Liu P, Sun Q, Nelson T, Brutnell TP (2010) The developmental dynamics of the maize leaf transcriptome. Nat Genet 42: 1060-1067**

Pubmed: [Author and Title](#)

CrossRef: [Author and Title](#)

Google Scholar: [Author Only](#) [Title Only](#) [Author and Title](#)

**Lohaus G, Hussmann M, Pennewiss K, Schneider H, Zhu J-J, Sattelmacher B (2000) Solute balance of a maize (Zea mays L.) source leaf as affected by salt treatment with special emphasis on phloem retranslocation and ion leaching. J Exp Bot 51: 1721-1732**

Pubmed: [Author and Title](#)

CrossRef: [Author and Title](#)

Google Scholar: [Author Only](#) [Title Only](#) [Author and Title](#)

**Lohaus G, Pennewiss K, Sattelmacher B, Hussmann M, Muehling KH (2001) Is the infiltration-centrifugation technique appropriate for the isolation of apoplastic fluid? A critical evaluation with different plant species. Phys Plant 111: 457-465**

Pubmed: [Author and Title](#)

CrossRef: [Author and Title](#)

Google Scholar: [Author Only](#) [Title Only](#) [Author and Title](#)

**Lunn JE, Furbank RT (1999) Tansley Review No. 105. Sucrose biosynthesis in C4 plants. New Phytol 143: 221-237**

Pubmed: [Author and Title](#)

CrossRef: [Author and Title](#)

Google Scholar: [Author Only](#) [Title Only](#) [Author and Title](#)

**Ma Y, Baker RF, Magallanes-Lundback M, DellaPenna D, Braun DM (2008) Tie-dyed1 and Sucrose export defective1 act**

**independently to promote carbohydrate export from maize leaves. *Planta* 227: 527-538**

Pubmed: [Author and Title](#)

CrossRef: [Author and Title](#)

Google Scholar: [Author Only](#) [Title Only](#) [Author and Title](#)

**Ma Y, Slewinski TL, Baker RF, Braun DM (2009) Tie-dyed1 encodes a novel, phloem-expressed transmembrane protein that functions in carbohydrate partitioning. *Plant Physiol* 149: 181-194**

Pubmed: [Author and Title](#)

CrossRef: [Author and Title](#)

Google Scholar: [Author Only](#) [Title Only](#) [Author and Title](#)

**Makela P, McLaughlin JE, Boyer JS (2005) Imaging and quantifying carbohydrate transport to the developing ovaries of maize. *Ann Bot* 96: 939-949**

Pubmed: [Author and Title](#)

CrossRef: [Author and Title](#)

Google Scholar: [Author Only](#) [Title Only](#) [Author and Title](#)

**Minchin PEH, Thorpe MR (1987) Measurement of unloading and reloading of photo-assimilate within the stem of bean. *J Exp Bot* 38: 211-220**

Pubmed: [Author and Title](#)

CrossRef: [Author and Title](#)

Google Scholar: [Author Only](#) [Title Only](#) [Author and Title](#)

**Mohanty A, Luo A, DeBlasio S, Ling X, Yang Y, Tuthill DE, Williams KE, Hill D, Zadrozny T, Chan A, Sylvester AW, Jackson D (2009) Advancing cell biology and functional genomics in maize using fluorescent protein-tagged lines. *Plant Physiol* 149: 601-605**

Pubmed: [Author and Title](#)

CrossRef: [Author and Title](#)

Google Scholar: [Author Only](#) [Title Only](#) [Author and Title](#)

**Ohshima T, Hayashi H, Chino M (1990) Collection and chemical composition of pure phloem sap from *Zea mays* L. *Plant Cell Physiol* 31: 735-737**

Pubmed: [Author and Title](#)

CrossRef: [Author and Title](#)

Google Scholar: [Author Only](#) [Title Only](#) [Author and Title](#)

**Patrick JW (2012) Fundamentals of phloem transport physiology. In *Phloem*. Wiley-Blackwell, pp 30-59**

Pubmed: [Author and Title](#)

CrossRef: [Author and Title](#)

Google Scholar: [Author Only](#) [Title Only](#) [Author and Title](#)

**Patrick JW, Botha FC, Birch RG (2013) Metabolic engineering of sugars and simple sugar derivatives in plants. *Plant Biotech J* 11: 142-156**

Pubmed: [Author and Title](#)

CrossRef: [Author and Title](#)

Google Scholar: [Author Only](#) [Title Only](#) [Author and Title](#)

**Porter GA, Knievel DP, Shannon JC (1985) Sugar efflux from maize (*Zea mays* L.) pedicel tissue. *Plant Physiol* 77: 524-531**

Pubmed: [Author and Title](#)

CrossRef: [Author and Title](#)

Google Scholar: [Author Only](#) [Title Only](#) [Author and Title](#)

**Rae AL, Perroux JM, Grof CPL (2005) Sucrose partitioning between vascular bundles and storage parenchyma in the sugarcane stem: a potential role for the ShSUT1 sucrose transporter. *Planta* 220: 817-825**

Pubmed: [Author and Title](#)

CrossRef: [Author and Title](#)

Google Scholar: [Author Only](#) [Title Only](#) [Author and Title](#)

**Reinders A, Sivitz A, Hsi A, Grof C, Perroux J, Ward JM (2006) Sugarcane ShSUT1: analysis of sucrose transport activity and inhibition by sucralose. *Plant Cell Environ* 29: 1871-1880**

Pubmed: [Author and Title](#)

CrossRef: [Author and Title](#)

Google Scholar: [Author Only](#) [Title Only](#) [Author and Title](#)

**Reinders A, Sivitz AB, Ward JM (2012) Evolution of plant sucrose uptake transporters. *Front Plant Sci* 3: 22. doi: 10.3389/fpls.2012.00022**

Pubmed: [Author and Title](#)

CrossRef: [Author and Title](#)

Google Scholar: [Author Only](#) [Title Only](#) [Author and Title](#)

**Rennie EA, Turgeon R (2009) A comprehensive picture of phloem loading strategies. *Proc Natl Acad Sci USA* 106: 14162-14167**

Pubmed: [Author and Title](#)

CrossRef: [Author and Title](#)

Google Scholar: [Author Only](#) [Title Only](#) [Author and Title](#)

**Riesmeier JW, Willmitzer L, Frommer WB (1992) Isolation and characterization of a sucrose carrier cDNA from spinach by functional expression in yeast. *EMBO J* 11: 4705-4713**

Pubmed: [Author and Title](#)

CrossRef: [Author and Title](#)

Google Scholar: [Author Only](#) [Title Only](#) [Author and Title](#)

**Riesmeier JW, Willmitzer L, Frommer WB (1994) Evidence for an essential role of the sucrose transporter in phloem loading and**

**assimilate partitioning. EMBO J 13: 1-7**

Pubmed: [Author and Title](#)

CrossRef: [Author and Title](#)

Google Scholar: [Author Only](#) [Title Only](#) [Author and Title](#)

**Rosenzweig C, Elliott J, Deryng D, Ruane AC, Müller C, Arneth A, Boote KJ, Folberth C, Glotter M, Khabarov N, Neumann K, Piontek F, Pugh TAM, Schmid E, Stehfest E, Yang H, Jones JW (2014) Assessing agricultural risks of climate change in the 21st century in a global gridded crop model intercomparison. Proc Natl Acad Sci USA 111: 3268-3273**

Pubmed: [Author and Title](#)

CrossRef: [Author and Title](#)

Google Scholar: [Author Only](#) [Title Only](#) [Author and Title](#)

**Rotsch D, Brossard T, Bihmidine S, Ying W, Gaddam V, Harmata M, Robertson JD, Swyers M, Jurisson SS, Braun DM (2015) Radiosynthesis of 6'-deoxy-6'[18F]fluorosucrose via automated synthesis and its utility to study in vivo sucrose transport in maize (Zea mays) leaves. PLOS ONE 10: e0128989**

Pubmed: [Author and Title](#)

CrossRef: [Author and Title](#)

Google Scholar: [Author Only](#) [Title Only](#) [Author and Title](#)

**Russell SH, Evert RF (1985) Leaf vasculature in Zea mays L. Planta 164: 448-458**

Pubmed: [Author and Title](#)

CrossRef: [Author and Title](#)

Google Scholar: [Author Only](#) [Title Only](#) [Author and Title](#)

**Ruzin S (1999) Plant Microtechnique and Microscopy. Oxford University Press, New York**

Pubmed: [Author and Title](#)

CrossRef: [Author and Title](#)

Google Scholar: [Author Only](#) [Title Only](#) [Author and Title](#)

**Sauer N (2007) Molecular physiology of higher plant sucrose transporters. FEBS Lett 581: 2309-2317**

Pubmed: [Author and Title](#)

CrossRef: [Author and Title](#)

Google Scholar: [Author Only](#) [Title Only](#) [Author and Title](#)

**Schmitt B, Stadler R, Sauer N (2008) Immunolocalization of Solanaceous SUT1 proteins in companion cells and xylem parenchyma: New perspectives for phloem loading and transport. Plant Physiol 148: 187-199**

Pubmed: [Author and Title](#)

CrossRef: [Author and Title](#)

Google Scholar: [Author Only](#) [Title Only](#) [Author and Title](#)

**Scofield G, Hirose T, Gaudron J, Upadhyaya N, Ohsugi R, Furbank RT (2002) Antisense suppression of the rice sucrose transporter gene, OsSUT1, leads to impaired grain filling and germination but does not affect photosynthesis. Funct Plant Biol 29: 815-826**

Pubmed: [Author and Title](#)

CrossRef: [Author and Title](#)

Google Scholar: [Author Only](#) [Title Only](#) [Author and Title](#)

**Scofield GN, Hirose T, Aoki N, Furbank RT (2007) Involvement of the sucrose transporter, OsSUT1, in the long-distance pathway for assimilate transport in rice. J Exp Bot 58: 3155-3169**

Pubmed: [Author and Title](#)

CrossRef: [Author and Title](#)

Google Scholar: [Author Only](#) [Title Only](#) [Author and Title](#)

**Sivitz AB, Reinders A, Ward JM (2005) Analysis of the transport activity of barley sucrose transporter HvSUT1. Plant Cell Physiol 46: 1666-1673**

Pubmed: [Author and Title](#)

CrossRef: [Author and Title](#)

Google Scholar: [Author Only](#) [Title Only](#) [Author and Title](#)

**Slewinski TL (2013) Using evolution as a guide to engineer Kranz-type C4 photosynthesis. Front Plant Sci 4: 212. doi:210.3389/fpls.2013.00212**

Pubmed: [Author and Title](#)

CrossRef: [Author and Title](#)

Google Scholar: [Author Only](#) [Title Only](#) [Author and Title](#)

**Slewinski TL, Baker RF, Stubert A, Braun DM (2012) Tie-dyed2 encodes a callose synthase that functions in vein development and affects symplastic trafficking within the phloem of maize leaves. Plant Physiol 160: 1540-1550**

Pubmed: [Author and Title](#)

CrossRef: [Author and Title](#)

Google Scholar: [Author Only](#) [Title Only](#) [Author and Title](#)

**Slewinski TL, Braun DM (2010a) Current perspectives on the regulation of whole-plant carbohydrate partitioning. Plant Sci 178: 341-349**

Pubmed: [Author and Title](#)

CrossRef: [Author and Title](#)

Google Scholar: [Author Only](#) [Title Only](#) [Author and Title](#)

**Slewinski TL, Braun DM (2010b) The psychedelic genes of maize redundantly promote carbohydrate export from leaves. Genetics 185: 221-232**

Pubmed: [Author and Title](#)

CrossRef: [Author and Title](#)  
Google Scholar: [Author Only Title Only Author and Title](#)

**Slewinski TL, Garg A, Johal GS, Braun DM (2010) Maize SUT1 functions in phloem loading. Plant Sig Behav 5: 687-690**

Pubmed: [Author and Title](#)  
CrossRef: [Author and Title](#)  
Google Scholar: [Author Only Title Only Author and Title](#)

**Slewinski TL, Meeley R, Braun DM (2009) Sucrose transporter1 functions in phloem loading in maize leaves. J Exp Bot 60: 881-892**

Pubmed: [Author and Title](#)  
CrossRef: [Author and Title](#)  
Google Scholar: [Author Only Title Only Author and Title](#)

**Slewinski TL, Zhang C, Turgeon R (2013) Structural and functional heterogeneity in phloem loading and transport. Front Plant Sci 4: 244. doi: 210.3389/fpls.2013.00244**

Pubmed: [Author and Title](#)  
CrossRef: [Author and Title](#)  
Google Scholar: [Author Only Title Only Author and Title](#)

**Smith JM, Leslie ME, Robinson SJ, Korasick DA, Zhang T, Backues SK, Cornish PV, Koo AJ, Bednarek SY, Heese A (2014) Loss of Arabidopsis thaliana Dynamin-Related Protein 2B reveals separation of innate immune signaling pathways. PLoS Pathog 10: e1004578**

Pubmed: [Author and Title](#)  
CrossRef: [Author and Title](#)  
Google Scholar: [Author Only Title Only Author and Title](#)

**Srivastava AC, Ganesan S, Ismail IO, Ayre BG (2008) Functional characterization of the Arabidopsis thaliana AtSUC2 Suc/H+ symporter by tissue-specific complementation reveals an essential role in phloem loading but not in long-distance transport. Plant Physiol 147: 200-211**

Pubmed: [Author and Title](#)  
CrossRef: [Author and Title](#)  
Google Scholar: [Author Only Title Only Author and Title](#)

**Sun Y, Reinders A, LaFleur KR, Mori T, Ward JM (2010) Transport activity of rice sucrose transporters OsSUT1 and OsSUT5. Plant Cell Physiol 51: 114-122**

Pubmed: [Author and Title](#)  
CrossRef: [Author and Title](#)  
Google Scholar: [Author Only Title Only Author and Title](#)

**Tang A-C, Boyer JS (2013) Differences in membrane selectivity drive phloem transport to the apoplast from which maize florets develop. Ann Bot 111: 551-562**

Pubmed: [Author and Title](#)  
CrossRef: [Author and Title](#)  
Google Scholar: [Author Only Title Only Author and Title](#)

**van Bel AJE (1996) Interaction between sieve element and companion cell and the consequences for photoassimilate distribution. Two structural hardware frames with associated physiological software packages in dicotyledons? J Exp Bot 47: 1129-1140**

Pubmed: [Author and Title](#)  
CrossRef: [Author and Title](#)  
Google Scholar: [Author Only Title Only Author and Title](#)

**van Bel AJE (2003) Transport phloem: low profile, high impact. Plant Physiol 131: 1509-1510**

Pubmed: [Author and Title](#)  
CrossRef: [Author and Title](#)  
Google Scholar: [Author Only Title Only Author and Title](#)

**van Bel AJE, Knoblauch M (2000) Sieve element and companion cell: the story of the comatose patient and the hyperactive nurse. Funct Plant Biol 27: 477-487**

Pubmed: [Author and Title](#)  
CrossRef: [Author and Title](#)  
Google Scholar: [Author Only Title Only Author and Title](#)

**Warmbrodt RD (1985) Studies on the root of Zea mays L.-structure of the adventitious roots with respect to phloem unloading. Bot Gazet: 169-180**

Pubmed: [Author and Title](#)  
CrossRef: [Author and Title](#)  
Google Scholar: [Author Only Title Only Author and Title](#)

**Weiner H, Blechschmidt-Schneider S, Mohme H, Eschrich W, Heldt HW (1991) Phloem transport of amino acids, comparison of amino acid contents of maize leaves and of the sieve tube exudate. Plant Physiol Biochem 29: 19-23**

Pubmed: [Author and Title](#)  
CrossRef: [Author and Title](#)  
Google Scholar: [Author Only Title Only Author and Title](#)

**Yadav UP, Ayre BG, Bush DR (2015) Transgenic approaches to altering carbon and nitrogen partitioning in whole plants: assessing the potential to improve crop yields and nutritional quality. Front Plant Sci 6: 275. doi: 210.3389/fpls.2015.00275**

Pubmed: [Author and Title](#)  
CrossRef: [Author and Title](#)  
Google Scholar: [Author Only Title Only Author and Title](#)

**Zelazny E, Borst JW, Muylaert M, Batoko H, Hemminga MA, Chaumont F (2007) FRET imaging in living maize cells reveals that**

**plasma membrane aquaporins interact to regulate their subcellular localization. Proc Natl Acad Sci USA 104: 12359-12364**

Pubmed: [Author and Title](#)

CrossRef: [Author and Title](#)

Google Scholar: [Author Only](#) [Title Only](#) [Author and Title](#)

**Zhang WH, Zhou YC, Dibley KE, Tyerman SD, Furbank RT, Patrick JW (2007a) Nutrient loading of developing seeds. Funct Plant Biol 34: 314-331**

Pubmed: [Author and Title](#)

CrossRef: [Author and Title](#)

Google Scholar: [Author Only](#) [Title Only](#) [Author and Title](#)

**Zhang X, Madi S, Borsuk L, Nettleton D, Elshire RJ, Buckner B, Janick-Buckner D, Beck J, Timmermans M, Schnable PS, Scanlon MJ (2007b) Laser microdissection of narrow sheath mutant maize uncovers novel gene expression in the shoot apical meristem. PLoS Genet 3: e101**

Pubmed: [Author and Title](#)

CrossRef: [Author and Title](#)

Google Scholar: [Author Only](#) [Title Only](#) [Author and Title](#)